July 2020

Development and Characterization of Robust and Cost-Effective Catalysts for Selective Biomass Upgrading to Fuels and Chemicals by Deoxydehydration

Bryan E. Sharkey

DEVELOPMENT AND CHARACTERIZATION OF ROBUST AND COST-EFFECTIVE CATALYSTS FOR SELECTIVE BIOMASS UPGRADING TO FUELS AND CHEMICALS BY DEOXYDEHYDRATION

A Dissertation Presented

By

BRYAN ELLIOTT SHARKEY

Submitted to the Graduate School of the
University of Massachusetts Amherst in partial fulfillment
of the requirements for the degree of

DOCTOR OF PHILOSOPHY

May 2020

Department of Chemical Engineering

DEVELOPMENT AND CHARACTERIZATION OF ROBUST AND COST-EFFECTIVE CATALYSTS FOR SELECTIVE BIOMASS UPGRADING TO FUELS AND CHEMICALS BY DEOXYDEHYDRATION

A Dissertation Presented

by

Bryan Sharkey

Approved as to style and content by:

_____

Friederike Jentoft, Chair

_____

Wei Fan, Member

_____

Kevin Kittilstved, Outside Member

_____

John Klier, Head,

Department of Chemical Engineering, University of

Massachusetts Amherst

ACKNOWLEDGEMENTS

This research was supported by the department of energy through grant DE-SC0001004. I would like to give my deepest thanks to my advisor Professor Friederike Jentoft. I would like to thank her for her expert guidance, advice, and support throughout my PhD. Her enthusiasm for science and my project was great encouragement, and I appreciate the opportunities that were given to present my work and interact with others in the field through the Catalysis Center of Energy Innovation. I would like to thank Professor Wei Fan and Professor Kevin Kittilstved for serving on my committee and providing valuable feedback and advice. I also thank Alana Denning, who was my predecessor on the deoxydehydration project in the group and spent valuable time to help me get up to speed on the project even as she was preparing to graduate.

I would like to express my gratitude and appreciation for my colleagues Dr. Koushik Ponurru, Eric Hernandez, Juili Parab, and Dr. Jincy Joseph. While we all worked on different projects, I felt the lab environment was very friendly, collaborative, and helpful. I thank you for your help, advice, and camaraderie over the years. ICP-MS proved to be a vital component of my work, so I would like to express my gratitude to Professor Stephen Eyles and the UMass Mass Spectrometry center, as well as Dr. Adam Graichen for his training and assistance. I thank Dr. Vivek Vattipalli for his assistance in BET surface area measurements. I thank Haneen Mansoor with her help and guidance in EPR measurements and Dr. Klaus Köhler for assistance in interpretation. I would also like to thank Dr. Anatoly Frenkel and Brookhaven National Lab for taking XAFS measurements on my samples.

I would like to thank my friends and family for their love and support. From the friends here at UMass and from back home, thank you I would like to give special thanks to my brother and my parents who have always been there for me even as we are scattered across the country. Thank you, Mom and Dad, for your endless love, support, and encouragement, thank you for helping me tow a U-Haul trailer 700 miles across the country to begin my PhD journey. My deepest

love and thanks to my partner Celina Abundis, who has been a pillar of love and support. My thanks also to the whole Abundis family who has been so welcoming and supportive, thank you for providing me a home away from home.

ABSTRACT

DEVELOPMENT AND CHARACTERIZATION OF ROBUST AND COST-EFFECTIVE CATALYSTS FOR SELECTIVE BIOMASS UPGRADING TO FUELS AND CHEMICALS BY DEOXYDEHYDRATION

MAY 2020

BRYAN SHARKEY, B.S.E. UNIVERISTY OF MICHIGAN ANN ARBOR

PHD, UNIVERISTY OF MASSACHUSETTS AMHERST

Directed by: Professor Friederike Jentoft

The use of biomass-derived ligno-cellulose as a possible alternative source of fuels and chemicals to fossil-based hydrocarbons has been an active area of research for both energy security and the search for more carbon neutral forms of energy. However, biomass offers many challenges based on processing and its high oxygen content. Various biomass upgrading routes, such as pyrolysis, fermentation, and hydrolysis, produce a variety of organic molecules with alcohol, carbonyl, and carboxylic functionality. The highly oxygenated compounds require catalytic upgrading before use as fuel or platform chemicals. One promising upgrading route is deoxydehydration, a reaction which combines a deoxygenation by a sacrificial reductant and dehydration in a single step to selectively convert vicinal diols into an olefin. This reaction has been demonstrated to be highly selective and effective at temperatures as low as 130 °C using homogeneous oxo-rhenium catalysts. The catalytic reaction involves the coordination of the diol with the metal center through a condensation reaction, reduction of the metal center by the sacrificial reductant, and finally the elimination of the alkene and re-oxidation of the catalytic metal center.

Oxo-rhenium complexes have proven to be very effective at deoxydehydration because they can easily undergo the necessary changes in coordination and oxidation state, however the high cost of rhenium and difficulty of homogeneous catalyst recovery make these catalysts untenable for large scale biomass upgrading. This thesis details work in developing more robust

and economical solid catalysts for deoxydehydration. A series of oxide-supported oxo-rhenium catalysts using silica, titania, alumina, iron oxide, and zirconia supports were synthesized and tested which demonstrate high activity for the deoxydehydration reaction, in some cases on par with benchmark homogeneous catalysts, and up to 95% selectivity. However, due to the liquid phase chemistry of the reaction, these catalysts demonstrated various propensities to deactivate over multiple runs due to the leaching of the active rhenium species. We undertook a study to determine which parameters control the leaching behavior. We observed that leaching was promoted by the presence of the diol. The severity of the leaching was dependent on not only the support, but the choice of reactant and solvent. It was also found that after complete diol conversion, the leached rhenium would precipitate out of the reaction mixture, enable a release and catch leaching mitigation strategy. Preliminary work using microporous zeolites as a support to inhibit leaching was conducted. A successful implementation of this strategy would require further investigation, however it was found that the acid site of the zeolite provided an anchoring site for the oxo-rhenium species which reduced leaching, but also lowered selectivity due to side reactions catalyzed by the acid site.

In an alternative strategy to mitigate the challenges associated with the high cost and rarity of rhenium, alternative redox active transition metals including vanadium, tungsten, molybdenum, and manganese were screened for deoxydehydration activity. The molybdenum catalysts were found to be the most promising, with the homogeneous ammonium heptamolybdate catalyst achieving 50% alkene yield and the oxide-supported molybdenum catalysts achieving 22% alkene yield using triphenylphosphine as the reductant. Interestingly, sodium molybdate was not found to be catalytically active under similar conditions. In investigating the role of the ammonium counterion, it was discovered that ammonium-based reductants such as ammonium chloride, ammonium sulfate, and urea are active reductants for molybdenum-catalyzed deoxydehydration. Vanadium catalysts also displayed catalytic activity for deoxydehydration using ammonium

chloride as a reductant with alkene yields of up to 14%.

TABLE OF CONTENTS

LIST OF TABLES

LIST OF FIGURES

LIST OF SCHEMES

CHAPTER 1

INTRODUCTION: DEOXYDEHYDRATION REACTION AS A TOOL FOR BIOMASS UPGRADING

1.1. Biomass Upgrading

Despite the growing concern of global warming due to fossil fuel emissions, oil remains the primary transportation fuel and is the source of many industrial chemicals.[1] The conversion of biomass to fuels and chemicals is an area of active research with the ultimate goal of transitioning from fossil feed stocks to renewable carbon sources. Lignocellulosic biomass forms the rigid structure of plants, comprising approximately 70% of dry plant matter by weight.[2] Lignocellulosic biomass is of great interest as a renewable and more carbon neutral source of fuels and platform chemicals as it is not competitive with crop food production, and the estimated land plant cell wall production is $150\text{-}170*10^9$ tons/year, which makes it potentially a very plentiful feedstock. However, biomass processing is made difficult by the challenge of first breaking down the highly complexed lignocellulosic structure, and by the very high oxygen content of biomass, corresponding to a near 1:1 ratio of carbon and oxygen. The products of primary processing, that is the fluids obtained through biomass pyrolysis or hydrolysis, therefore must be upgraded by extensive deoxygenation.[3]

1.2. Deoxydehydration

One potential biomass upgrading reaction of interest is deoxydehydration (DODH), which targets the vicinal OH groups characteristic of sugars and sugar alcohols. This transformation combines a deoxygenation using a sacrificial reductant, and a dehydration, into a single catalytic cycle, thus producing an alkene from a diol (Scheme 1.1). It does so by combining a deoxygenation by a sacrificial reductant, and a dehydration into a single step with the reaction being thermodynamically driven by the oxidation of the reductant, and the elimination of water, as seen in the mechanism shown in Scheme 1.2.

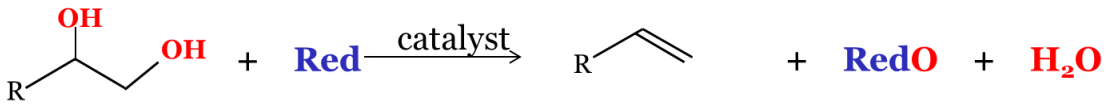

Scheme 1.1 Deoxydehydration reaction to convert a vicinal diol into an alkene by combined dehydration and deoxygenation

DODH was discovered by Cook and Andrews in 1996 who achieved over 90% selectivity to the alkene by using methyltrioxorhenium as the active complex in a homogeneously catalyzed reaction with triphenylphosphine as a reductant.[4] The portfolio of soluble catalysts for deoxydehydration has since been expanded, including improving activity by using bulky ligands on rhenium catalysts,[5] as well as identifying molybdenum,[6,7] and vanadium[8,9] complexes capable of carrying out deoxydehydration. An array of reductants has been successfully employed, including triphenylphosphine, sulfite,[10–12] gaseous CO and H_2,[13] elemental reductants,[14] hydroaromatic reductants,[15] and secondary alcohols.[16,17]

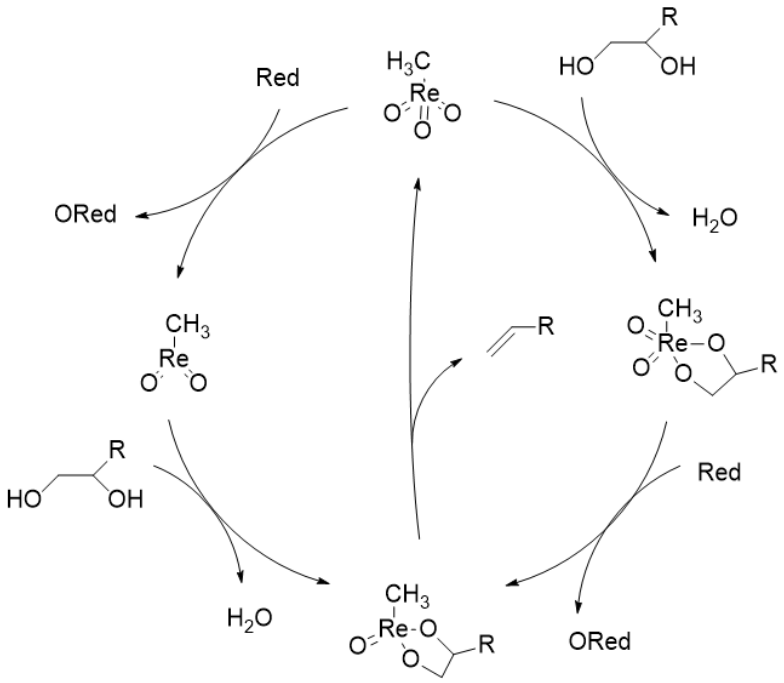

Scheme 1.2 Generalized DODH reaction mechanism with methyltrioxorhenium pictured as catalyst. There are three fundamental steps, condensation with the diol to form a glycolate intermediate, reduction of the catalyst metal center, and elimination of the alkene which reforms the more oxidized form of the catalyst.

The applicability of deoxydehydration was explored on a wide variety of polyol substrates. Cyclic diols were tested to see whether a particular orientation of the OH groups is needed; and cis-diols were generally found to be reactive, whereas steric constraints can apply to trans-cyclic diols such as 1,2-transcyclohexanediol.[18] For larger polyols, such as C4-C6 sugar-derived polyols, there was the question of whether initial reaction of an interior pair of vicinal OH groups would inhibit complete conversion of the remaining, further spaced OH groups. However, Shiramizu and Toste demonstrated complete conversion of erythritol (a 1,2,3,4-tetrol) to butadiene and proposed a mechanism in which the rhenium catalyst also facilitates a hydroxyl and double bond shift.[18] There is agreement that the reaction has three fundamental steps, a reduction step in which the catalyst oxidation state decreases by 2, a condensation step in which the diol coordinates with the oxo-metal site to form a glycolate, and an elimination step in which the catalytic site is re-oxidized and the olefin is eliminated. The sequence of the first two steps is not firmly established.[12,17,19–22]

1.3. Solid Deoxydehydration Catalysts

Due to the high cost and rarity of rhenium, there is significant interest in developing a stable solid catalyst for deoxydehydration. The principal strategy pursued towards this goal has been to heterogenize known active rhenium complexes. In 2013, Denning et al. reported a carbon-supported perrhenate catalyst that was active, selective and versatile with respect to substrate and reducing agent but was also found to deactivate as a result of leaching.[23] Sandbrink et al. tested a variety of oxides as supports for oxo-rhenium and assessed the obtained catalysts with 1,2-hexanediol as reactant and 3-octanol as secondary alcohol reductant and solvent.[24] The authors found that they could produce a relatively stable ReO_x/TiO_2 catalyst when it was pre-reduced. Tomishige and coworkers tested a variety of ceria-supported oxo-rhenium catalysts with added noble metal promoters, including palladium,[25] platinum,[26] and gold.[27] The group developed a gold nanoparticle promoter that was capable of activating H_2 as reductant for deoxydehydration, while the resulting alkenes were not hydrogenated into less valuable alkanes. Leaching was reported to

be insignificant. Li and Zhang sought to attach rhenium catalysts on polymer supports by various strategies that relied on amine-type ligands and ionic ammonium groups. However, these catalysts all demonstrated some leaching during DODH of diethyl tartrate with 3-pentanol as reductant and solvent.[28] Our collaborators, Nicholas and coworkers, tried using a catecholate ligand with a tether as an anchoring strategy, but rhenium was found to leach.[29]

1.4. Objectives, Strategy, and Thesis Outline

In order to make deoxydehydration an industrially feasible process, it is important to develop robust solid catalysts that can be used repeatedly. This is especially relevant to rhenium catalysts as it is a very rare and valuable metal, valued at $1290/lb.[30] Two approaches were pursued in this thesis to produce more robust and industrially feasible catalysts for deoxydehydration.

The first approach is to anchor the rhenium catalyst on a support. Upon pursuing this project, only one supported rhenium catalyst used in deoxydehydration had been reported using carbon as a support. For this catalyst deactivation by leaching is of prime concern.[23] Since the typical substrates of interest are large polar molecules, such as sugar-derived polyols, a solvent is required because their size and polarity make solid-gas phase reactions less feasible. In order to more strongly bind the rhenium catalyst to the support, a variety of oxides were tested as supports. Chapter 2 will cover the development and testing of oxide-supported rhenium catalysts for deoxydehydration.

In general, solid catalyst activity and stability in solution phase processing is of importance in relation to upgrading reactions for biomass-derived feedstock.[31] Moreover, leaching of active species from solid catalysts is a common phenomenon in liquid phase processing and can be a key challenge to developing stable solid catalysts for conversion of non-volatile reactants. There are multiple examples of dissolution of supported noble metal species.[32,33] Leaching is not always easy to detect and requires a number of tests.[34–36] Chapter 3 will cover our investigation of solid rhenium deoxydehydration catalyst stability, especially in regard to the leaching behavior of the active

species and the considerations necessary when testing whether the deoxydehydration catalysis is truly heterogeneous.

Due to the rarity and high cost of rhenium, the second approach to making a more practical deoxydehydration catalyst is to find an alternative redox-active transition metal which can readily undergo the necessary change in coordination and oxidation state to enable the necessary catalytic steps. That is namely the condensation of the metal center with the diol to form a glycolate, the deoxygenation by a sacrificial reductant, and the elimination of the alkene product. Some progress has recently been made on this front. Kwok et al. demonstrated the gas phase conversion of 2,3-butanediol to butene at 400 °C using a VO_x/SiO_2 catalyst.[37] Oxide-supported molybdenum catalysts were reported to be catalytic by Sandbrink et al.[38] and Sharkey et al.[29], however, only with limited selectivity to the deoxydehydration product. Chapter 4 will cover our investigation of alternative metals to rhenium for deoxydehydration and detail the results of screening oxide supported tungstate, vanadate, molybdate, and manganese catalysts.

CHAPTER 2

INVESTIGATION OF SUPPORTED OXO-RHENIUM CATALYSTS FOR DEOXYDEHYDRATION

2.1. Introduction

The substrates of interest for deoxydehydration are primarily biomass-derived polyols. Due to the high oxygen content of these feeds, often in a 1:1 carbon-to-oxygen ratio, they tend to be relatively large polar molecules. In order to facilitate the reaction, it becomes necessary to dissolve the substrates in a solvent for a liquid phase reaction. Homogeneous catalysts, such as the methyltrioxorhenium tested by Cook and Andrews[4] are difficult to recover once they become dissolved in the solution. Further, this homogeneous rhenium is prone to form long oligomers which will foul the side of the reaction vessel and is also difficult to recover the catalyst in this form. Denning et al.[39] tested the first supported rhenium catalyst using activated carbon as a support; however, this catalyst was found to deactivate on repeated runs.

The strategy we chose to pursue was to screen oxide supports, which are more polar than the previously tested carbon support, to anchor rhenium species. The supports were classical oxides well known in heterogeneous catalysis, specifically titania, zirconia, alumina, silica, and iron oxide. A key advantage of these oxide supports is that they are relatively inexpensive, are used extensively in industry, and a support with a surface oxo-metal species can be synthesized relatively simply using incipient wetness impregnation. This synthesis technique involves dissolving a precursor of the desired species in a volume of water corresponding to the pore volume of the support. This precursor solution can then be added to the pre-dried support producing a paste. This technique is enough to give relatively good dispersion of the surface species as it is dispersed across the surface by the capillary action of the water. This paste is then dried, followed by a calcination, which is a heat treatment in the presence of air. The calcination process is to attempt to bond the surface

species to the support, and possibly remove any undesired component of the precursor. For example, ammonium salt precursors are convenient as the ammonium counterion is easily removed by decomposition-combustion during the calcination process. Characterization of the support surface area was important to decide on a rational loading of the active species, which would ideally be less than the monolayer coverage with the goal of producing a mono-dispersed active species.

These supported catalysts were characterized by UV-Vis and FTIR spectroscopy to probe the nature of the supported rhenium species. The supports were tested for catalytic activity, either for deoxydehydration or a side reaction. The oxide-supported rhenium catalysts were also tested for catalytic activity and selectivity in comparison to the homogeneous catalysts such as methyltrioxorhenium. Screening reaction conditions were chosen to be similar to those used by Cook and Andrews[4] to give a good basis of comparison to previous results in homogeneous DODH catalysis literature.

2.2. Materials and Methods

2.2.1. Catalyst Preparation and Characterization

A variety of catalysts were prepared by incipient wetness impregnation of ammonium perrhenate (Sigma Aldrich) onto P25 TiO_2 (Sigma Aldrich), fumed SiO_2 (Evonik Aerosil 150), ZrO_2 (MEL Chemicals, G2 hydrous zirconia), α-Fe_2O_3 (US Research Nanomaterials, Inc), and γ-Al_2O_3 (Alfa Aesar) at 4 wt% rhenium and subsequent calcination. The zirconia was from a hydrous zirconia precursor (G2 hydrous zirconia, MEL Chemicals). If listed, ZrOH indicates that the hydrous zirconia was used, ZrO_x or ZrO_2 indicates that the hydrous zirconia was pre-calcined at 550 °C for 2 h, prior support impregnation. The supports were pre-dried in a muffle furnace at 115 °C for at least 8 h. Ammonium perrhenate was dissolved in an amount of deionized water corresponding to the pore volume of the pre-dried support to produce a 4 wt% rhenium catalyst (0.5-1.5 mL per 1000 mg of support). The impregnated support was dried in a muffle furnace at 115 °C for at least 8 h followed by calcination in a tube furnace at 420 °C for 4 h. The relatively

mild calcination conditions were selected to mitigate loss of rhenium through formation and sublimation of the highly volatile Re_2O_7 species.

Support and catalyst surface areas were determined by N_2 adsorption and BET analysis using an Autosorb iQ2 (Quantachrome instruments). The catalysts were pre-treated in vacuum for 12 h at a temperature of 300 °C, isotherms were measured at 77 K.

The catalysts and supports were spectroscopically characterized using diffuse reflectance FTIR and UV-Vis spectroscopy using a Harrick Praying Mantis Accessory with a 1 cm diameter sampling cup. FTIR spectroscopy was performed using a Perkin Elmer Spectrum 100 spectrometer. UV-Vis spectroscopy was performed using a Perkin Elmer Lambda 950 UV-Vis-NIR spectrometer.

2.2.2. Reaction Procedure

For the initial catalytic screening, benzene (Sigma Aldrich, anhydrous) and toluene (Sigma Aldrich, anhydrous) were selected as a non-polar solvents which should not induce solubility of the perrhenate. A non-polar solvent is also desirable as Morris et al.[40] suggests the more polar solvents reduce catalytic activity by coordinating with the active species. 1,2-Decanediol (Sigma Aldrich, 98%) was chosen as a soluble and easily quantifiable reductant which gives an expected product of 1-decene. Triphenylphosphine (Sigma Aldrich) was used as reductant for its solubility in non-polar solvent, easy quantification by GC-FID, and 1:1 stoichiometric consumption with the diol in deoxydehydration.

Catalytic test reactions were carried out in a 15 mL glass pressure tube rated at 150 psig (Ace Glass) equipped with a Teflon-coated stir bar. Since the reactions are conducted above the boiling point of the solvents at autogeneous pressure, care must be taken that the mixture´s vapor pressure does not exceed the rating of the vessel at the reaction temperature. The glass reactor was heated in a silicone oil bath with a magnetic stirrer (IKA hot plate). The reported temperature is

from a K-type thermocouple that was placed into the glass reactor's thermowell and read by a MicroDAQ thermometer. Post reaction in the standard procedure, the reactor was cooled in a room temperature water bath. The catalyst and reaction solution were separated either at room temperature by centrifugation (10 min at 1500 rpm).

2.2.3. Post Reaction Analysis

The composition of the reaction mixture was quantitatively analyzed by using an Agilent 7890B GC with an Agilent HP-5 column (30 m, 0.320 mm diameter, 025 μm film) and flame ionization detection. Retention times and response factors were determined with the help of standards. Diol conversion was calculated from measured final concentration and the initial concentration of diol known from preparation of stock solution of solvent, diol, and internal standard. Yields are based on the initial diol concentration. Reductant consumption is based on the yield of triphenylphosphine oxide.

Error bars indicate 3 experimental replicates from independent test reactions under the same conditions for both GC-FID and ICP-MS measurements; error is reported as the mean ± 1 standard deviation.

Side products of the reaction were characterized using gas chromatography with detection by mass spectroscopy (GC-MS), using an Agilent 7890B GC with an Agilent HP-5 column (30 m, 0.320 mm diameter, 0.25 μm film) which fed into an Agilent 5977A MSD mass spectrometer. Fragmentation patterns were characterized against the NIST library.

2.3. Supported Oxo-Rhenium Catalyst Characterization

Oxide-supported rhenium catalysts using SiO_2, TiO_2, α-Fe_2O_3, ZrO_2, and γ-Al_2O_3 were prepared using incipient wetness impregnation using ammonium perrhenate as the rhenium precursor. Catalyst rhenium loading, as determined by the amount of rhenium added in the incipient wetness preparation, and support and catalyst surface area, as measured by BET absorption isotherms, are shown in Table 2.1.

Table 2.1: Oxide-supported rhenium catalyst loading and surface area measurements.

Catalyst	Rhenium Content (wt%)	Support BET Surface Area (m^2/g)	Catalyst BET Surface Area (m^2/g)
ReO_x/TiO_2	4.09	53.2	51.5
ReO_x/ZrO_2	4.09	99.5	87.6
ReO_x/SiO_2	3.90	300[a]	204
ReO_x/Fe_2O_3	4.24	42.7	45
ReO_x/Al_2O_3	4.30	151.6	122.5

[a] Manufacturer's information

The catalysts, the supports, and the rhenium precursor were also characterized by diffuse reflectance UV-Vis spectroscopy, and diffuse reflectance FTIR in order to characterize the supported rhenium species.

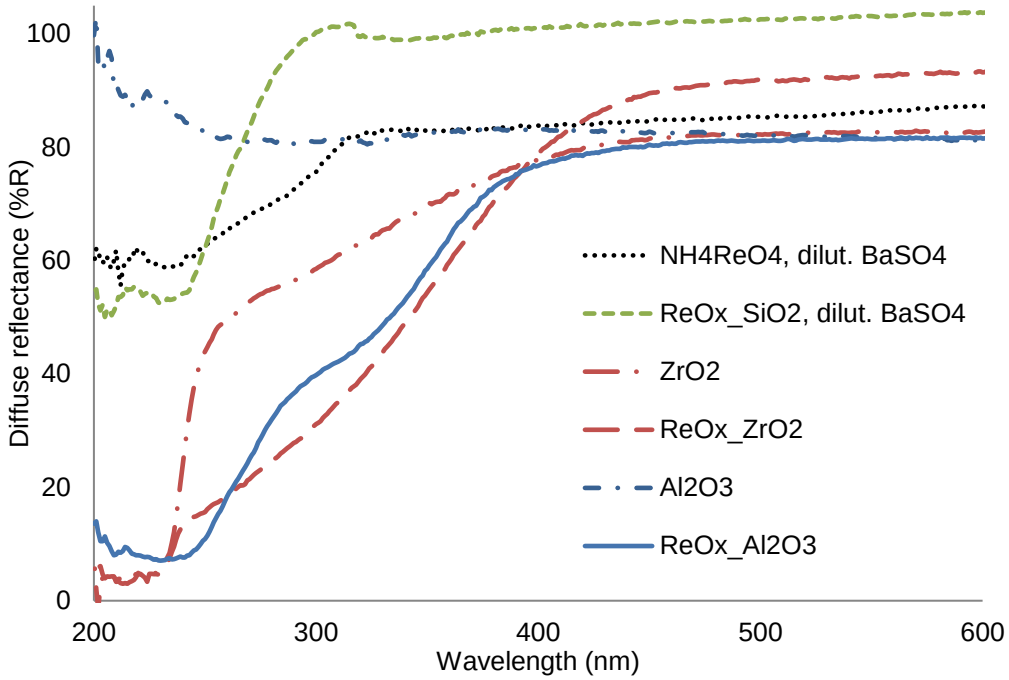

Figure 2.1: Diffuse reflectance UV-Vis spectra collected of supported rhenium catalysts and supports.

From the UV-Vis spectra of catalysts and supports seen in Figure 2.1, we observe the ligand-to-metal charge transfer band of ReO_4^- at 233 nm. The spectra from the TiO_2 and α-Fe_2O_3 supports and supported catalysts are not pictured as the strong absorption of the supports obscures possible ReO_x species absorption bands. Zirconia also absorbs strongly at around 240 nm. The perrhenate band is observed for ReO_x/SiO_2 with an absence of other major bands, indicating weak interaction with support. The perrhenate band is slightly shifted to longer wavelengths for ReO_x/Al_2O_3, with an additional band present around 320 nm, indicating a support effect. The zirconia-supported catalysts demonstrate broad absorption from 250 to 500 nm for ReO_x/ZrO_2 which may also be indicative of rhenium-support interaction.

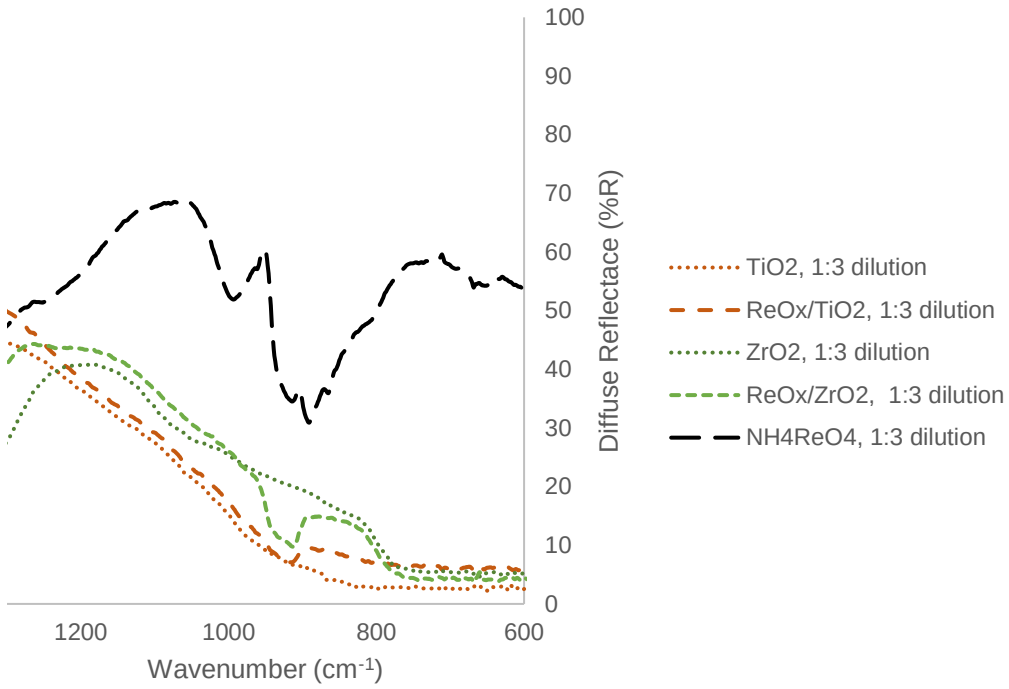

Figure 2.2: Diffuse reflectance FTIR spectra collected of the ammonium perrhenate precursor, TiO_2 support, ReO_x/TiO_2, ZrO_2 support, and ReO_x/ZrO_2 catalysts diluted by a 3 to 1 ratio in KBr.

Diffuse reflectance FTIR spectra were measured for the ammonium perrhenate precursor as well as all the supports (TiO_2, ZrO_2, Al_2O_3, Fe_2O_3, and SiO_2) and all the prepared oxide-supported rhenium catalysts after diluting with 3 times as much KBr by weight and pre-drying in a muffle furnace at 115 °C prior to measuring. The $\nu_{as}(Re(=O)_3)$ bands of the supported rhenium species are Raman active. Raman spectra for these catalysts were not measured, however band assignments reported by Lee and Wachs[41,42] are 977 cm^{-1} for SiO_2, 975 cm^{-1} for TiO_2, and 941 cm^{-1} for ZrO_2. We observe IR active bands for ReO_x/TiO_2 and ReO_x/ZrO_2, as seen in Figure 2.2, around 911 cm^{-1} which correspond with the 920 cm^{-1} and 906 cm^{-1} bands reported by Lee and Wachs for the rhenium/support oxygen bridging bonds ν_s(Ti-O-Re) and ν_s(Zr-O-Re), which suggests a bond formation between the surface rhenium species and the support.

2.4. Catalyst Activity

2.4.1. Control Reactions

In order to assess the effectiveness of our supported catalysts, a set of control reactions were run to test the support for catalytic activity, solvent effects, and for detectable side reactions catalyzed by either the supports or supported rhenium catalysts.

2.4.1.1. Support Reactivity

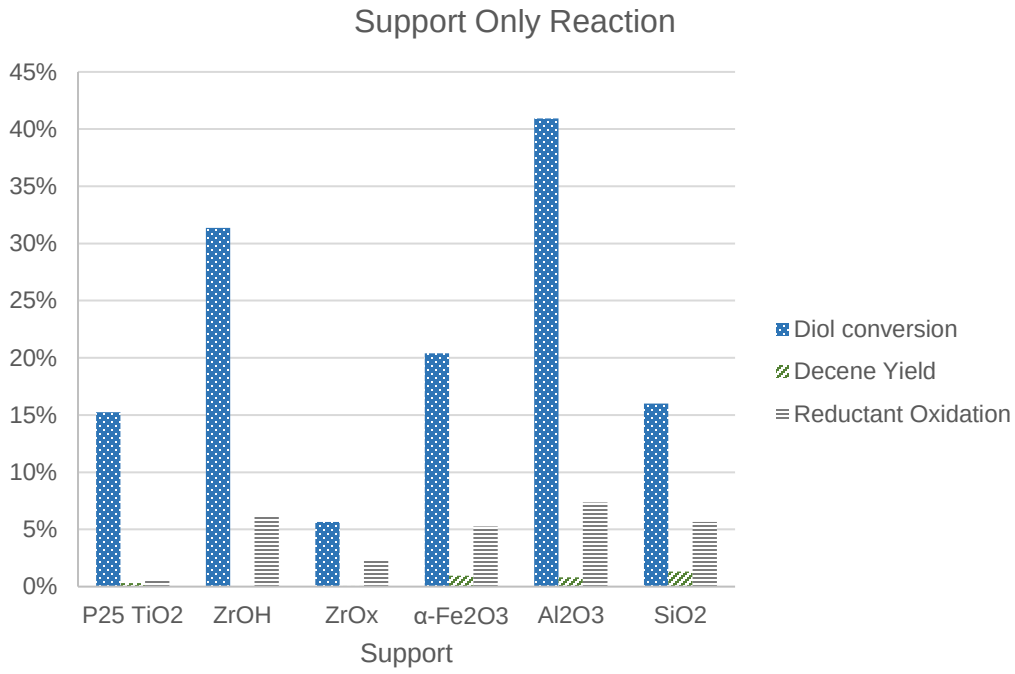

Figure 2.3: Support reactivity, Reaction conditions: Temp. 165 °C, time 20 h, solvent benzene, 0.2 M 1,2-decanediol, 0.23 M PPh_3.

In order to test whether any of the supports were active in catalyzing deoxydehydration, we pre-dried the support for 12 h at 115 °C in a muffle furnace prior to reaction at long time and high temperature to test for any support catalytic activity at relevant temperatures (Figure 2.3). For all supports, total decene yield was under 2% with no other major side products observed. The 1,2-decanediol disappearance is attributable to diol adsorption on the support.

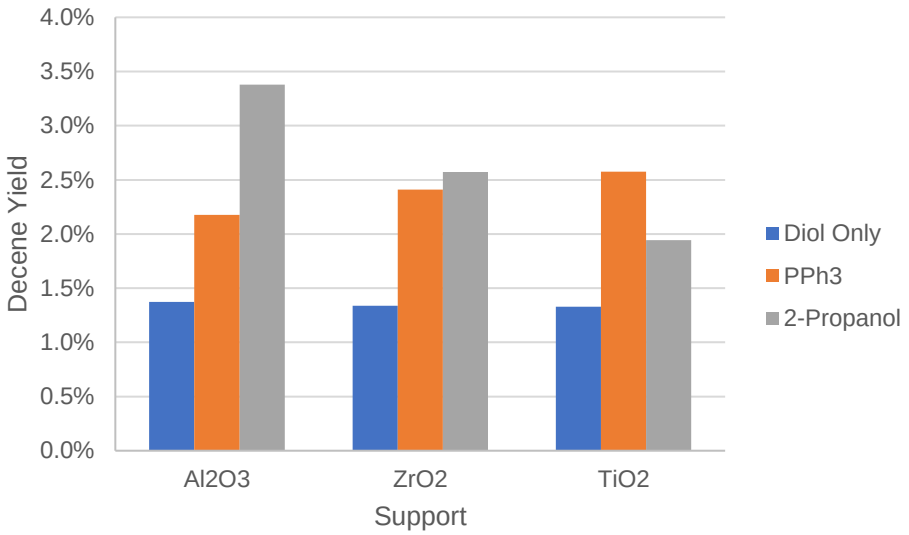

Figure 2.4: Support only reactivity vs reductant. Reaction conditions: Temp. 150 °C, time 20 h, solvent benzene, 0.2 M 1,2-decanediol, 0.23 M PPh_3.

2.4.1.2. Solvent Effect

Benzene was initially selected as a solvent for comparability to previous work undertaken by Cook and Andrews,[4] the Nicholas group[11] and the Jentoft group;[23] however, we wanted to switch to alternative solvents such as toluene and *p*-xylene as they have a lower vapor pressure and pose lower health risks. The reactivity of ammonium perrhenate for DODH was tested for the 3 solvents, as shown in Figure 2.5. Using toluene and *p*-xylene lowered activity indicating lowered activity due to lower solubility of the catalyst, or a deleterious effect associated with the bulkier solvent molecules. Based on weighing safety vs reactivity, toluene was used extensively in subsequent experiments, while *p*-xylene was not due to the very low catalyst activity. Morris et al.[40] tested rhenium catalyst activity in a variety of solvents, including benzene, chloroform, tetrahydrofuran, acetonitrile, and pyridine. They reported much higher activities with the less polar benzene and chloroform in relation to the more polar tetrahydrofuran, acetonitrile, and pyridine. The lower activity was attributed to the more polar solvents coordinating with the rhenium species, inhibiting activity.

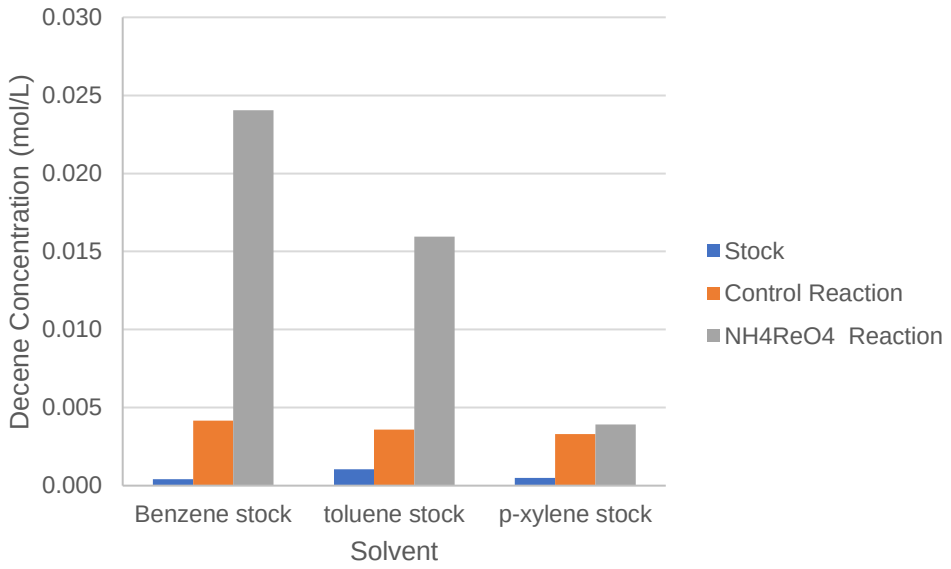

Figure 2.5: Solvent effect on 1,2-decanediol deoxydehydration. Reaction conditions: temp. 150 °C, time 20 h, solvent benzene, 0.2 M 1,2-decanediol, 0.23 M PPh_3.

2.4.1.3. Double Bond Isomerization

Initial rhenium reactivity experiments were conducted at 180 °C for 24 h in benzene solvent with triphenylphosphine reductant. These conditions were well beyond 100% diol conversion, and time and temperature were reduced to test catalyst activity. At the elevated temperature additional GC-peaks were observed near the 1-decene peak. Using GC-MS, it was determined that these were 1-decene isomers with internal double bonds suggesting that the rhenium catalysts are capable of catalyzing double bond migration, however, when reaction temperatures were lowered to 150 °C, no internal olefins were observed. Since terminal olefins are more valuable than internal olefins, suppressing double bond isomerization is important.

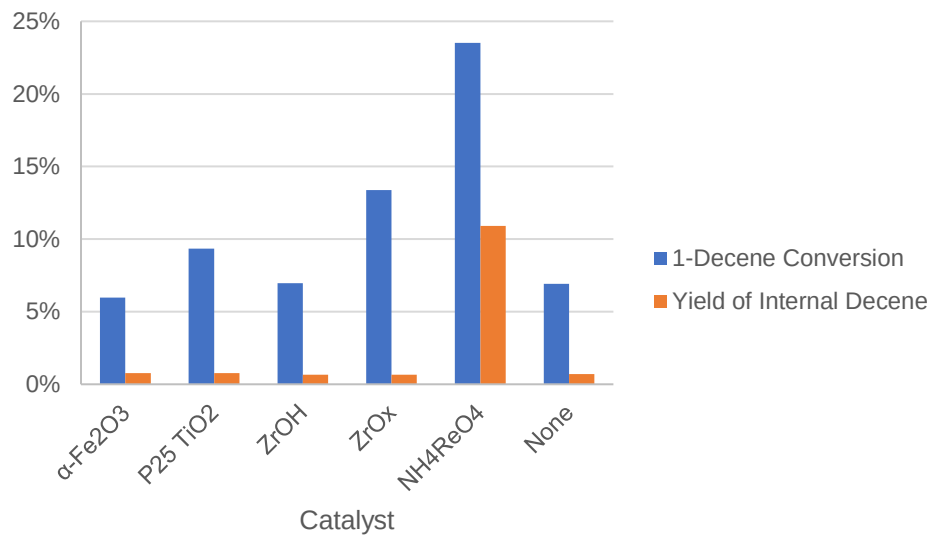

Figure 2.6: Double bond isomerization. Reaction conditions: temp. 165 °C, time 20 h, solvent benzene, 0.2 M 1-decene, 0.23 M PPh_3.

2.4.1.4. Solubility Effect for Homogeneous Catalysts

From the test of ammonium perrhenate deoxydehydration activity in a variety of solvents in Figure 2.5, we see that the reactivity for the homogeneous catalyst is highly dependent on the solvent. A possible explanation is that the variation of solubility of the homogeneous ammonium perrhenate catalyst in each solvent is a large driver in the catalyst activity.

To test whether the kinetics of dissolving the homogeneous catalyst in the solvent is a major driver in catalyst activity, we tested the ammonium perrhenate catalyst activity as received versus the effect of grinding the catalyst, thereby increasing surface area to speed up the dissolution; and to test whether exposure to the diol in the solution prior to the reaction can dissolve the catalyst to make it more active, the ammonium perrhenate was mixed with the diol and solvent and held at reaction temperature for 30 minutes prior to the introduction of the triphenylphosphine reductant.

Table 2.2: Ammonium perrhenate reactivity with 0.23 M triphenylphosphine reductant in toluene solvent with and without pre-grinding treatment and pre-mixing with diol and solvent.

Catalyst	Temp (°C)	Time (h)	Pre-ground Catalyst	Pre-reaction Diol Mixture	Activity (mol alkene)(mol Re)$^{-1}$h^{-1}
NH_4ReO_4	150	0.5	No	No	0.9
NH_4ReO_4	150	0.5	Yes	No	9.6
NH_4ReO_4	150	0.5	No	Yes	6.7
NH_4ReO_4	150	0.5	Yes	Yes	12.1

From Table 2.2, we see that both pre-grinding the catalyst, and pre-mixing the catalyst with the diol solution greatly increase the catalytic activity of the ammonium perrhenate, with the application of both pre-treatments producing the most active catalyst. This demonstrates that fully dissolving the catalyst is important for producing the most active form of the catalyst. This also means that when comparing the activity of homogeneous catalysts for deoxydehydration, there are additional factors that will affect relative catalyst activity, including the crystal size of the catalyst, and solvent and diol choice. The poor solubility of the ammonium perrhenate explains the relatively low activity of the ammonium perrhenate in subsequent experiments, and makes the more soluble methyltrioxorhenium a better benchmark in terms of the activity of homogeneous deoxydehydration catalysts.

2.4.2. Supported Rhenium Catalyst Activity

2.4.2.1. Triphenylphosphine Reductants

As seen in Figure 2.7, all supported rhenium catalysts were highly selective towards decene, the expected DODH reaction product. However, we see a strong relationship between the support used and catalyst activity. While the most active SiO_2 and TiO_2 supported catalysts demonstrated activity at least on par with methyltrioxorhenium, the homogeneous catalyst benchmark, the Al_2O_3, Fe_2O_3 and ZrO_2 catalysts were considerably less active. This support effect may be due to stronger interaction between the support and the perrhenate catalyst, which will be discussed further in Chapter 3.

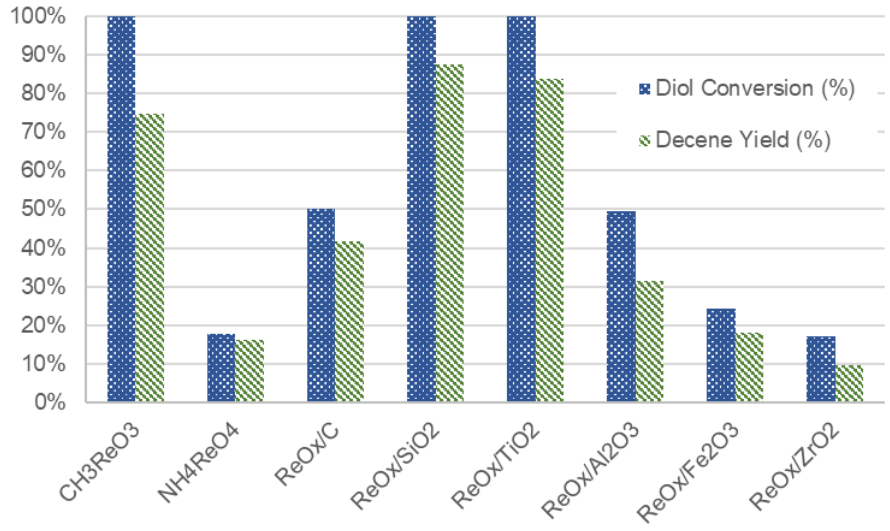

Figure 2.7: Reactivity of supported rhenium catalysts as compared to homogeneous benchmarks, methyltrioxorhenium and ammonium perrhenate. Reaction conditions: Temp. 150 °C, time 40 min, solvent benzene, 0.2 M 1,2-decanediol, 0.23 M PPh_3.

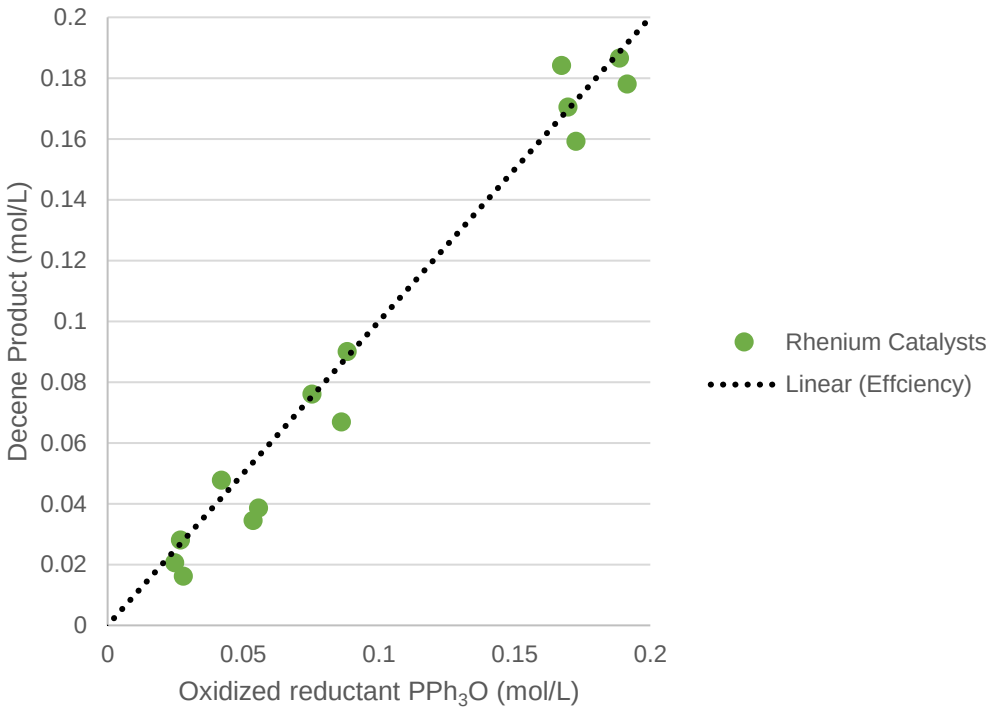

Figure 2.8 Reductant efficiency, molecules of decene produced per triphenylphosphine reductant consumed.

As seen in Figure 2.8, the triphenylphosphine reductant was also consumed very efficiently with a near 1:1 consumption of triphenylphosphine and production of 1-decene. The high decene selectivity along with efficient reductant use validate the deoxydehydration reaction scheme (Scheme 1.1)

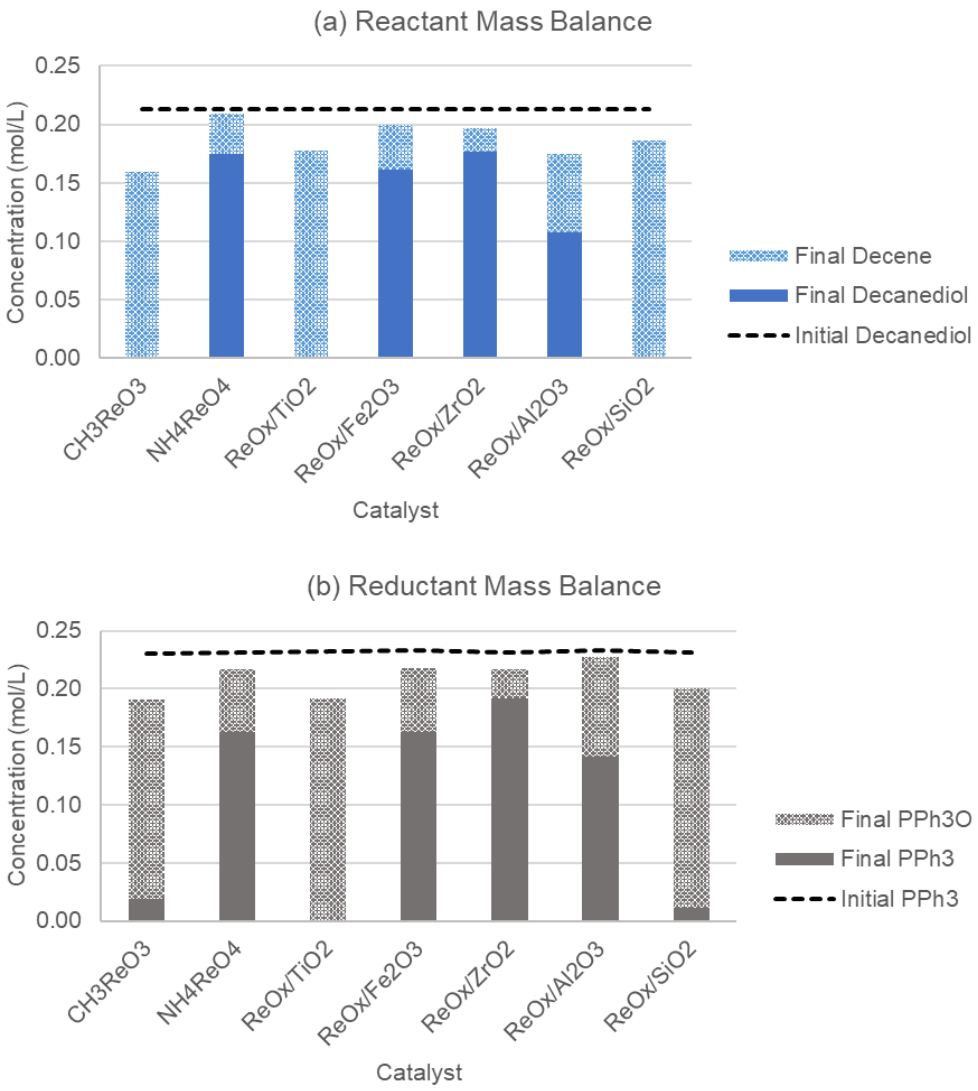

Figure 2.9 Mass balance of diol reactant and decene product (a) and reductant and oxidized reductant (b) for the rhenium catalysts. Reaction conditions: Temp. 150 °C, time 40 min, solvent benzene, 0.2 M 1,2-decanediol, 0.23 M PPh_3, diol:Re=20.

Figure 2.9 shows the mass balance for the 1,2-decanediol (a) and triphenylphosphine (b) and their DODH products observed for the rhenium catalyst reactions given in Figure 2.7. We see that most of the 1,2-decanediol and triphenylphosphine is accounted for in most reactions, however the discrepancy can be as high as 25% of the initial diol and 20% of the initial triphenylphosphine. No unexplained GC peaks were observed for these reactions, so the discrepancy is likely primarily

due to adsorption on the support (e.g. Al_2O_3) or precipitate in the case of homogeneous catalysts, or possibly the formation of heavy compounds not observed by GC-FID.

Table 2.3: Supported rhenium catalyst activity using triphenylphosphine reductant. Reaction conditions: Temp. 150 °C, time 40 min, solvent toluene, 0.2 M 1,2-decanediol, 0.23 M PPh_3, Diol:Re=20.

Catalyst	Diol Conversion (%)	Alkene Yield (%)	Selectivity (%)	Activity (mol alkene)(mol Re)$^{-1}h^{-1}$
CH_3ReO_3	99.8	74.7	74.9	24.4
NH_4ReO_4	17.8	16.2	90.8	5.1
ReO_x/TiO_2	100.0	83.6	83.6	27.7
ReO_x/Fe_2O_3	24.3	18.1	74.5	6.0
ReO_x/ZrO_2	17.1	9.7	56.7	3.5
ReO_x/Al_2O_3	49.4	31.4	63.6	10.4
ReO_x/SiO_2	100.0	87.6	87.6	31.0

We find that these supported perrhenate-based catalyst are active and selective for deoxydehydration. The most active TiO_2 and SiO_2 supported catalysts exhibit turnover frequencies of 27.2 and 30.5 (mol decene)(mol Re)$^{-1}h^{-1}$, which is comparable to our benchmark homogeneous methyltrioxorhenium catalyst with a turnover frequency of 24 (mol decene)(mol Re)$^{-1}h^{-1}$ and ammonium perrhenate at 0.9 (mol decene)(mol Re)$^{-1}h^{-1}$. However, after these reactions, we observe a color change in the reaction supernatants for both supported and homogeneous catalysts, which seemed to indicate the presence of leached species. The color change was often the most severe for the ReO_x/TiO_2 and ReO_x/SiO_2, perhaps indicating that the high activity arises from easy dissolution of the rhenium due to weak support interaction and high dispersion on the support. Further discussion of catalyst stability and leaching will be covered in Chapter 3, including spectroscopic characterization of supernatants.

2.4.2.2. Secondary Alcohol Reductants

Secondary alcohols have also been reported as effective reductants for DODH.[43] The activity of the titania and zirconia-supported rhenium catalysts was tested for activity using 2-propanol and 3-octanol as both the solvent and reductant for deoxydehydration, as seen in Table 2.4.

Table 2.4: Rhenium catalyst activity with secondary alcohol reductants. Reaction Conditions: 150 °C, the listed secondary alcohol was used as the solvent, 0.23 M of the diol was added, diol:Re=20.

Catalyst	Time (min)	Reductant	Reactant	Alkene Yield (%)	Activity (mol alkene)(mol Metal)$^{-1}$h^{-1}
NH_4ReO_4	40	2-Propanol	1,2-decanediol	13	4.0
ReO_x/TiO_2	30	2-Propanol	1,2-decanediol	1	0.6
ReO_x/ZrO_2	60	2-Propanol	1,2-decanediol	2	0.6
ReO_x/TiO_2	30	2-Propanol	1,2-hexanediol	6	4.4
ReO_x/ZrO_2	60	2-Propanol	1,2-hexanediol	6	2.3
NH_4ReO_4	40	3-Octanol	1,2-decanediol	11	3.2
ReO_x/TiO_2	20	3-Octanol	1,2-decanediol	27	26.8
ReO_x/ZrO_2	60	3-Octanol	1,2-decanediol	26	8.3
ReO_x/TiO_2	20	3-Octanol	1,2-hexanediol	5	5.3
ReO_x/ZrO_2	60	3-Octanol	1,2-hexanediol	7	2.3

As seen in Table 2.4, secondary alcohol reductants were less active than triphenylphosphine. In the literature, higher temperatures are usually selected possibly indicating a higher energy barrier for the reduction step,[24,43] or inhibited activity due to the higher solvent polarity.[40]

2.5. Conclusions

Oxide supports were tested as a strategy of anchoring an oxo-rhenium species to create a heterogeneous deoxydehydration catalyst. As supported catalysts for deoxydehydration was a new field in the beginning of our investigation, with the first supported catalyst being demonstrated in 2013,[23] we verified that the tested oxide supports, silica, alumina, zirconia, and titania did not

catalyze any significant side reactions and thus were viable as supports. It was found that significant amounts of diol could be adsorbed on the oxide supports, which can make it difficult to close the mass balance for the diol reactant, however at high conversion, high yields and selectivities of the alkene product are observed, indicating that support adsorbed diol could subsequently be converted. The oxide-supported rhenium catalysts were found to be active and selective with the expected stoichiometric conversion of the reactant and reductant. The activity of the supported catalyst varied widely depending on the support. Titania- and silica-supported catalysts demonstrated activities on par with the homogeneous benchmark, methyltrioxorhenium. Investigation into the stability of these catalysts over multiple runs will be covered in Chapter 3.

CHAPTER 3

CATALYST DEACTIVATION AND LEACHING BEHAVIOR OF OXIDE-SUPPORTED RHENIUM CATALYSTS IN DEOXYDEHYDRATION

3.1. Introduction

In Chapter 2, we observed that supported rhenium catalysts were highly active for deoxydehydration, though the reactivity was highly variable depending on the support. It was also noted that the separated reaction supernatant was discolored, possibly indicating the presence of a soluble rhenium species. In previous literature, deactivation over multiple runs through leaching was noted to be an issue.[23] In developing a heterogeneous catalyst, especially when using a valuable metal like rhenium, catalyst stability is paramount, so an effort was made to study supported rhenium catalyst stability and leaching behavior. In this chapter we will explore how the leaching behavior of the oxide-supported rhenium catalysts depend on choice of support in section 3.2, how the reaction conditions effect leaching behavior in section 3.3, discuss possible leaching mitigation strategies in section 3.4, and finally review preliminary exploration in using microporous supports to inhibit leaching in section 3.5.

3.2. Experimental Methods

Catalyst preparation and characterization and reaction procedure were carried out as described in Chapter 2. For testing solubility effects and catalytic performance, a range of diol reactants, solvents, and reductants were employed. The diol reactants were 1,2-decanediol (Sigma Aldrich) and 1,2-hexanediol (Sigma Aldrich). The solvents used were benzene (Sigma Aldrich, anhydrous), toluene (Sigma Aldrich, anhydrous), 1,4-dioxane (Sigma Aldrich, anhydrous), 3-octanol (Sigma Aldrich, 99%), and 2-propanol (Sigma Aldrich, anhydrous 99.5%). Triphenylphosphine (Sigma Aldrich) was the default reductant. Triphenylphosphine oxide (Sigma Aldrich) was used for calibration to quantify reductant oxidation. Some reactions were performed

without a reductant, or with a secondary alcohol reductant, or with a secondary alcohol solvent. *n*-hexadecane was added as an internal standard for GC-FID analysis.

The amount of leached rhenium was quantified by ICP-MS. The ICP-MS samples were prepared by drying 0.1 mL of reaction supernatant to remove the solvent. The leftover solid was then digested in 5 mL of 5 wt % HNO_3 for 12 h at a temperature of 80 °C. Then a 0.2 mL aliquot of the digestion solution was filled up to 10 mL with additional 5 wt % HNO_3 for a total dilution factor of 2500x. The rhenium content of these solutions was measured by a Perkin Elmer NexION350D ICP-MS. A higher concentration standard solution was used to create 7 rhenium calibration standards between 0.1 and 500 ppb. The dilution factor was used to back-calculate the concentration of leached rhenium in the reaction solution.

The standard reaction volume was 5 mL containing 0.20 M of diol, 0.23 M of triphenylphosphine (*i.e.*, a slight excess of reductant), 0.10 M of *n*-hexadecane, and catalyst corresponding to an equivalent of 0.01 M of rhenium and a diol-to-rhenium molar ratio of 20:1.

In order to characterize leaching at the elevated reaction temperatures, hot filtration was performed to separate the reaction liquids from the solid catalyst at reaction temperature. The filtration was performed using a filter disk (porosity 10-20 μm). Since reactions were carried out at temperatures above the normal boiling point of the solvent, the filter disk was connected to the reactor top via a valve, such that immediate filtration at reaction temperature became possible.

The post reaction solution was also characterized by UV-Vis transmission spectroscopy and EPR to characterize the solubilized rhenium. UV-visible transmission spectra of reaction supernatants were measured using a PerkinElmer Lambda 900 UV-vis-NIR spectrometer. The supernatant solution was diluted with excess solvent one in three parts by volume. The solutions were placed in 1 cm quartz cuvettes, and the pure solvent served as a reference. EPR spectra of reaction supernatants were collected at room temperature in 4 mm quartz EPR tubes (Wilmead-Glass) using a Bruker Elexsys E-500 EPR with ER 4105DR cavity.

Error bars indicate 3 experimental replicates from independent test reactions under the same conditions for both GC-FID and ICP-MS measurements; error is reported as the mean ± 1 standard deviation.

3.3. Catalytic and Solubility Experiments

All oxide-supported catalysts were screened for their activity in decanediol DODH. Homogeneous catalysis with methyltrioxorhenium and heterogeneous catalysis with previously reported ReO_x/C were used for benchmarking. Since the catalysts differed significantly in their activity, an average rate of 1-decene formation was determined at comparable conversions (within ± 10%) to eliminate any reaction order-related rate effects. The most active supported catalysts, ReO_x/TiO_2 and ReO_x/SiO_2 were found to have turnover frequencies to 1-decene (mol decene per mol rhenium and hour) similar to homogeneous methyltrioxorhenium on a per rhenium basis, that is, 27.3 h^{-1} for ReO_x/TiO_2, 30.3^{-1} for ReO_x/SiO_2 as compared to 24.0 h^{-1} for methyltrioxorhenium. Re/C was also highly active as previously observed,[23] whereas all other oxide-supported catalysts were less active (Figure 3.1a). For a given catalyst, selectivity to the alkene product was largely invariant to diol conversion, between about 80-90% for ReO_x/TiO_2 and ReO_x/SiO_2. Consistently, the amount of triphenylphosphine oxide formed was proportional to the amount of decene with little deviation.

The solid catalysts were recovered and re-tested repeatedly with fresh reaction mixtures to monitor stability over multiple uses. The development of the DODH performance over five batch reactions is shown in Figurea, normalized to total catalyst mass, as the rhenium content becomes unknown after the first use. Because of the decreasing amount of catalyst in these experiments, the uncertainty in the rate increases during later uses.

The initially most active catalysts, ReO_x/SiO_2, ReO_x/TiO_2, and ReO_x/C, deactivated considerably even after a single use. In contrast, the initially less active catalysts, ReO_x/ZrO_2, ReO_x/Fe_2O_3, and ReO_x/Al_2O_3, were more stable. ReO_x/ZrO_2, ReO_x/Fe_2O_3 even consistently

demonstrated a slightly higher activity in the second run in comparison to the first use. In order to investigate the cause for deactivation, the quantity of leached rhenium was determined by ICP-MS. The results in Figure 3.1b indicate a strong correlation between the leached rhenium and both the activity of the catalyst for a given run, and loss in activity observed in subsequent runs. The first correlation suggests that solubilized rhenium species contribute to the observed DODH activity.

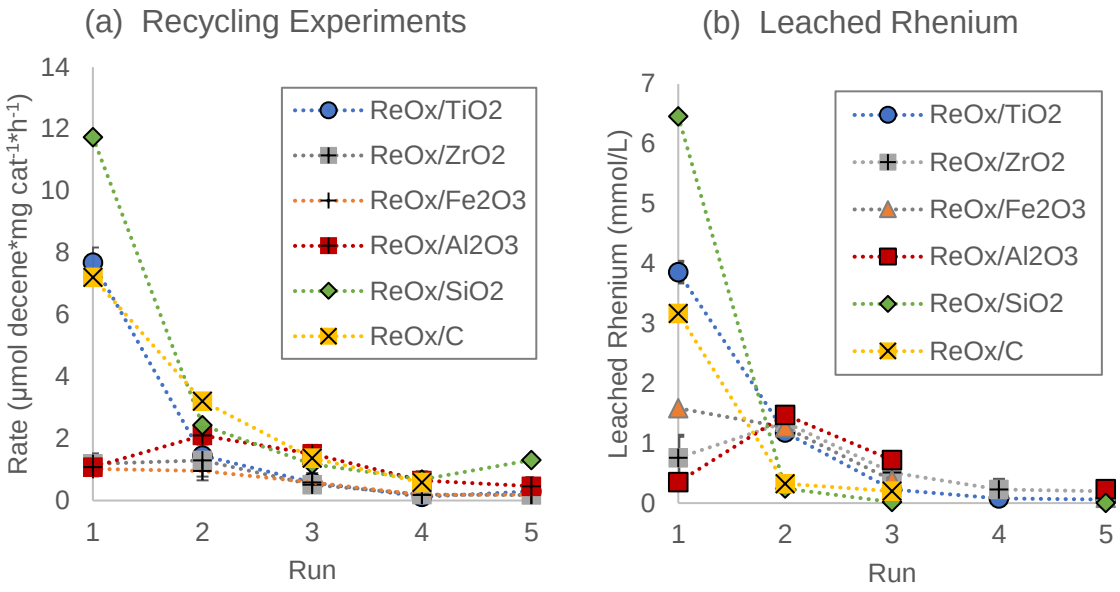

Figure 3.1: (a) Catalysts activity over multiple uses, (b) Leached rhenium concentration as measured by ICP-MS over the 5 recycle runs of (a). Reaction conditions: temp. 150 °C, time 15-40 min (40-60% diol conversion), solvent toluene, 0.2 M 1,2-decanediol, 0.23 M PPh_3, diol:Re=20.

The amount of rhenium leached was measured for each of the repeat runs, and the cumulative amount of rhenium leached into the reaction solution by the supported catalysts was calculated. By normalizing the amount of rhenium lost to the total initial rhenium content on the catalyst from the incipient wetness impregnation, the fraction of rhenium lost by run was obtained, as seen in Figure 3.2. The ReO_x/SiO_2 catalyst, which deactivated most quickly, lost most of its rhenium to the reaction solution in the first run. The other catalysts leached more gradually, with ReO_x/TiO_2 losing about 80% of its rhenium content after 5 runs, while the other oxide-supported catalysts lost about 50% of their rhenium content after 5 runs.

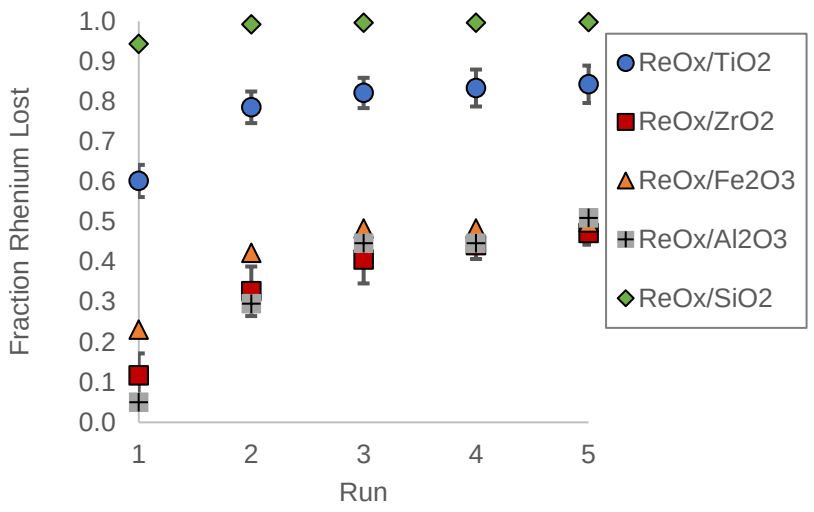

Figure 3.2: Fraction of rhenium leached over several recycle runs. Reaction conditions: Temp. 150 °C, time 15-40 min (40-60% diol conversion), solvent toluene, 0.2 M 1,2-decanediol, 0.23 M PPh_3, diol:Re=20.

These experiments would indicate that the solubilized rhenium species may be more active, but there seem to be firmly attached rhenium species on Al_2O_3, ZrO_2, Fe_2O_3, and to a lesser extent on TiO_2. For further investigations, we chose to focus on ReO_x/TiO_2 as an active but quickly deactivating catalyst, and ReO_x/ZrO_2 as a less active but more stable catalyst.

Hot filtration tests were performed for ReO_x/TiO_2 and ReO_x/ZrO_2 catalysts to investigate whether rhenium is redeposited on the support when the reaction mixture is cooled. Figure 3.3 shows the amount of leached rhenium measured by ICP-MS for three differently obtained reaction supernatants. In all cases, the catalytic reaction was started at a temperature of 150 °C for a duration designed to achieve an intermediate conversion, which depended on the catalyst. The reaction medium was then separated from the solid by hot filtration at the reaction temperature (150 °C) or at an intermediate temperature (100 °C). Alternatively, separation was accomplished by centrifugation at room temperature. It can be seen that the separation temperature did not have a significant effect on the amount of rhenium detected in the liquid, indicating that cooling the reaction mixture does not cause precipitation or redeposition of rhenium species. This result demonstrates that the solubility of the leached rhenium complexes is not a strong function of

temperature, and measurements made after separation at ambient temperature properly represent the amount of rhenium leached under reaction conditions. Separations in this chapter (including those conducted to generate Figures 3.1 & 3.2) were thus conducted at room temperature unless otherwise indicated, because of the difficulty of separating under autogeneous pressure and recovering the catalyst from the filter disk.

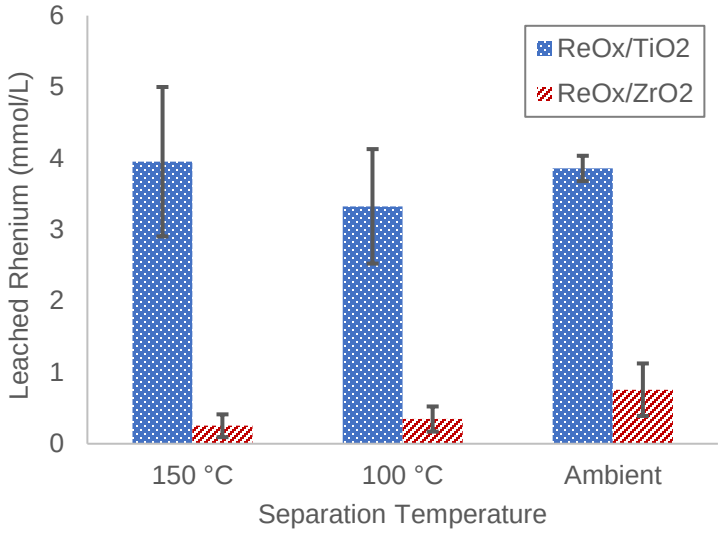

Figure 3.3: Leached rhenium vs. catalyst separation temperature. Reaction conditions: Temp. 150 °C, time 10 min ReO_x/TiO_2, 60 min ReO_x/ZrO_2 (40-60% diol conversion), solvent toluene, 0.2 M 1,2-decanediol, 0.23 M PPh_3, diol:Re=20. Separation at 150 °C performed by filtration at set reaction time; separation at 100 °C performed by filtration after reaction at 150 °C and transfer to 80 °C oil bath to cool for 5 min; separation at ambient temperature performed by centrifugation after cooling in water bath.

To test whether elevated temperatures are needed to solubilize rhenium in the first place, the amount of rhenium leached into an unheated reaction mixture was compared with that leached under reaction conditions. As seen in Figure 3.4, for ReO_x/TiO_2, the degree of leaching at room temperature was similar to that at reaction temperature. In contrast, ReO_x/ZrO_2 demonstrated almost no rhenium leaching at low temperature. These observations indicate different ReO_x-support interaction for these two catalysts. The interaction is weak between ReO_x and TiO_2, whereas it is strong between ReO_x and ZrO_2, requiring elevated temperatures to induce leaching.

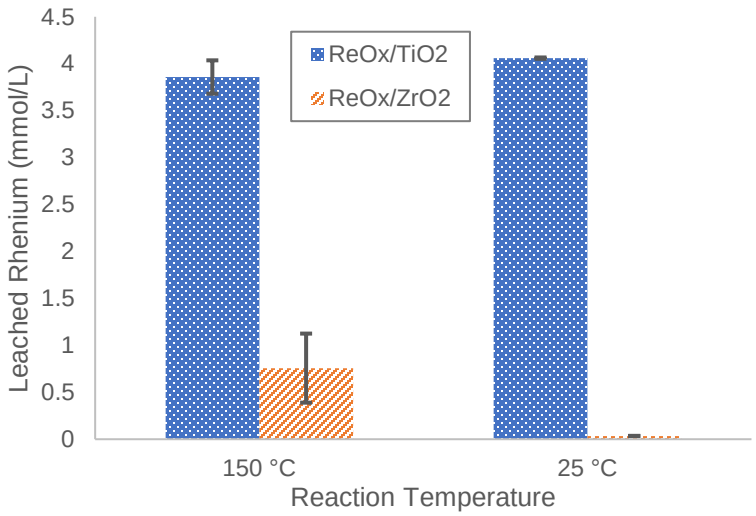

Figure 3.4: Reaction temperature vs. room temperature leaching. Reaction conditions: Temp. 150 °C, time 15 min ReO_x/TiO_2, 60 min ReO_x/ZrO_2 (40-60% diol conversion), solvent toluene, 0.2 M 1,2-decanediol, 0.23 M PPh_3, diol:Re=20.

To test the effect of loading, ReO_x/TiO_2 and ReO_x/ZrO_2 catalysts containing 1 and 2 wt % rhenium were prepared, and the rhenium leaching during reaction was compared with that of the 4 wt % rhenium catalysts (Figure 3.5). For both TiO_2 and ZrO_2 supported catalysts, the lower loadings resulted in significantly less leaching and a higher fraction of retained rhenium over several uses of the catalysts. However, the deoxydehydration rates per rhenium were not favorable, as seen in Table 3.1, suggesting that the more strongly bound rhenium species in the lower-loading catalysts tend to have lower activity for DODH and become largely inactive after several runs.

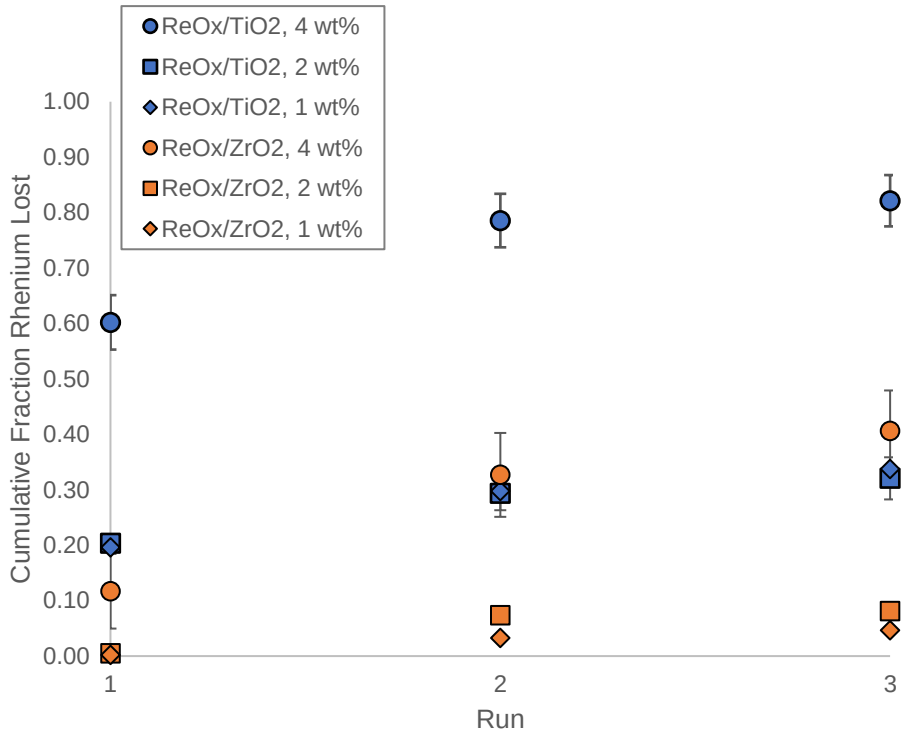

Figure 3.5: Catalyst leaching vs. loading. Reaction conditions: Temp. 150 °C, time 15-60 min, solvent toluene, 0.2 M diol, 0.23 M PPh_3, diol:Re=20.

Table 3.1: Catalytic activity of titania- and zirconia-supported catalysts with various rhenium loadings

Catalysts		Turnover frequency (mol decene)(mol Re)$^{-1}$ h^{-1} *		
Composition	Rhenium content (wt%)	Run 1	Run 2	Run 3
ReO_x/TiO_2	3.87	36.3±1.6	16.4±8.4	12.0±4.6
ReO_x/TiO_2	1.86	17.8±2.5	4.2±0.6	0.0±0.0
ReO_x/TiO_2	0.97	10.6±2.7	4.4±0.4	0.7±1.3
ReO_x/ZrO_2	3.88	5.5±1.8	7.0±2.6	3.7±3.1
ReO_x/ZrO_2	1.88	0.2±0.4	2.3±0.1	0.5±0.4
ReO_x/ZrO_2	1.02	0.0±0.0	0.8±0.1	0.0±0.0

**__Reaction conditions:__ Temp. 150 °C, time 15-60 min, solvent toluene, 0.2 M diol, 0.23 M PPh_3, diol:Re=20. Conversion <25% for 1 and 2 wt% loadings. Max. conversion for 4 wt% was 40% (ReO_x/TiO_2). Turnover frequencies referenced to rhenium content corrected for leached fraction. Uncertainties are 1 standard deviation from 3 tests.*

A series of supernatant-catalyzed reactions were performed to measure the catalytic activity of solubilized rhenium species and compare with that of solid catalysts. For a given catalyst, Figure 3.6 contains two data points (from two separate batch experiments), representing reaction progress with the solid catalyst present. Decene concentrations increased linearly with time, consistent with a constant rate of reaction and a zero-order reaction, which was also seen by Dethlefsen and Fristrup in a reaction kinetics investigation with homogeneous catalysts.[19,35] After the first reaction, the solid catalyst was removed, and only the reaction liquids were heated again to reaction temperature to monitor for additional conversion. Cumulative product formation is shown as a function of overall reaction time for these experiments, that is, the second set of data points (at longer time) for each catalyst represents the sum of initial and supernatant activity. It is expected that if there are no active solubilized species, the product yield should not further increase for the second reaction. Any increase in alkene yield indicates active solubilized species and generally contributions from homogeneous catalysis, which was evidently the case. To discriminate between heterogeneous and homogeneous catalysis contributions, cumulative product yields obtained with solid and supernatant need to be compared with that obtained with solids at the same overall reaction time. For both ReO_x/TiO_2 and ReO_x/ZrO_2 supernatants, the cumulative decene yield is below the linear trajectory seen for the solid catalysts, indicating a large portion of the catalytic activity comes from soluble species, but not all.

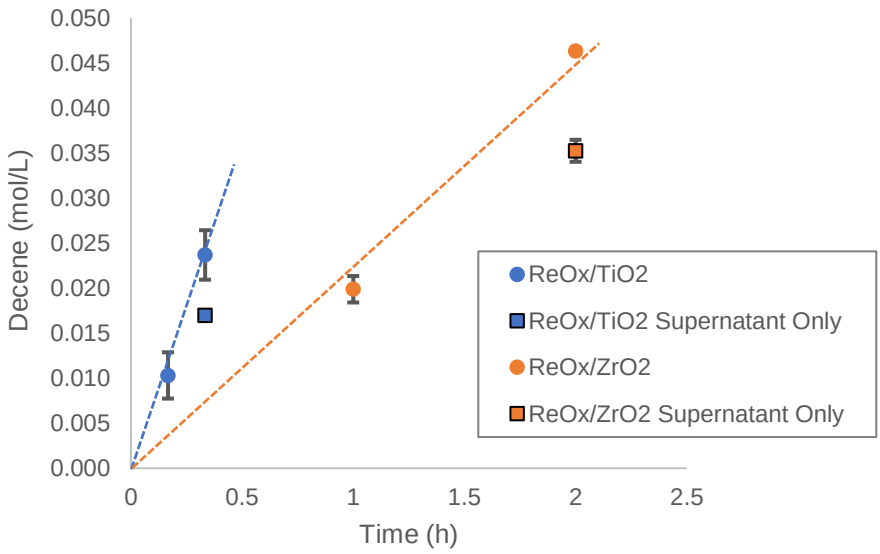

Figure 3.6: Hot filtration supernatant activity test. Solid catalyst reaction conditions: Temp. 150 °C, time 15-60 min, solvent toluene, 0.2 M diol, 0.23 M PPh_3, diol:Re=40. Supernatant reaction conditions: Separated reaction filtrate from shorter reaction time was run for an additional 15 or 60 min at 150 °C without any solid catalyst. Lines are to guide the eye only.

To further assess the relative contributions of homogeneous and heterogeneous catalysis, the rate of product formation during the reaction with the solid present was normalized in two different ways, while the supernatant rate was normalized to the amount of solubilized rhenium as determined by ICP-MS (Figure 3.7). If both rates are normalized to soluble rhenium, then a higher rate results for the initial run with solid present than for the supernatant, indicating that there is a heterogeneous catalysis contribution from supported rhenium in the solid. This contribution was significant only for the ReO_x/ZrO_2 catalyst. Comparison of the rate normalized to total supported rhenium in the first run with the rate per dissolved rhenium species in the supernatant run indicates a higher rate per rhenium in the supernatant, suggesting the dissolved species are more active on a per rhenium basis.

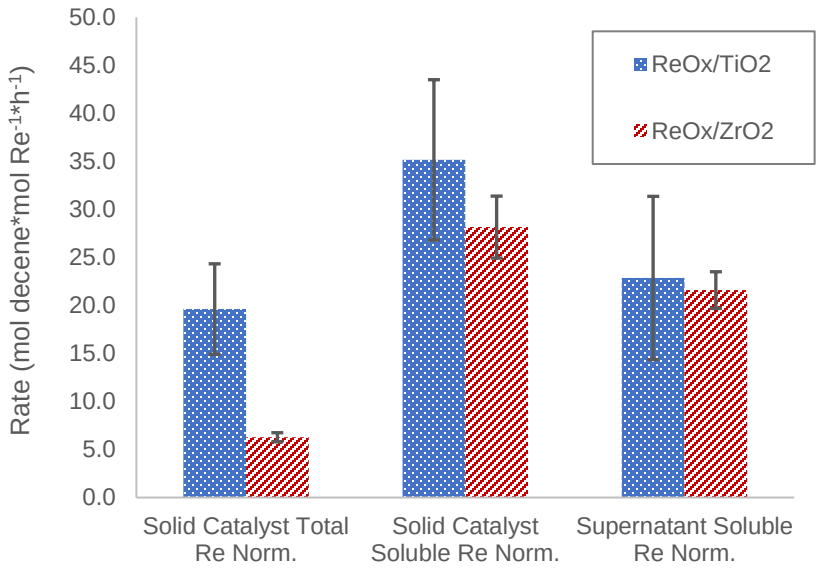

Figure 3.7: Solid vs supernatant reaction yield per total rhenium or solubilized rhenium measured via ICP-MS. Initial reaction conditions: Temp. 150 °C, time 15-60 min, solvent toluene, 0.2 M diol, 0.23 M PPh_3, diol:Re=20. Supernatant reaction conditions: Separated reaction filtrate from the initial reaction was run for an additional 15 or 60 min at 150 °C without any solid catalyst. The activity is normalized to the solubilized rhenium as measured by ICP-MS.

3.4. Solvent and Ligand Effect on Rhenium Leaching

The data in Figure 3.1 indicate a strong influence of the support on the propensity of rhenium to leach. However, a comparison with literature data suggests there might be additional factors affecting stability. Little to no leaching was reported by Sandbrink et al.[24], whose most stable catalysts were a ReO_x/TiO_2 material and an even better, pre-reduced variant of this ReO_x/TiO_2 material. Tazawa et al.[27] found their $ReO_x/Au/CeO_2$ catalyst to lose only minor amounts of rhenium, corresponding to less than 0.25% of the loaded amount. Since the ReO_x/TiO_2 catalyst used in the present work is fundamentally similar to the non pre-reduced catalyst used by Sandbrink et al., the significant differences in leaching behavior require explanation. We hypothesized that in addition to the support, the solvent is likely to have an influence and, based on the proposed mechanism, also the reactant. If the species on the supported catalysts are similar to the perrhenate

precursor, which was demonstrated for the carbon support, then, as a charged inorganic moiety, they are not expected to be very soluble in the non-polar solvent toluene. During the catalytic cycle though, the rhenium complex receives new ligands. The proposed reaction mechanism for deoxydehydration involves a vicinal diol forming a glycolate with the active rhenium site followed by elimination of the alkene product. The glycolate intermediate would likely be far more soluble than the perrhenate alone, especially if the diol has a large non-polar region as with 1,2-decanediol, as illustrated in Scheme 3.1. The glycolate intermediates shown in the figure are based on published structures, for example, by Ahmad et al.[11] or by Shakeri et al.[22]

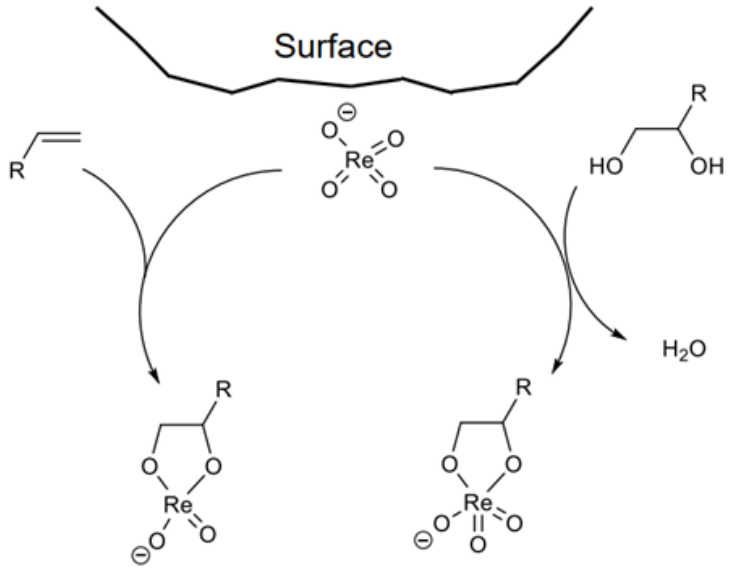

Scheme 3.1: Leaching hypothesis: Perrhenate (ReO_4^-) is not appreciably soluble in non-polar solvents, however diol and decene have surfactant-like properties when acting as a chelating ligand.

To test the theory of a chelating ligand inducing solubility of rhenium complexes, test reactions were performed to see which species present in the reaction might be capable of solubilizing rhenium, as seen in Figure 3.8. Negligible leaching is observed for the catalyst in the solvent alone, or in the presence of the triphenylphosphine reductant. The most severe leaching is seen when the diol is present in absence of any other reductant, with slightly less leaching in

reaction conditions with both diol and triphenylphosphine in the medium. The 1-decene product also seemed to be capable of inducing rhenium dissolution, demonstrating that in addition to a soluble Re(VII) glycolate, there exists a soluble Re(V) glycolate. This behavior was observed for ReO_x/TiO_2, but not ReO_x/ZrO_2. The difference is likely due to a greater energetic barrier from stronger ReO_x-ZrO_2 interaction. Based on the results in Figure 3.8, it is evident that mainly the diol causes leaching, by coordinating with the rhenium.

To test whether the leaching effect observed when using a vicinal diol was caused merely by the presence of an alcohol group coordinating with the rhenium species, 1-butanol was tested as a primary alcohol, and 1,4-butanediol was tested as an α,ω-diol. These molecules were not measurably converted into any products at relevant reaction conditions and did not induce any significant rhenium leaching for either a titania- or a zirconia-supported catalyst. This result suggests that a vicinal diol is necessary to form the solubilized intermediate, likely by undergoing dehydration to form the soluble rhenium glycolate intermediate, as illustrated in Scheme 3.1. Interestingly, Shiramizu and Toste demonstrated that 2-butene-1,4-diol can be converted to butadiene using methyltrioxorhenium as catalyst and proposed an isomerization reaction to a vicinal diol followed by DODH.[18] Evidently, the double bond enables this rearrangement.

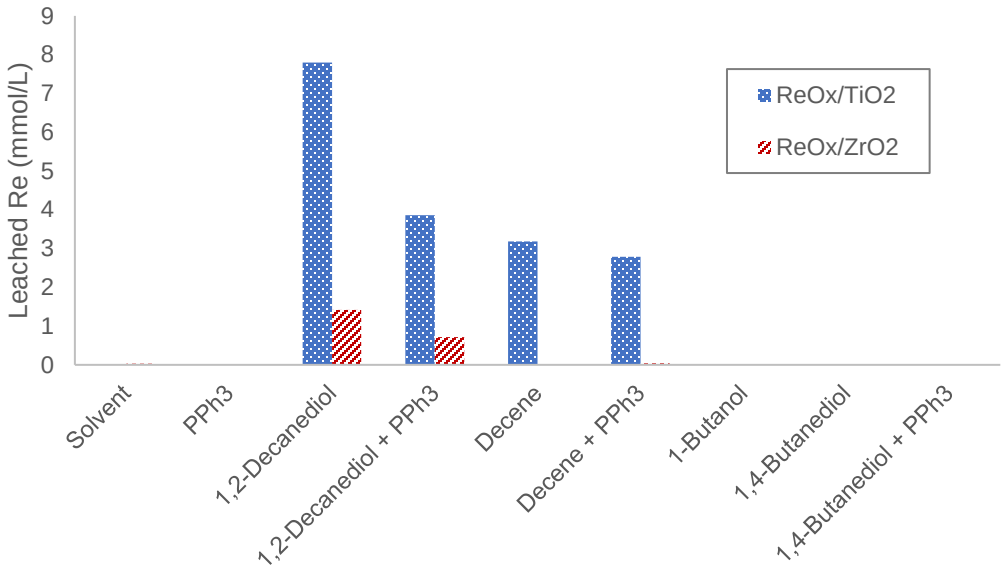

Figure 3.8: Ligand effect. Reaction Conditions: Temp. 150 °C, time 15 min for ReO_x/TiO_2, 60 min for ReO_x/ZrO_2, solvent toluene, 0.2 M 1,2-decanediol, 1-butanol, or 1,4-butanediol if noted, 0.23 M PPh_3 if noted, 0.2 M 1-decene if noted, diol:Re=20.

If the diol forming a glycolate complex with the rhenium is the primary cause of leaching, then it follows that the combination of diol and solvent may strongly control the degree of leaching. To further test this hypothesis, solvents with varying polarity were employed, which were toluene, 1,4-dioxane, 3-octanol, 2-propanol and water in order of increasing polarity. To ascertain the effects of the diol presence as such and of its hydrocarbon tail length, the options 1,2-decanediol, 1,2-hexanediol, and no diol were combined with the various solvents. The ReO_x/TiO_2 catalyst was chosen for this purpose, and it was principally active with all tested reductant, solvent and reductant combinations.

Figure 3.9 shows the amount of leached rhenium for the ReO_x/TiO_2 catalyst across the range of diols and solvents. In the no-diol condition, rhenium leaching was low for toluene, 1,4-dioxane, 3-octanol and 2-propanol though it did increase slightly with increasing solvent polarity. Rhenium leaching was significant when water was used, as expected for an inorganic, presumably

ionic species. When diol was present, leaching was most prominent in the non-polar solvent and diminished as the solvent polarity increased. This effect was consistently more pronounced for 1,2-decanediol than for 1,2-hexanediol, showing the larger hydrocarbon tail exacerbates the diol-induced leaching.

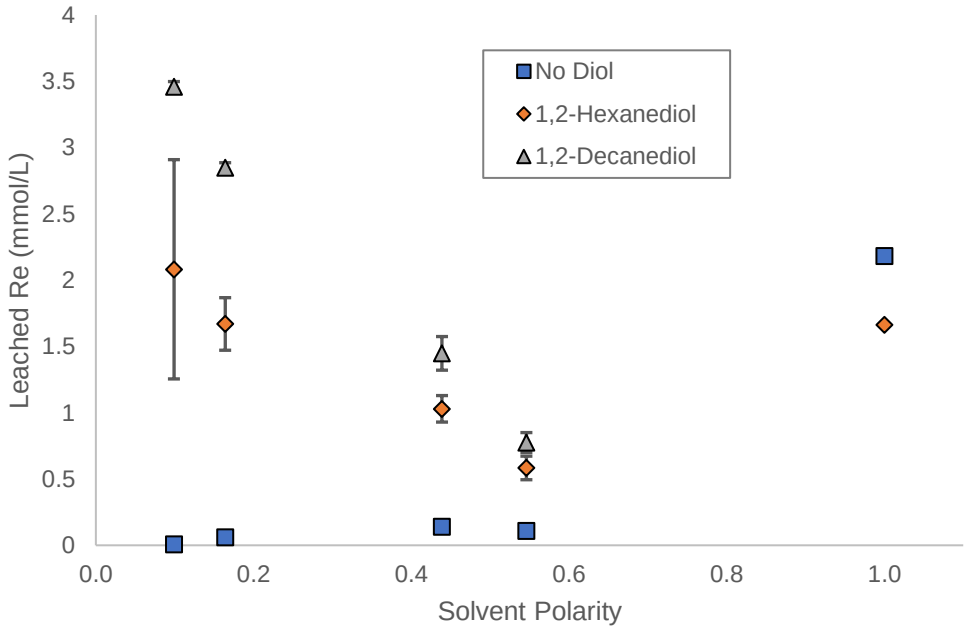

Figure 3.9: Solvent effect. Reaction Conditions: Temp. 150 °C, time 15 min for ReO_x/TiO_2, solvents toluene, 1,4-dioxane, 3-octanol, 2-propanol, and water in order of increasing polarity,[44] 0.2 M 1,2-decanediol or 1,2-hexanediol if noted, 0.23 M PPh_3 for toluene and 1,4-dioxane reactions, diol:Re=20.

Since the diol induces rhenium solubility, we were curious whether driving the reaction to 100% diol conversion would cause rhenium species to redeposit, or whether they would persist as soluble species. To test this hypothesis, the ReO_x/ZrO_2 and ReO_x/TiO_2 catalysts were operated to final diol conversions of 40-60% or 100%. Figure 3.10a shows catalytic activity of the fresh and recycled catalysts after both complete and partial diol conversion. The recovered catalyst demonstrated significantly higher activity in the second use if the first reaction was stopped only after complete diol conversion. Even more striking is the analysis of leached rhenium observed by ICP-MS after the first use of the catalysts (Figure 3.10b); while significant amounts of leached

rhenium were detected at incomplete conversion, the amount of solubilized rhenium was negligible at complete diol conversion. These measurements imply that rhenium is re-deposited onto the support or precipitated at complete diol conversion. Since the activity of the recovered catalyst does not correspond to that of the fresh catalyst even though there are almost no soluble rhenium species, additional deactivating processes must be inferred.

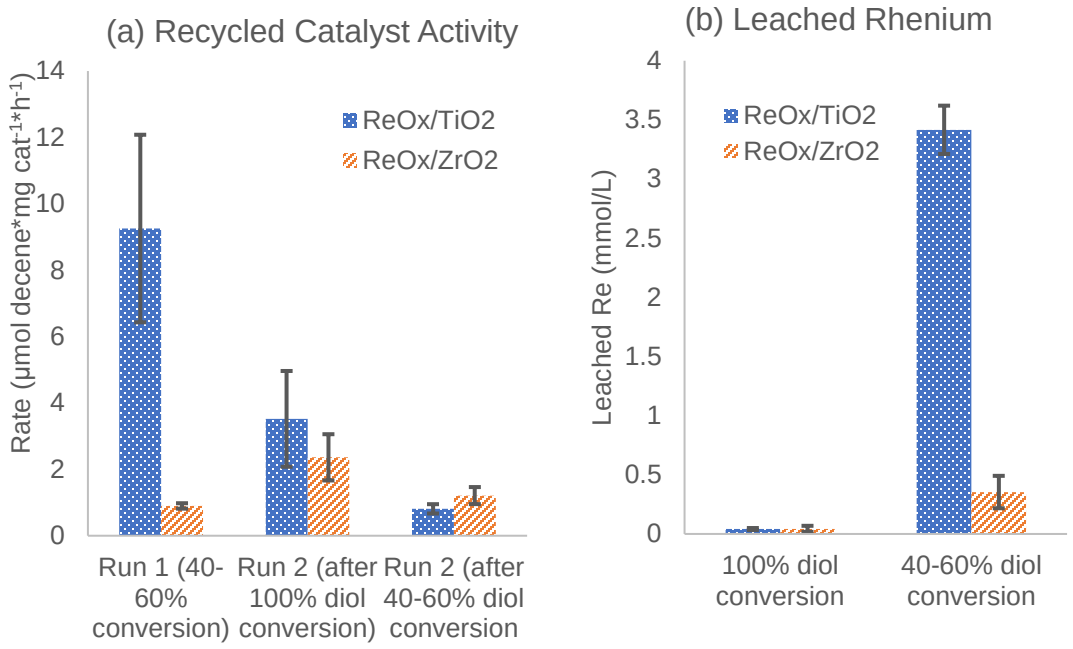

Figure 3.10: Diol conversion effect. Reaction Conditions: temp. 150 °C, time ReO_x/TiO_2 15 min incomplete and 60 min complete conversion, ReO_x/ZrO_2 1 h incomplete and 3 h complete conversion, solvent toluene, 0.2 M 1,2-decanediol, 0.23 M PPh_3 diol:Re=20. (a) Catalytic activity of the fresh catalyst and of the recycled catalyst after complete or incomplete diol conversion in the initial run. (b) Leached rhenium as measured by ICP-MS after either complete or incomplete diol conversion.

To gain insight into the nature of the solubilized rhenium species, UV-vis and EPR spectra of the supernatants were recorded at room temperature within 24 h of generation, as color changes occurred both with temperature and also during storage. EPR spectra indicate small concentrations of paramagnetic species. Spectra of solutions generated with diol only or diol and a secondary alcohol reductant showed a weak signal at g=1.910, with a hyperfine coupling of a(Re) = 260 G = $232x10^{-4}$ cm^{-1}. These spectra are consistent with Re(VI), but the weak signal indicates a minority

species given the concentrations measured by ICP and the typically excellent spectra obtainable with Re(VI) solutions. In presence of PPh_3, a signal with g = 2.263 is observed; chemically, Re(IV) is a likely species assuming further reduction. UV-vis spectra were characterized by a band at 493-499 nm for PPh_3-driven DODH of diols in various solvents. Without PPh_3, a band at 400 nm was observed when the solvent was dioxane, suggesting a different predominant oxidation state and perhaps also coordination of dioxane. The region of perrhenate absorption (229 nm) was generally obscured by strong solvent absorption. The simplicity of the UV-vis spectra suggests there are very few different species; however, given the many options for the rhenium oxidation state and the significant wavelength shifts that occur for both charge transfer and d-d transitions with coordination and nature of the ligands, it was not possible to assign these transitions. The bands did disappear with complete conversion of the diol, confirming the diol as one of the ligands and consistent with reprecipitation of rhenium.

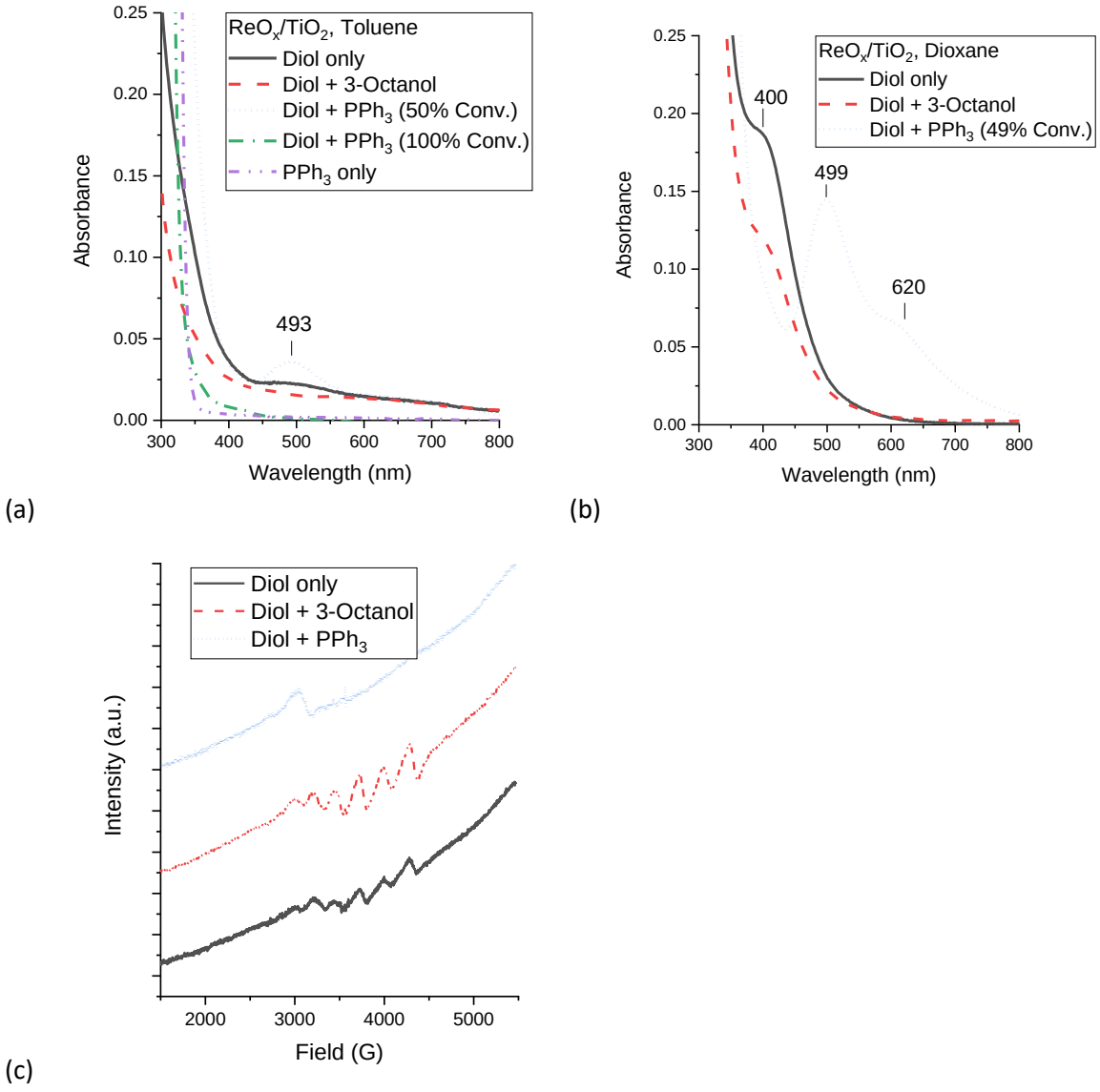

Figure 3.11: (a) UV-vis spectra of reaction supernatants in (a) toluene and (b) 1,4 dioxane solvent. (c) EPR spectra of reaction supernatants using ReO_x/TiO_2 catalyst, toluene solvent, 1,2-decanediol reactant with either no additional reductant, triphenylphosphine reductant, or 3-octanol reductant. Reaction conditions: Temp. 150 °C, time 15 min, ReO_x/TiO_2 catalyst 4 wt% loading, solvent toluene, 0.2 M diol (conversion indicated), 0.23 M PPh_3 or 3-octanol reductant if indicated, diol:Re=20.

3.5. Discussion of Leaching Effects

3.5.1. Catalyst Optimization by Activity and Stability

A strong role of the support for both ReO_x activity and stability emerges from the combined data of Denning et al.,[23] Ota et al.,[27] Sandbrink et al.,[24] and the present work. Ota et al. investigated catalysts consisting of a support, ReO_x as active component, and palladium as a promoter for DODH of 1,4 anhydroerythritol. Among a series of supports including carbon, SiO_2, TiO_2, ZrO_2, CeO_2, Al_2O_3, La_2O_3, Y_2O_3, MgO and CaO, the oxide CeO_2 was found to give the most active catalyst in the presence of palladium. Sandbrink et al. did not add a noble metal and reported an activity ranking for ReO_x/support in the order of carbon > SiO_2 > TiO_2 > ZrO_2, while finding the TiO_2-supported ReO_x material to be the most stable, particularly after a pre-reduction of the catalyst. The data in Figure 3.1a confirm the high activity of oxo-rhenium moieties supported on carbon, SiO_2, and TiO_2, but Figure 3.1b and Figure 3.7 suggest that much of the activity of these catalysts stems from leached species. The high supernatant activity (Figure 3.6) also demonstrates that the entire cycle can be homogeneous without temporary deposition, suggesting true homogeneous contributions and not a coupled homogeneous-heterogeneous cycle.

The support plays a primary role for the leach resistance of oxo-rhenium complexes and sets the activation barrier for detachment. The mechanism of detachment depends on the bond to the support. A weakly, van der Waals-bound species may simply be solubilized. An option to release charged moieties is ion exchange, during which the rhenium complex is replaced by another ion with like charge. However, the reactants and reagents are expected to be neutral molecules, making this mechanism unlikely. Alternatively, ligand exchange may occur, and the support moiety that serves as a ligand in the complex is replaced by another ligand. Perrhenate behaves like other oxido anions with a single charge such as nitrate or perchlorate, and is expected to not have a strong affinity to most surfaces. The decisive role of the diol suggests that detachment is promoted by ligand addition or ligand exchange.

With respect to stability as measured by performance of the recycled solid, the successfully employed supports are reducible except for Al_2O_3, and the most easily reducible supports among those investigated, CeO_2 and TiO_2, give the highest activity. Sandbrink et al.[24] reported improved catalyst stability for ReO_x/TiO_2 if the catalyst was pre-reduced and ascribed this phenomenon to the lower solubility of rhenium complexes with lower oxidation states. In light of the aggregate results of several groups, stronger attachment of oxido-rhenium moieties on a reduced support is an alternative interpretation. In the experiments by Tomishige and coworkers,[25–27] CeO_2 may be easily reduced through spillover of hydrogen from the noble metals. The stability of the Al_2O_3-supported ReO_x catalyst may be understood on the basis of the findings of Zhang et al.[45] They report on supported oxido-rhenium metathesis catalysts and found the rhenium species to be interacting with silica via a single oxygen bridge, whereas with alumina, an additional interaction via a hydroxyl group was observed. This increased rhenium-support interaction could be responsible for both the lower activity and the increased stability that is seen with ZrO_2, Al_2O_3, and Fe_2O_3 supports relative to SiO_2 and TiO_2 supports in Figure 3.1.

A second important factor is the loading of the rhenium. Figure 3.2 shows that the leached fraction depends on the support and that the amount leached decreases as the loading decreases. While the maximum loading could be explored by preparing catalysts with different loadings, it can be predicted by the cumulative leaching experiment in Figure 3.2. Since the initial rhenium loading was 4 wt%, the data suggest that SiO_2 is not a good support at any loading, TiO_2 should be limited to securely attaching around 1 wt%, and all others to about 2 wt% rhenium. The data in Figure 3.5, which compiles rhenium leached from catalysts with different loadings, are consistent with this prediction; zirconia retains rhenium better than titania. The amounts may vary depending on support source, support pretreatment, and rhenium precursor. They are however far below monolayer coverages, which are estimated to be 8.0, 3.7, 8.2, and 3.3 wt% for Al_2O_3, TiO_2, ZrO_2 and SiO_2, respectively, on the basis of the surface areas of the catalysts in Table 1 and the densities

calculated by Wachs.[46] Sandbrink et al. applied between 3.5-5.5 wt% rhenium and found leaching (as measured by filtrate activity and rhenium concentration in solid) to occur only in the initial use of ReO_x/TiO_2 and to be insignificant afterwards. Even though CeO_2 was not tested here, the 1 wt.% Re loading used by Tomishige and co-workers probably significantly lowered the risk of leaching.

Considering all reports on supported ReO_x catalysts and their suitability for DODH, the following conclusion can be drawn: If true heterogeneous catalysis is desired, then low rhenium loadings on supports such as ZrO_2, CeO_2, Al_2O_3 and Fe_2O_3, and on TiO_2 with suitable treatments are most promising. However, the data in Table 3.1 demonstrate that while lower loadings result in less leaching, the observed DODH rates per rhenium decline at the same time. There are two potential reasons for lower rates at low loadings, fewer homogeneous contributions and lower activity of more strongly bound surface species. The first is ruled out by the calculation in Table 3.1. Figure 3.6 indicates that homogeneous contributions dominate for high loadings, raising the general question about the contribution of heterogeneous DODH catalysis. The literature on supported catalysts is in favor of heterogeneous catalysis, and even some literature on soluble complexes suggests that a solid is the active species, resulting in an induction period.[47] However, other authors concluded that oligomerization of soluble catalyst leads to inactive species.[17,19]

3.5.2. Causes of Leaching

The results in Figure 3.9 show that the pristine solid catalyst ReO_x/TiO_2 is reasonably stable in the reaction medium. It is the reaction of oxido-rhenium with diol that promotes leaching, which supports the hypothesis that a glycolate complex is the soluble species. The glycolate can be formed through condensation of oxido-rhenium species with a diol. Decene is also effective in solubilizing rhenium, presumably because a glycolate can be formed through addition of decene (Scheme 3.1), which is the reverse reaction of the third step of DODH, the alkene elimination. It is evident that steps of the catalytic cycle lead to formation of soluble species. At complete diol conversion, the amount of dissolved rhenium is negligible (Figure 3.10). This scenario is reminiscent of

observations made with palladium catalysts for Heck and Suzuki couplings.[48–53] Dissolved palladium that forms during the course of the reaction serves as active species in these coupling reactions. The palladium is redeposited on the support at the end of the reaction; however, the high number of components in these reactions prevents the clear relationship between leaching and reactants or products that is seen in Figure 3.8 for rhenium-catalyzed DODH.

While the leached complexes could not be exactly identified, some knowledge could be gleaned from the aggregate information. Since primary alcohols and α,ω-diols did not induce leaching, the complexes are likely to be have diol-derived ligands. The complexes were not thermally or long-term stable, underlining the dynamics observed by others.[47] UV-vis spectra presented well-defined bands, suggesting well-defined species. EPR spectra suggest paramagnetic species such as Re(VI) and Re(IV) are a minority, consistent with the Re(VII)/Re(V)-based homogeneous catalysis cycle proposed by Ahmad et al.[11]

The association of catalyst with the reactant as primary cause of leaching presents challenges, both in detecting and in mitigating leaching, as discussed in the following.

3.5.3. Detecting Leaching

The detection of leached species and homogeneous catalysis contributions requires accounting for a number of phenomena as illustrated by Sheldon et al.,[34] and, consequently, leach tests call for cautious experimenting[54] and may be augmented by application of scavengers, for example thiols in Heck and Suzuki couplings.[35] Mercury has been used as a poison for solid metals to demonstrate heterogeneous catalysis, but this test is also associated with difficulties.[55]

The most common recommendation is hot filtration followed by testing of the filtrate for activity,[56] which addresses the issue of redeposition of leached species onto the support upon cooling. For the rhenium species, the effect of the separation temperature is rather minor, as seen in Figure 3.3, indicating that at the test conditions, solubility of the leached rhenium species is not

a limiting factor and saturation is not reached, or solubility is not strongly temperature dependent. The fact that the concentration of leached rhenium is the same at room temperature and at 150 °C for some catalysts (ReO_x/TiO_2) corroborates that the leached species are well soluble (Figure 3.4). In contrast, elevated temperatures were needed for other catalysts (ReO_x/ZrO_2) to overcome the detachment barrier and induce leaching in the first place.

In some cases, continued reaction of the catalyst with the substrate after separation has led to an inactive state of the catalyst and long induction periods in subsequent tests that can disguise supernatant activity.[34] Such a scenario can be avoided if the reaction is run to completion, that is, to 100% conversion, and for the test, more reactant is later added to the filtrate. This approach would fail here; if leaching is stimulated by the reactant, then it becomes undetectable at 100% conversion (Figure 3.10). In fact, at a reactant-to-catalyst ratio of 20 and an assumed diol-to-rhenium stoichiometry in the solubilized complexes of 1:1, conversions beyond 95% imply insufficient ligand availability. Soomro et al.[36] found a more complex relationship for Suzuki-Miyaura couplings, where in some cases the concentration of dissolved palladium passed through a maximum at 60% conversion even though the relative catalyst concentration was only 0.1 mol%. This observation and other data presented by the authors indicate that reagents and other additives also play a role for palladium solubilization. Their observations are not unique, for example, Sheldon saw chromium leaching from CrAPO-5 as a result of oxidation by a hydroperoxide which was added as a stoichiometric oxidant.[34] In contrast to these reports, the effect of conversion on leaching of rhenium from ReO_x/TiO_2 and ReO_x/ZrO_2 during DODH is absolutely clear (Figure 3.10), and the effect of PPh_3 is rather minor (Figure 3.8).

Sheldon et al.[34] also pointed out that recycled catalyst activity can be deceiving if the leached amount is very small but highly active. Indeed, upon second and further uses, which are representative of lower initial rhenium loadings, the activity of many solids remains more or less constant (Figure 3.1). In contrast the ICP analysis of the filtrate provides a sensitive measurement

and thus an unambiguous account of trace amounts of leached rhenium (Figure 3.1, Figure 3.2).

3.5.4. Leaching Mitigation Through Choice of Reaction Conditions

Ideally, the interaction between support and active moiety is so strong that leaching is kinetically hindered and prevented in the first place. If the activation barrier for detachment is high enough as appears to be the case for ReO_x/ZrO_2 (cf. Figure 3.3 and Figure 3.4), then lowering the reaction temperature should suppress leaching.

If detachment is principally possible, then the solubilities of all forms of the catalyst in the cycle, that is, in its original form and after association with a reactant or reagent in the solvent have a considerable influence. In the present case, minimizing solubility is challenging because of opposite trends. The pristine ReO_x/support catalyst, presumably containing an inorganic ion as active rhenium moiety, is not appreciably soluble in nonpolar organic solvents. In contrast, the glycolate complexes with their hydrophobic hydrocarbon tails are more soluble in nonpolar solvents than in polar solvents. As seen in the leaching map in Figure 3.9, the optimal solvent polarity for minimal leaching is the minimum resulting from combination of the solubility curves of the various catalyst forms. The optimal solvent is also a function of the reagent and of course must still be favorable for catalyst operation. A survey of recent DODH reports shows that Sandbrink et al.[24] converted hexanediol and octanediol and used 3-octanol as the solvent and reductant. Indeed, slightly more leaching was observed for octanediol than for hexanediol, as the leaching map in Figure 3.9 would have predicted. Tomishige and co-workers[25–27] combined 1,4-dioxane as the solvent with a variety of substrates and found little leaching with glycerol as the reactant,[27] suggesting that this combination works well together with the catalyst.

Solvents are typically chosen with the goal of dissolving reactants and products. It is seen here that with a heterogenized catalyst, the leach resistance becomes an additional criterion for selecting a solvent; and the solvent must be adapted to the reactant to lower the solubility of the catalyst-reactant complex.

An additional complication is the formation of water as a reaction product, which as per Figure 3.9 promotes rhenium leaching, at least of the oxo-anions used here. Its fate depends on the miscibility with the solvent. Solubility in toluene, which was used for most of the reactions, is low at 0.027 M,[57] and indeed a second phase forms if larger amounts are added. This scenario could be problematic if the catalyst partitions to the aqueous fraction, while also implying ease of separation.

3.5.5. Release and Catch Catalysis

Since leaching is difficult to suppress entirely for rhenium-catalyzed DODH, an interesting alternative solution to this issue is a 'release and catch' catalytic scheme, where the active species becomes partially homogeneous during the reaction, but is then redeposited on the support, similar to what has been demonstrated for other liquid phase reactions such as the Suzuki couplings.[36] Figure 3.10 shows that dissolved rhenium species can be precipitated when the reaction is driven to complete diol conversion, which can additionally be promoted by excess reductant. Another possible benefit of excess reductant is that the reduced form of the catalyst is less likely to react with decene. However, the recycled catalysts do not reach the activity of the original catalyst, indicating that some rhenium is transformed into an inactive solid. The release and catch scheme thus has potential, but requires further optimization.

3.6. Rhenium Encapsulation in Microporous Zeolites

Rhenium solubilization was found to be induced by the diol forming a glycolate with the active rhenium species. We hypothesized that if the oxo-rhenium species is deposited within a microporous zeolite, the bulky glycolate intermediate may have reduced mobility within the zeolite pore. Though there has not been any reported use of zeolites in DODH catalysis, rhenium deposition on zeolites have been demonstrated by several groups. Wu et al.[58] used incipient wetness impregnation to deposit ammonium perrhenate rhenium precursors on MFI and MWW zeolite. CVD methods have also been used to deposit rhenium using methyltrioxorhenium and Re_2O_7 onto HZSM-5.[59]

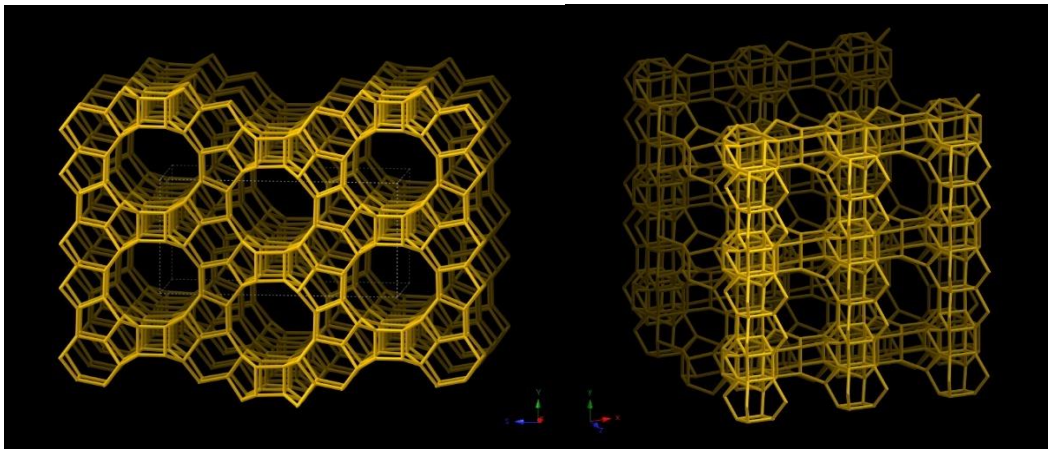

Figure 3.12: Zeolite framework of Beta/ BEA zeolite on [1 0 0] axis (left) and [0 0 1] axis (right) from IZA database of zeolite structures.[60]

The major parameters which will be considered for this study are the zeolite pore size, zeolite acidity, rhenium deposition technique, and the reactant and reductant size and identity. We choose to select zeolite beta (BEA), pictured in Figure 3.12, as it is a large pore zeolite in which a 5.95 Å kinetic diameter sphere can diffuse through the pores with a cavity space of 6.68 Å.[60] This larger pore size was selected to allow the diffusion of the perrhenate precursor and diol reactants through the pore and allow for the formation of the glycolate intermediate within the zeolite. A potential complicating factor is if pore confinement sterically hinders reactivity of the rhenium species within the pore. However, the pores should be small enough to inhibit diffusion of the glycolate intermediate outside of the zeolite. This size effect can be studied using various diols, such as 1,2-hexanediol, 1,2-decanediol, and diethyltartrate in order of increasing size, and the bulky triphenylphosphine versus smaller secondary alcohol reductants.

Wu et al. reported that the perrhenate species preferentially attach to the Si-O-Al Brønsted acid site, so both a siliceous and high acid site density zeolite were tested. Both incipient wetness and CVD have been employed to incorporate rhenium into zeolites in the literature,[59,61] for initial testing incipient wetness was employed due to ease of synthesis, though CVD could also be employed in future testing. Since we are working with a microporous catalyst, diffusion effects

into the zeolite will become significant which will affect kinetics, and larger reactants and reductants may not be able to fit into the pores.

3.6.1. Zeolite Catalyst Preparation, Rationale, and Reaction Conditions

The beta zeolites were obtained from Zeolyst. Two different beta zeolites were used: BEA-19 (Zeolyst, CP814C) which has a Si:Al ratio of 19, and BEA-150 (Zeolyst, CP811C-300) which has a Si:Al ratio of 150. The silicon to aluminum ratio dictates the acidity of the zeolite as the bridging oxygen between the silicon and aluminum in the framework has a Brønsted acidic hydrogen. By using zeolites with varying concentrations of Brønsted acid sties, we hoped to test whether this acidic site can provide a rhenium binding site as reported by Wu et al.[58] The zeolites as obtained from Zeolyst were in their ammonium form, and in order to decompose the ammonium and obtain the hydrogen form (H-BEA) of the zeolites, they were first calcined at 500 °C for 3 hours. Rhenium was introduced to the zeolites using incipient wetness impregnation with ammonium perrhenate as the rhenium precursor which was dissolved in a volume of deionized water corresponding to the pore volume of the zeolite support.

Table 3.2: BEA zeolite catalysts of varying acidities impregnated with rhenium.

Catalyst	Re loading (wt%)	mmol Al	mmol Re
ReO_x/BEA 19	3.9	1.73	0.34
ReO_x/BEA 150	3.9	0.24	0.34

The composition of prepared rhenium zeolite catalysts can be seen in Table 3.2. ReO_x/BEA19 catalyst contains an excess of acid sites compared to the rhenium loading, with roughly 5 acid sites for every rhenium atom. The ReO_x/BEA150 has a deficit of acid site as compared to rhenium loading, with just over 1 rhenium atom per acid site. In order to evaluate the zeolite catalyst, 4 wt% loading ReO_x/TiO_2 and ReO_x/ZrO_2 were used as controls.

3.6.2. Zeolite Supported Rhenium Catalyst Results

The ReO_x/Zeolite catalsyts were tested using 1,2-hexanediol, 1,2-decanediol, and diethyltartrate in order to test the effect of substrate size. Increasing the size of the reactant can either inhibit the reaction due to slower diffusion, or steric effects within the pore reducing reactivity. 2-propanol was used as the solvent and reductant to ensure that the reductant would not be hindered by diffusion limitations. Refer to Chapter 2 for reaction conditions and procedures.

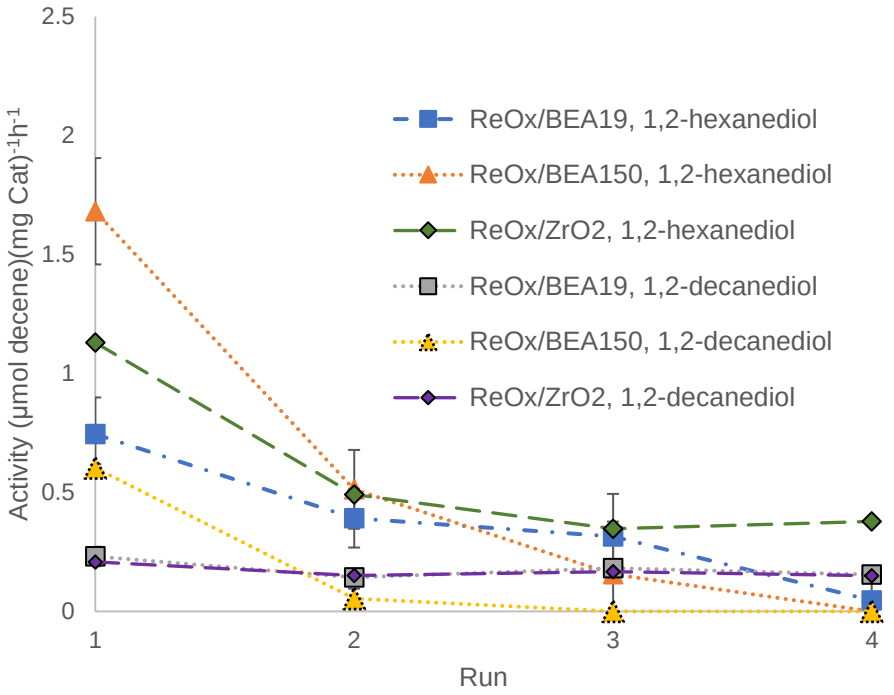

Figure 3.13: Zeolite-supported rhenium catalyst DODH activity over 4 consecutive runs. Reaction conditions: 150 °C, 55 minutes for 1,2-hexanediol reactions, 90 minutes for 1,2-decanediol, 2-propanol solvent and reductant, 0.2 M diol, diol:Re=20.

The zeolite catalysts were active for deoxydehydration over multiple runs, as seen in Figure 3.13, however the benchmark zirconia-supported catalyst had similar initial activty and retained higher activity over multiple runs, suggesting that this initial screening of rhenium zeolites does not offer an advantage over previously tested catalyts. Interestingly however, while the less acidic BEA150 catalyst lost most of its activity in the first run, the more acidic BEA19 was a much more stable catalyst, though its initial deoxydehydration activty was lower. This greater stability lends

some credence to the idea put forward by Wu et al.[58] that the acidic silicon-aluminum oxygen bridging site has an affinity towards the rhenium species.

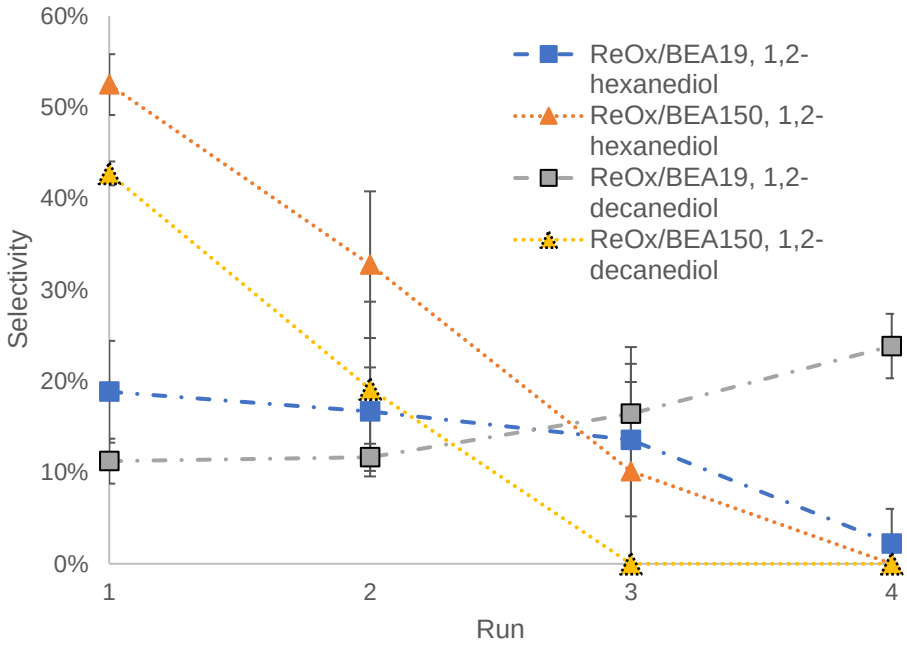

Figure 3.14: Zeolite-supported rhenium catalyst selectivity over multiple runs. Reaction conditions: 150 °C, 55 minutes for 1,2-hexanediol reactions, 90 minutes for 1,2-decanediol, 2-propanol solvent and reductant, 0.2 M diol, Diol:Re=20.

The reason for the lower initial activity observed for the more acidic ReO_x/BEA19 catalyst can be seen by looking at the selectivity shown in Figure 3.14. Both catalysts actually had similar diol conversion, however the more acidic zeolite forms side products, greatly reducing selectivity. However, over multiple runs, the more acidic zeolite catalyst ReO_x/BEA19 is more stable, while ReO_x/BEA150 loses selectivity as the catalyst deactivates after the first run. In runs of the BEA19 and BEA150 without the introduction of rhenium the 1,2-decanediol was largely converted, however decene was not formed. The product peaks are consistent with what could be expected of acid-catalzyed dehydration produts of the 1,2-decanediol.. This explains the low selectivity of the zeolite-supported rhenium catalysts, especially for the more acidic ReO_x/BEA19.

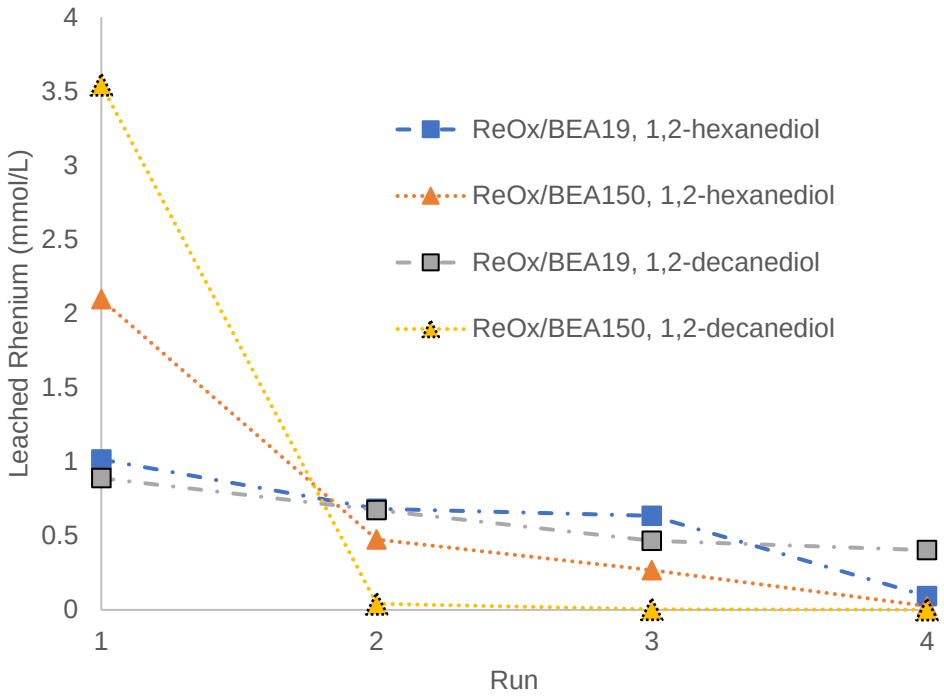

Figure 3.15: Zeolite-supported catalyst rhenium leaching by ICP-MS.

From the ICP-MS we see that there is not a large difference in leaching whether using the 1,2-hexanediol or 1,2-decanediol substrate, though the 1,2-hexanediol demonstrated slightly higher leaching due to the relatively polar 2-propanol solvent. The acidity of the zeolite framework had a strong effect on leaching. The less acidic ReO_x/BEA150 leached most of its rhenium after the first run, however the more acidic ReO_x/BEA19 catalyst steadily leached rhenium over the 4 runs. This explains the loss in activity of the BEA150 catalysts versus the relative stability of the BEA19 catalysts observed in Figure 3.15 and further supports the reported interaction between the acid site and the oxo-rhenium species.

3.6.3. Microporous Supports for Rhenium DODH Catalyst Conclusions

The siliceous zeolite framework does not seem to be a very strongly binding support for the perrhenate species, similar to what is observed for the tested fumed silica support. This effect may arise from the relatively negatively charged silica surface and the perrhenate anion, or possibly just from the lack of strong bridging rhenium-oxygen-silicon bond. The presence of acid sites in

the zeolite did suppress the rhenium leaching, however, introduction of the Brønsted acid site lowered selectivity to the deoxydehydration product by catalyzing side reactions. With the size of substrate and zeolite pore tested, there does not seem to be a strong suppression of rhenium leaching through encapsulation of the rhenium species.

This preliminary study of microporous supports for deoxydehydration shows some promise that the rate of leaching can be slowed by the presence of an acid site. There is a very large parameter space using microporous supports. There may be an effect if a smaller-pore zeolite was employed, though the choice of substrate and its size may dictate the possible pore sizes which makes it difficult to make a one size fits all catalyst. It may also be helpful to optimize the rhenium to acid site ratio to provide binding sites for the rhenium without a large excess of Brønsted acid sites. Further, if this line of research were to be persued it would be useful to identify whether the rhenium species were primarily surface species, or whether they were entrapped in the micropore network. This could be verified in part using transmission electron microscopy, or using the technique by Wu et al.[58] who applied FTIR-spectroscopy to track the replacement of the acidic hydrogens with rhenium.

Alternative encapsulation strategy would be to use a deoxydehydration catalyst with very bulky homogenoues catalyst and then employ a ship in the bottle strategy. This has been demonstrated for the Grubbs catalyst by Yang et al.[62] in which a bulky second generation Grubbs catalyst was entrapped in SBA-1, a small pore, mesoporous silica. The surface of the SBA was then functionalized through silylation with dichlorodiphenylsilane which reduced the pore size of the SBA, trapping the catalyst within the cages of the SBA.

CHAPTER 4

INVESTIGATION OF ALTERNATIVE MORE ECONOMICAL METALS FOR DEOXYDEHYDRATION

4.1. Introduction

From Chapter 3, we see that during liquid phase deoxydehydration catalysis, the supported catalytically active species is prone to leaching. This leaching issue is exacerbated by the formation of a glycolate intermediate, and further the active species must be able to easily able to undergo changes in oxidation and coordination, so attempts to more strongly bind the active species may reduce reactivity. Though leaching mitigation strategies will be beneficial to producing a more practical catalyst, due to the high cost of rhenium, it would be more ideal to start working with a cheaper transition metal that is capable of similar redox catalysis as rhenium. Namely, the metal must be able to coordinate and form the glycolate intermediate, and easily undergo the ±2 oxidation state redox couple necessary for the initial reduction and re-oxidation in the elimination of the alkene from the glycolate. From that starting point, we wanted to survey group V, VI, and VII transition metals.

We started by exploring oxide-supported vanadium, manganese, molybdenum, and tungsten catalysts which are all widely used as oxide-supported redox catalysts[63–68] and are relatively cheap and abundant in relation to rhenium.[69]

4.2. Molybdenum Catalysts

Developing supported molybdenum catalysts for DODH was of great interest because of the relative abundance and low cost of molybdenum compared to rhenium, the fact that it is a well-known redox catalyst capable of undergoing the change in oxidation state required for deoxydehydration, as well as the fact that homogeneous molybdenum catalysts have been demonstrated to be active for DODH when coordinated with bulky ligands.

4.2.1. Catalyst Preparation and Characterization

Using the same oxide supports used for the supported rhenium catalysts, a series of supported molybdenum catalysts were synthesized using incipient wetness impregnation. Ammonium heptamolybdate tetrahydrate (Sigma Aldrich) was used as the molybdenum precursor. A similar procedure was used as in the rhenium preparation outlined in section 2.1, however 550 °C for 4 h was used for the calcination as molybdenum sublimation was not as large of a concern.

Table 4.1: Molybdenum catalyst loading and surface area measurements.

Catalyst	Molybdenum Content (wt%)	Support BET Surface Area (m^2/g)	Catalyst BET Surface Area (m^2/g)
MoO_x/TiO_2	9.3	53.2	49.8
MoO_x/ZrO_2	9	99.5	81.8
MoO_x/SiO_2	10.1	300	
MoO_x/Fe_2O_3	9.1	42.7	29.9
MoO_x/Al_2O_3	8.8	151.6	143.2

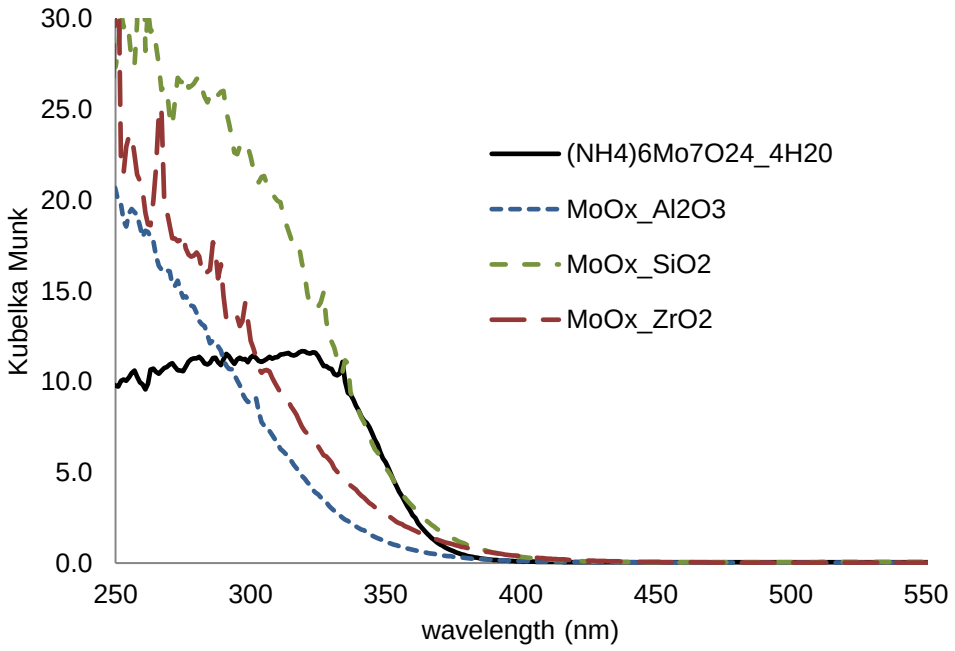

Figure 4.1: Diffuse reflectance UV-vis spectra converted to Kubelka-Munk function of oxide-supported molybdenum catalysts and ammonium heptamolybdate, the molybdenum precursor used in the synthesis of the supported catalyst.

From UV-Vis spectra taken of the molybdenum precursor and catalysts shown in Figure 4.1, we see that the heptamolybdate precursor has an absorption edge of around 350 nm. This is

shared by the silica-supported molybdenum catalyst, however the zirconia and alumina supported catalysts absorb at shorter wavelengths. As noted by Weber,[70] the absorption edge of the molybdate species is dependent on the degree of oligomerization where the more oligomerized forms have lower energy absorption edges. This would imply that the silica-supported molybdenum catalyst retains its poly-molybdate form from the heptamolybdate precursor or reforms poly-molybdate upon calcination, while the alumina and zirconia supported molybdate has higher energy absorption bands indicating the breakdown of the molybdate into smaller molecules and/or a greater degree of interaction between the molybdate and the support.

4.2.2. Molybdenum Catalyst Reactivity with Triphenylphosphine Reductant

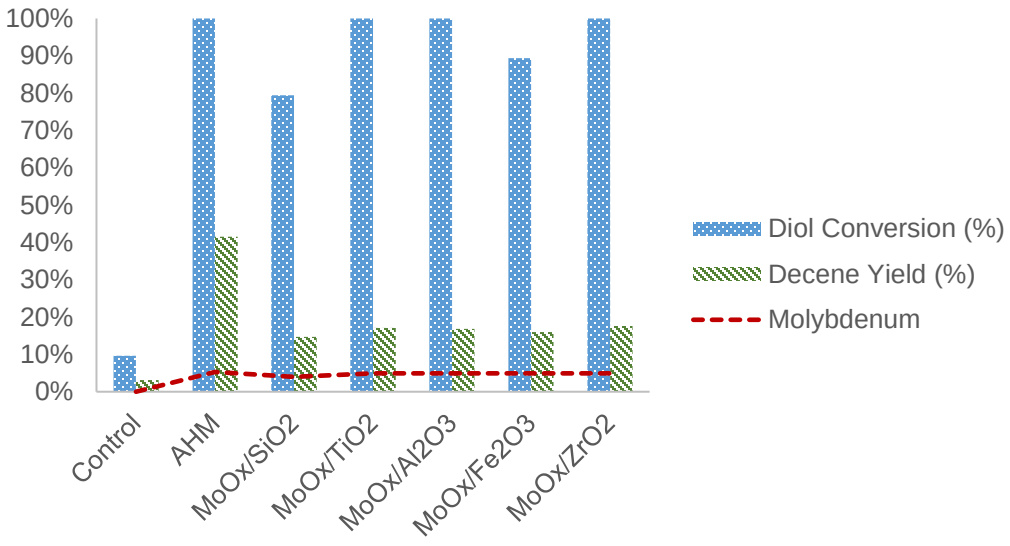

Figure 4.2 Supported molybdenum catalyst reactivity, AHM represents ammonium heptamolybdate tetrahydrate used as a homogeneous benchmark catalyst. Reaction conditions: temp. 180 °C, time 24 h, solvent benzene, 0.2 M 1,2-decanediol, 0.23 M PPh_3, diol:Mo=20.

The supported molybdenum catalysts were initially tested at 150 °C, however, they only achieved stoichiometric conversion to the decene product as compared to the molybdenum content of the supported catalysts. To see whether we could demonstrate that the molybdenum is truly catalytic, we tested at 180 °C, as seen in Figure 4.2. In this case, we see at least 3 times more

decene produced compared to the molybdenum content, indicating that the supported molybdenum is catalytic. For the supported catalysts, the DODH selectivity is largely independent of support. The low selectivity of the molybdenum catalysts is born out in that we see an abundance of side products in the chromatograms. Molybdenum oxides are known to be active catalysts for hydrogenation, dehydration, and condensation.[71] When the reaction mixture was analyzed by GC-MS, we saw compounds that are likely dehydration products and some heavier compounds that are likely condensation products.

Table 4.2: Supported molybdenum catalyst reactivity with triphenylphosphine reductant. Reaction conditions: Temp. 180 °C, time 24 h, solvent benzene, 0.2 M 1,2-decanediol, 0.23 M PPh_3, diol:Mo=20, 9 wt% Mo loading.

Catalyst	Temp (°C)	Time (h)	Diol Conv (%)	Alkene Yield (%)	Selectivity (%)	Activity (mol alkene)(mol Metal)$^{-1}h^{-1}$
Control	24	180	10	3	32	
$(NH_4)_6Mo_7O_{24}$	24	180	100	42	42	0.33
MoO_x/SiO_2	24	180	79	15	18	0.16
MoO_x/TiO_2	24	180	100	17	17	0.15
MoO_x/Al_2O_3	24	180	100	17	17	0.15
MoO_x/Fe_2O_3	24	180	89	16	18	0.14
MoO_x/ZrO_2	24	180	100	18	18	0.15

4.2.3. Molybdenum Catalyst Oligomerization Effect

Curiously, we regularly observed greater activity and selectivity using the homogeneous precursor, ammonium heptamolybdate tetrahydrate (AHM). A study was conducted to ascertain the reason for the greater selectivity. The initial hypothesis was that the greater degree of molybdate oligomerization, which is known to enhance reducibility, was responsible for enabling the redox behavior that facilitates DODH. Further, the initial molybdenum catalysts had a relatively high molybdenum loading.

Table 4.3: Zirconia-supported molybdenum catalysts with alternate incipient wetness impregnation conditions, calcined for 4 hours.

Catalyst	Precursor	Deposition Method	Deposition Solvent	Calcination Temp °C	Mo wt %
MoO_x/ZrO_2 AHM IW	$Mo_7O_{24}^{6-}$	incipient wetness	water	550	5.1%
MoO_x/ZrO_2 MoO_4 MeOH	MoO_4^{2-}	evaporative deposition	methanol	300	3.1%
MoO_x/ZrO_2 AHM MeOH	$Mo_7O_{24}^{6-}$	evaporative deposition	methanol	300	3.2%

To test the molybdenum oligomerization hypothesis, mono-molybdate, di-molybdate and hepta-molybdates were tested as homogeneous catalysts. Because the poly-molybdates can dissociate into mono-molybdate in water,[72] it is likely that dissolving the ammonium heptamolybdate precursor in water for incipient wetness impregnation would result in the deposition of mono-molybdate on the support. In order to counteract that, an alternative deposition technique was applied to try and retain the poly-molybdate structure. Zirconia-supported molybdate catalysts were prepared using mono-molybdate and hepta-molybdate precursors and using methanol to disperse the precursor. Because the precursors were less soluble in methanol, evaporative deposition was used, and the calcination temperature was lowered to 300 °C to avoid oligomerization or dispersion. The alternate preparation technique was tested against the standard incipient wetness impregnation, see Table 4.3. Sodium molybdate (Sigma Aldrich) and molybdenum trioxide (Alfa Aesar) were employed to test the effect of the counter cation and form of molybdenum oxide respectively.

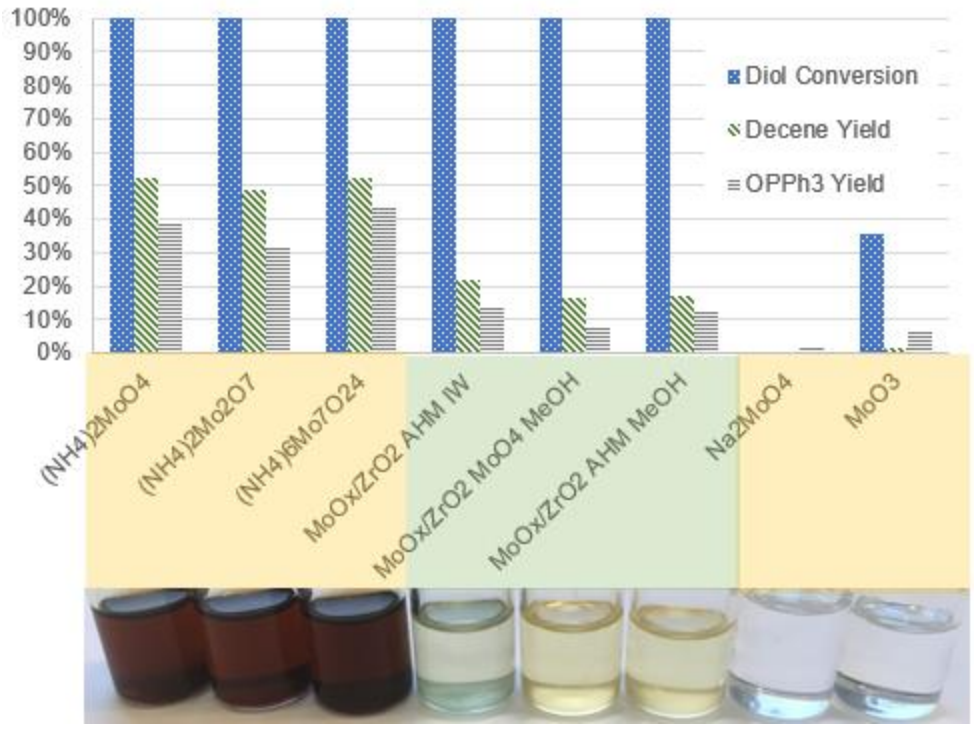

Figure 4.3 Molybdenum catalyst selectivity, testing the effect of oligomerization, support, counterion, and form of molybdenum oxide. Reaction conditions: temp. 180 °C, time 21 h, solvent toluene, 0.2 M 1,2-decanediol, 0.23 M PPh_3, diol:Mo=20, molybdenum loading 3.0-3.3 wt %.

The degree of molybdate oligomerization was not observed to have a significant effect on DODH selectivity for the homogeneous ammonium molybdate precursors. However, both sodium molybdate and molybdenum trioxide were inactive, indicating that the coordination state of the molybdenum was an important factor, and that the counterion plays a large effect on the activity of molybdate. The high DODH activity of ammonium molybdate has also been reported in the literature by Navarro et al.[73] and Sandbrink et. al.,[38] however, the source of the effect of the ammonium counterion remains unresolved. Possibilities are increased solubility of the catalysts, or a lower energy barrier of the reduction for the metal center with varying the cation for perrhenate as was reported by Shakeri et al.[22]

For the supported catalysts, the incipient wetness catalyst had slightly higher yield suggesting the alternative deposition method employed was not beneficial, however further

characterization would be needed to determine how the molybdenum sites on these catalysts differ. Due to the differing loading, deposition method, and calcination temperature, as noted in Table 4.3, it is unclear how much of the oligomerization of the precursor is retained after deposition. Further, it has been noted that rhenium catalysts, especially methyltrioxorhenium, is prone to oligomerize during deoxydehydration.[74,75] The similar conversion across the mono, di, and hepta-molybdate could be because they are quickly transformed to a similar mixture of species under reaction conditions regardless of their original form.

Shorter 5 h reactions were run to achieve incomplete diol conversion in order to assess molybdenum catalyst turnover frequency and selectivity. Ammonium molybdate catalysts were found to achieve selectivities to the DODH 1-decene product of 48.5-52.3% with a turnover frequency of 0.79-1.21 (mol decene)(mol Mo)$^{-1}$h^{-1}, while our zirconia-supported catalysts were able to achieve a selectivity of 16.7-21.7% with a turnover frequency of 0.23-0.26 (mol decene)(mol Mo)$^{-1}$h^{-1}. While the catalytic activity and selectivity of the much cheaper molybdenum catalysts are promising, further improvement in activity and selectivity is required. Beyond that, like rhenium, supported molybdenum catalysts are seen to leach as evidenced by the color change of the supernatant and tests of supernatant activity, indicating the presence of active soluble molybdenum species.

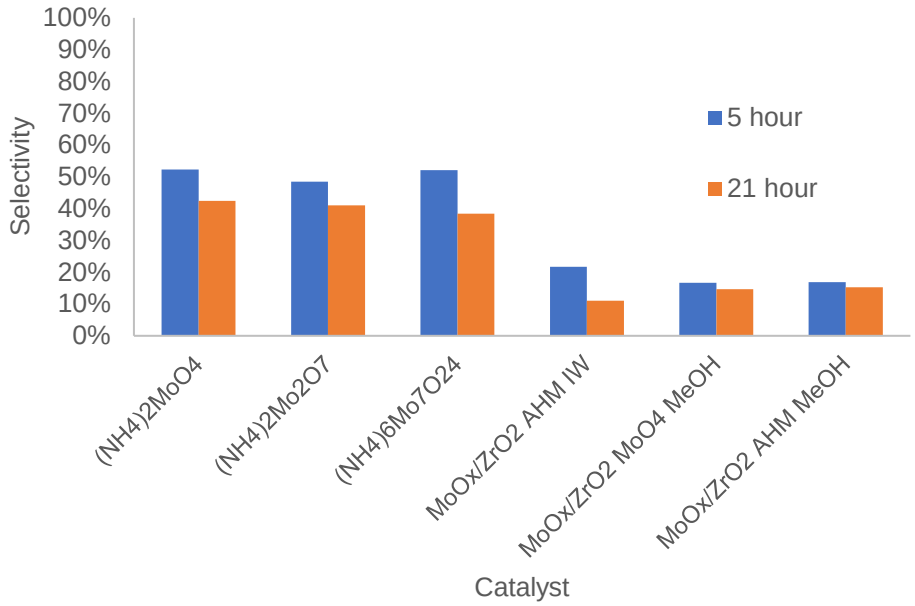

Figure 4.4: Reaction time and selectivity for molybdenum catalysts. Reaction Conditions: 180 °C, 5 or 21 hour reaction, 0.2 M 1,2-decanediol, 0.23 M triphenylphosphine, Diol:Mo=20.

The selectivity for the 5 hour reaction at incomplete diol conversion and the selectivity for the 21 hour reaction with complete diol conversion (from Figure 4.3) are shown in Figure 4.4. We see that the shorter reaction resulted in higher DODH selectivity across all tested catalysts, indicating either that the DODH product can be subsequently converted to a side product, or that the selectivity decreases as the reaction proceeds. Table 4.4 shows the molybdenum reaction conversions, yield, selectivity and activities for the reactions using triphenylphosphine as the reductant.

Table 4.4: Molybdenum catalyst oligomerization effect, reaction yields and activities. Reaction Conditions: 180 °C, 5 or 21 hour reaction, 0.2 M 1,2-decanediol, 0.23 M triphenylphosphine, diol:Mo=20.

Catalyst	Time (h)	Diol Conversion (%)	Alkene Yield (%)	Selectivity (%)	Activity (mol alkene)(mol Metal)$^{-1}$h^{-1}
$(NH_4)_2MoO_4$	21	100	52	52	0.49
	5	74	32	42	1.21
$(NH_4)_2Mo_2O_7$	21	100	48	48	0.42
	5	62	25	41	0.79
$(NH_4)_6Mo_7O_{24}$	21	100	52	52	0.42
	5	54	21	38	0.83
MoO_x/ZrO_2 AHM IW	21	100	22	22	0.20
	5	52	6	11	0.23
MoO_x/ZrO_2 MoO4 MeOH	21	100	17	17	0.16
	5	37	5	15	0.23
MoO_x/ZrO_2 AHM MeOH	21	100	17	17	0.16
	5	43	7	15	0.26
Na_2MoO_4	21	0	0	0	0.00
MoO_3	21	35	2	4	0.01

4.2.4. Molybdate Counterion Effect

From Figure 4.3, we see the ammonium counterion seemed to play a critical role in the reactivity of our molybdate catalysts, as ammonium molybdate is quite active while sodium molybdate was not active at all. One hypothesis was that the ammonium ion is either acting as a reductant itself, or at least converting the molybdate into an active catalyst in some way. To see whether an ion exchange of the sodium counterion with ammonium could cause sodium molybdate to become active, a small amount (0.02 M) of NH_4Cl was added to see if the addition of ammonium could active the molybdate.

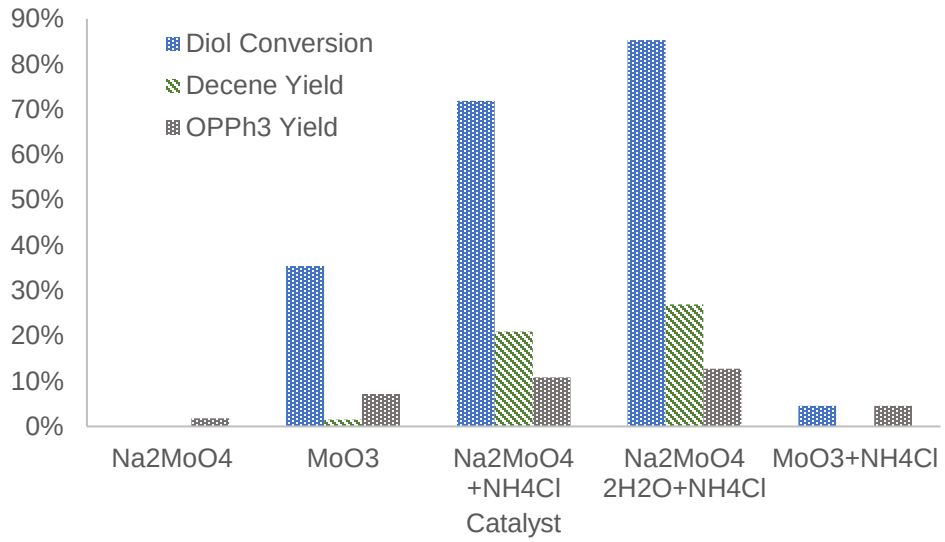

Figure 4.5: Molybdenum counterion effect: adding 0.02 M NH_4Cl. Reaction conditions: 180 °C, 5 h, 0.2 M 1,2-decanediol, 0.23 M triphenylphosphine, diol:Mo=20.

As seen in Figure 4.5, adding ammonium chloride to the reaction mixture makes the sodium molybdate active, however the molybdenum trioxide remains inactive. This suggests that the ammonium is necessary in order to activate the molybdate catalyst, and that deoxydehydration activity is sensitive to the original coordination state of the molybdenum, as molybdenum trioxide remains inactive. In addition to adding ammonium chloride, we also wanted to see if the presence of sodium or chloride ions could affect the reactivity of the ammonium molybdate and zirconia supported catalysts, so reactions with a small amount (0.02 M) of sodium chloride (Sigma Aldrich) added.

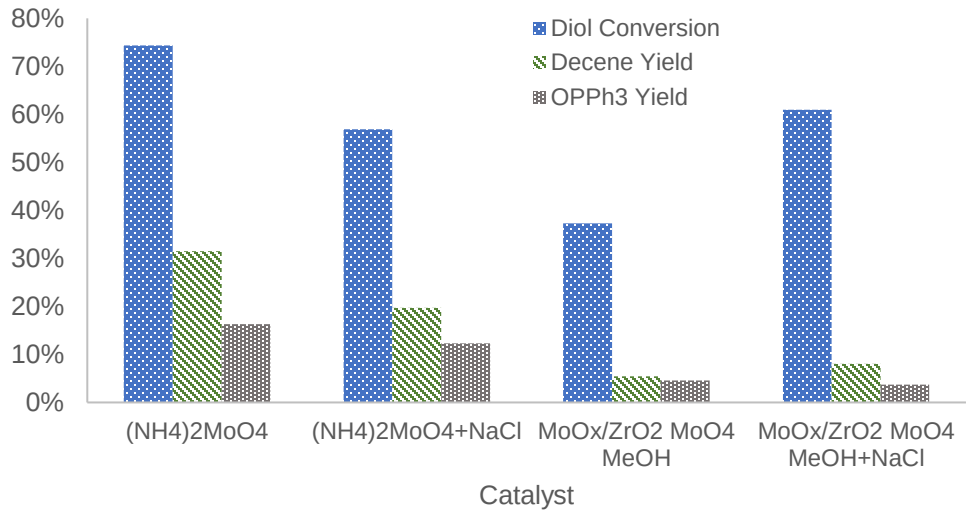

Figure 4.6: Molybdenum counterion effect: adding 0.02 M NaCl. Reaction conditions: 180 °C, 5 h, 0.2 M 1,2-decanediol, 0.23 M triphenylphosphine, diol:Mo=20.

4.2.5. Ammonium-Based Reductants

From Figure 4.5, we see that adding ammonium chloride to the sodium molybdate catalyst even in small concentrations (2:1 ammonium-to-molybdenum ratio), makes the sodium molybdate catalyst active. This suggests that the ammonium is necessary to activate the homogenous molybdate catalysts. The supported molybdenum catalysts on the other hand are active even in the absence of ammonium, as the counterion of the ammonium heptamolybdate would be decomposed during the calcination. A key question is how the ammonium is activating the molybdate. Possibly resulting from the proton transfer from the ammonium ion to the molybdate to form molybdic acid, a ligand exchange of an oxo-group for the ammonia or acting as a reductant for DODH.

In looking at the literature for a possible explanation, there is significant precedent for using ammonium, ammonia, and urea as a reductant for molybdenum catalysts in selective catalytic reduction.[76] Selective catalytic reduction is typically used as an environmental catalysis to remove NO_x from fossil fuel emissions by reducing it to N_2.[77] This is necessary because NO_x compounds are dangerous pollutants that are highly reactive oxidizers which are hazardous to health and lead to the formation of ground level ozone and smog.

To test whether ammonium could act as a reductant for deoxydehydration, we tested three different ammonia-based reductants. In addition to ammonium chloride (Sigma Aldrich), ammonium sulfate (Sigma Aldrich) was tested to see whether the choice in anion was significant. Urea (Sigma Aldrich) was also tested as an ammonia like reductant which is produced in high quantities[78] and is often employed as a reductant in catalytic converters for SCR.[76] These reductants were screened against the zirconia-supported MoO_x/ZrO_2 catalyst, and the homogeneous sodium molybdate catalyst. Sodium molybdate was chosen as it did not have an ammonium counterion which could obscure results. Table 4.5 shows the resulting deoxydehydration activity of these catalysts with ammonium-based reductants.

Table 4.5: Molybdenum catalyst reactivity with ammonium and urea reductants. Reaction conditions: 180 °C, 5 h, toluene solvent, 0.2 M 1,2-decanediol, 0.23 M reductant (NH_4Cl, $(NH_4)_2SO_4$, or urea), diol:Mo=20.

Catalyst	Reductant	Diol Conversion (%)	Alkene Yield (%)	Selectivity (%)	Activity (mol alkene)(mol Mo)$^{-1}$h^{-1}
Na_2MoO_4	NH_4Cl	86.1 ± 6.1	25.2 ± 4.6	29.4 ± 6.4	0.85 ± 0.08
MoO_x/ZrO_2	NH_4Cl	72.1 ± 13.2	8.3 ± 3.4	12.0 ± 5.6	0.26 ± 0.10
Na_2MoO_4	Urea	94.3 ± 4.7	13.0 ± 3.4	13.7 ± 3.1	0.50 ± 0.16
MoO_x/ZrO_2	Urea	84.6 ± 6.6	7.7 ± 4.6	9.4 ± 6.4	0.27 ± 0.16
Na_2MoO_4	$(NH_4)_2SO_4$	28.4 ± 5.7	4.9 ± 1.4	17.1 ± 1.6	0.18 ± 0.05
MoO_x/ZrO_2	$(NH_4)_2SO_4$	100 ± 0	6.6 ± 0.3	6.6 ± 0.3	0.21 ± 0.01

**experiments were run in triplicate to produce error bars.*

All tested reductants were active for DODH with both the supported MoO_x/ZrO_2 and Na_2MoO_4 catalysts. Ammonium chloride was found to be the most active and selective reductant and was especially effective for the homogeneous sodium molybdate catalyst with a turnover frequency of about 0.85 (mol decene)(mol Mo)$^{-1}$h^{-1} and 30% selectivity to the decene product. The choice of reductant was less impactful on the activity of the supported catalyst, which was lower than the homogeneous sodium molybdate catalyst in all cases but the ammonium sulfate reductant. The low activity of the ammonium sulfate may also be due to poor solubility and the larger crystal size.

Figure 4.7 shows the sensitivity of the sodium molybdate activity depending on the reductant and the relatively similar activity seen for the zirconia-supported catalyst.

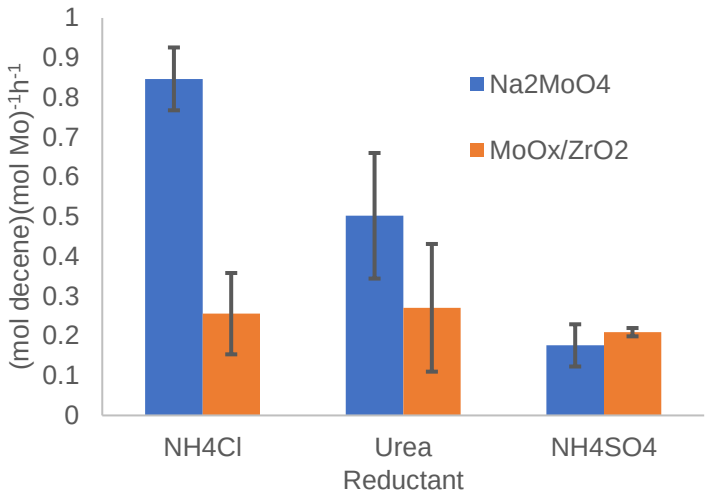

Figure 4.7: Molybdenum catalyst turn over frequency using ammonium-based reductants (ammonium chloride, ammonium sulfate, or urea). Reaction conditions: 180 °C, 5 hours, toluene solvent, 0.23 M 1,2-decanediol, 0.23 M reductant, diol:Mo=20.

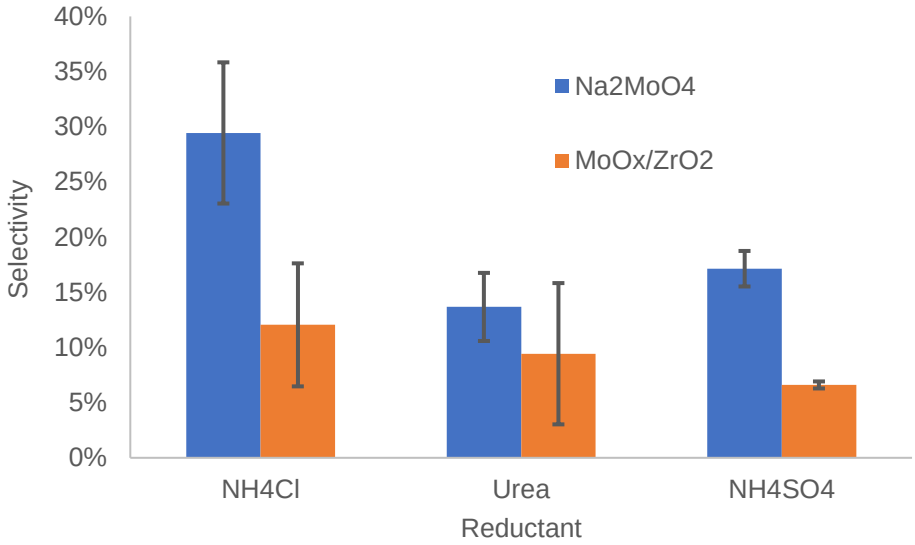

Figure 4.8: Molybdenum catalyst selectivity using ammonium-based reductants (ammonium chloride, ammonium sulfate, or urea). Reaction conditions: 180 °C, 5 h, toluene solvent, 0.23 M 1,2-decanediol, 0.23 M reductant, diol:Mo=20.

As seen in Figure 4.8, the selectivity is higher for the sodium molybdate catalyst than for the zirconia-supported molybdenum catalyst, with ammonium chloride displaying the highest selectivity among the ammonium-based reductants. In order to assess how selectivity evolves with

reaction time for the ammonium reductant, a set of 10 h reactions were conducted using the sodium molybdate catalyst and NH_4Cl reductant, as they were the most active and selective combination of catalyst and ammonium reductant, Figure 4.9. While the conversion is quite high for these conditions with 86% diol conversion after 5 hours, after 10 hours we see essentially complete diol conversion and the yield increases from 25 to 33%. This large gain in yield results in a slight increase in selectivity for the longer reaction from 29.4 to 34%. This increase in selectivity is a reversal of what was observed for the ammonium molybdate catalysts using triphenylphosphine as the primary reductant.

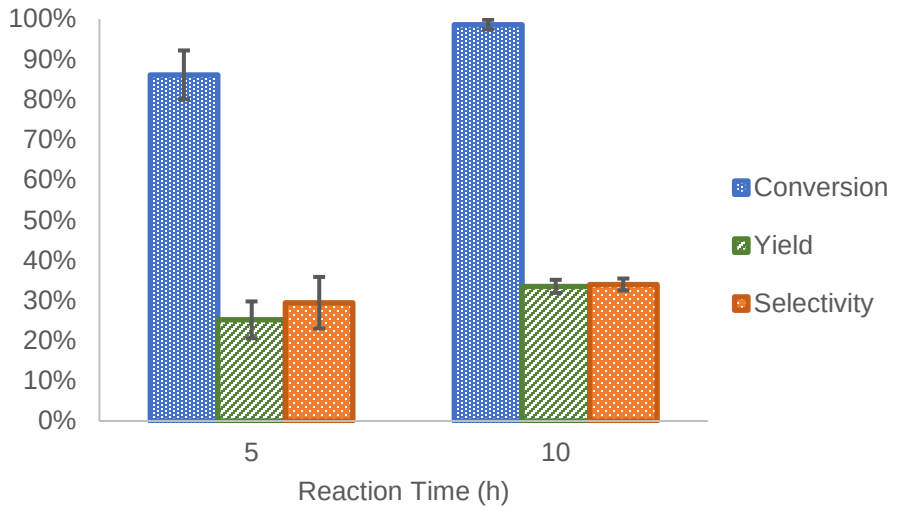

Figure 4.9: Ammonium chloride reaction time effect. Reaction conditions: Na_2MoO_4 catalyst, 180 °C, 5 or 10 hours, 0.02 M 1,2-decanediol, 0.23 M NH_4Cl, diol:Mo=20.

While the ammonium chloride is found to be an active reductant for molybdenum DODH, it is less active than the combination of ammonium molybdate catalyst with triphenylphosphine as a reductant. This would seem to suggest that triphenylphosphine is an effective reductant for the molybdate catalyst, but only in the presence of ammonium, raising the question of whether the ammonium reacts or performs a ligand exchange to create an active form of molybdenum, or acts in a redox couple with the triphenylphosphine. A set of experiments with varying amounts of

ammonium chloride and triphenylphosphine were performed to try and understand this relationship, seen in Figure 4.10.

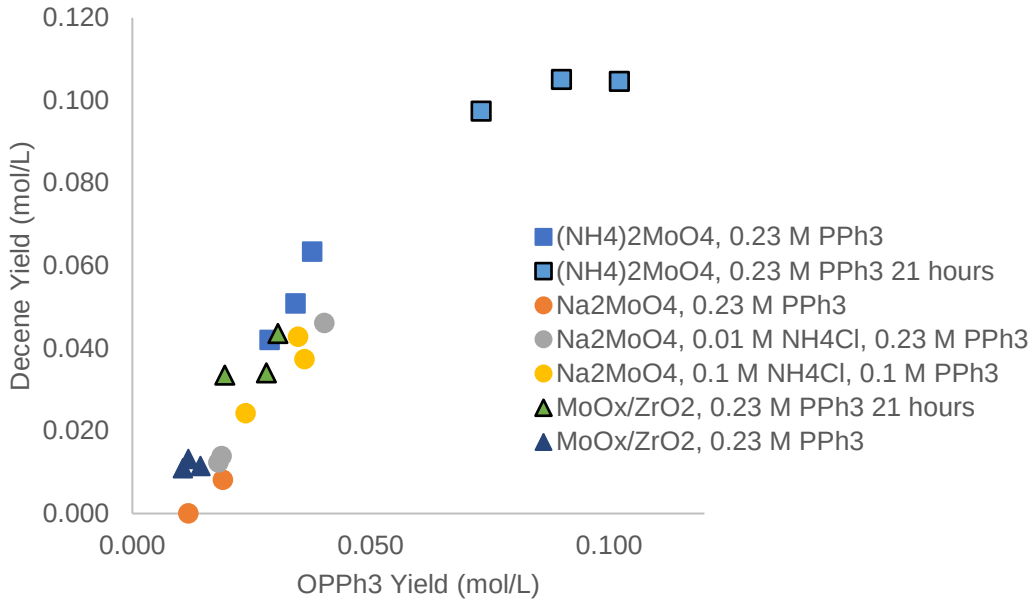

Figure 4.10: Triphenylphosphine reductant efficiency with varied ammonium concentrations. Reaction conditions: 180 °C, 5 hours unless otherwise noted, toluene solvent, 0.2 M 1,2-decanediol, 0.23 M triphenylphosphine, varied ammonium concentrations, diol:Mo=20.

For perfect reductant efficiency in deoxydehydration, a 1:1 production of triphenylphosphine oxide and decene would be expected, as observed for rhenium in Figure 2.8. From Figure 4.10, we observe a positive correlation between decene and triphenylphosphine oxide yield across the ammonium molybdate, sodium molybdate, and MoO_x/ZrO_2 catalysts, however there is some triphenylphosphine yield even when there is no decene yield as with the sodium molybdate catalyst in the absence of any ammonium. The reactions of the sodium molybdate catalyst with added external ammonium chloride display very close to a 1:1 ratio of decene to triphenylphosphine oxide yield regardless of whether 0.1 or 0.01 M of ammonium chloride is added.

For the ammonium molybdate and MoO_x/ZrO_2 reactions, the decene production is slightly higher than the triphenylphosphine oxide production. For the ammonium molybdate catalysts, this

might be explained by the ammonium acting as a reductant for the molybdate. However, in the 21 hour reaction the ammonium molybdate catalyst reaction yielded close to a 1:1 ratio of decene and triphenylphosphine oxide. Likewise, for the MoO_x/ZrO_2 catalysts, the excess decene is within 0.01 M of the triphenylphosphine oxide, which is the concentration of molybdenum in the reaction mixture.

From these results, it appears that the presence of ammonium has an activating effect on the molybdate catalysts when using triphenylphosphine as the reductant. However, ultimately the triphenylphosphine will be oxidized as the reducing agent. Deducing the mechanism for this behavior would be an open area of research. It may be that the ammonium and triphenylphosphine act as a redox couple, or perhaps ammonia can act as a ligand coordinated with the reduced molybdate followed by a ligand exchange with the diol to form glycolate intermediate. It would be especially useful to determine the fate of the ammonium nitrogen atoms in deducing their role.

4.2.6. Secondary Alcohol Reductants

Secondary alcohols have been reported as effective reductants for molybdenum DODH.[7,79] We carried out experiments using 2-propanol solvent which also acts as the reductant in order to assess molybdenum activity using secondary alcohol reductants vs triphenylphosphine and ammonium.

Table 4.6: Secondary alcohol reductants activity. Reaction conditions: 180 °C, 5 hour, 0.2 M 1,2-decanediol, 2-propanol solvent and reductant, diol:Mo=20.

Catalyst	Diol Conversion (%)	Alkene Yield (%)	Selectivity (%)	Activity (mol alkene)(mol Metal)$^{-1}h^{-1}$
Na_2MoO_4	7.9 ± 3.2	1.2 ± 0.2	16.5 ± 3.5	0.04 ± 0.01
MoO_x/ZrO_2	24.4 ± 1.6	4.9 ± 0.6	20.1 ± 2.1	0.16 ± 0.02

From Table 4.6, sodium molybdate is practically inactive, as was observed for the triphenylphosphine reductant, again indicating that the ammonium counterion is likely required to

activate the molybdate. Secondary alcohol reductants are still active for supported catalyst but less so than triphenylphosphine and ammonium chloride reductants.

4.2.7. Major Side Products of Molybdenum-Catalyzed Deoxydehydration

While the molybdenum catalysts are less active than similar rhenium catalysts, the major obstacle to using molybdenum catalysts remains their lower selectivity. While we observed selectivities up to 50% for the ammonium molybdate catalyst with triphenylphosphine reductant, the selectivity is lower for most other catalysts. This is especially apparent for the supported catalysts which peak at around 20% selectivity. In order to better understand how to improve the selectivity of the molybdenum catalysts, it would first be important to characterize the dominant side reactions. To this end, reaction supernatants of the molybdenum catalysts were studied using GC-MS.

GC-MS was used to characterize the major side products of the molybdenum reactions with 2-propanol, triphenylphosphine, ammonium chloride, ammonium sulfate, and urea reductants. When using triphenylphosphine as a reductant, the primary products were 1-decene (deoxydehydration product), 2-decanone and decanal, 2 different size ranges of larger compounds, likely oligomers forming from 1,2-decanediol. Secondary alcohol DODH for molybdenum catalysts has many different side products including decene internal isomers; a variety of aldehydes, ketones, and alcohols from the original 1,2-decanediol; ether formation with the 2-propanol solvent; and some oligomeric compounds.

Interestingly, the ammonium chloride, ammonium sulfate, and urea reductants resulted in a very similar mix of side products which varied considerably depending on whether sodium molybdate or MoO_x/ZrO_2 was used as the catalyst. For both catalysts, we do not observe the aldehyde, ketone, and alcohol functionalized side products. Distinctive peaks of larger, longer retention time molecules were found when using ammonium-based reductants for both sodium molybdate and MoO_x/ZrO_2, though these large molecules tend to elute primarily in one peak for

the sodium molybdate catalysts, and in a variety of longer retention time peaks later on for the zirconia-supported catalysts. Their similar fragmentation pattern likely indicates the presence of various isomers of these large oligomers formed from the 1,2-decanediol reactant.

The lack of carbonyls and alcohols could be explained by their conversion to imines and amines which would consume the aldehyde and alcohol side products seen when using ammonium-based reductants.[80–83] The question which needs to be resolved is whether the large oligomerized side products are nitrogen-containing. Due to the distinct difference between the supported and unsupported catalyst side products, it appears that the zirconia support may be active in catalyzing a side reaction or inducing additional reactivity for the supported molybdenum catalyst. As we see the supported molybdenum catalysts are less selective than their homogeneous counterparts, a more detailed investigation into the role of the support is warranted.

4.3. Tungsten Catalysts

While rhenium is very effective for DODH, its high cost and rarity motivate us to find cheaper and more abundant oxo-metal compounds to make the reaction feasible at industrial scale. Tungsten is a good candidate because it is well studied as a supported oxide catalyst and can form a surface 'di-oxo' structure similar to rhenium.[84,85]

4.3.1. Tungsten Catalyst Preparation

Oxide-supported tungsten catalysts were prepared using incipient wetness impregnation using an ammonium tungstate precursor dissolved in 1-1.5 mL of DI water corresponding to the pore volume of about 1000 mg of pre-dried P25 TiO_2, ZrO_2, and γ-Al_2O_3 support to produce a roughly 4 wt% W catalyst. The impregnated catalysts were dried in a muffle furnace at 115 °C for at least 8 hours, followed by a calcination for 2 hours at 550 °C. The tungsten content and support surface areas for these catalysts are listed in Table 4.7.

Table 4.7: Oxide-supported tungsten catalysts.

Catalyst	Tungsten Content (wt%)	Support BET Surface Area (m^2/g)
WO_x/TiO_2	3.9	53.2
WO_x/ZrO_2	3.8	99.5
WO_x/Al_2O_3	3.9	151.6

4.3.2. Tungsten Catalyst Reactivity

The supported tungsten catalysts were tested for DODH catalytic activity at 150 and 180 °C using 1,2-decanediol as reactant, triphenylphosphine as reductant, and toluene as the solvent.

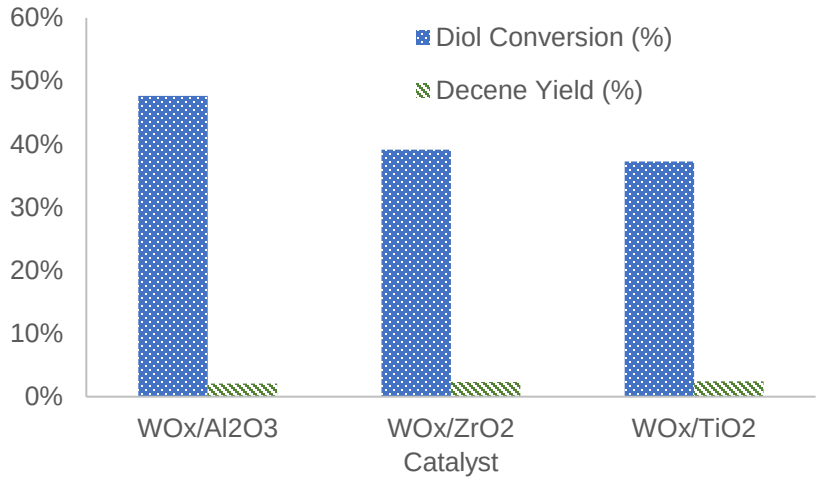

Figure 4.11: Tungsten catalyst reactivity with triphenylphosphine reductant. Reaction conditions: Temp. 150 °C, time 12 h, solvent toluene, 0.2 M 1,2-decanediol, 0.23 M PPh_3, diol:W=20.

The catalytic test results for the supported tungsten oxide catalysts performed at 150 °C can be seen in Figure 4.11. At 40% diol conversion in the tested conditions, we observe between 2.1-2.4% yield of decene. Similar decene yields were observed when using 2-propanol as the solvent which also acts as a secondary alcohol reductant. To test whether increasing the reaction temperature can increase the deoxydehydration alkene yield, the supported tungsten catalysts were tested at 180 °C for 20 h using triphenylphosphine as the reductant and toluene as the solvent. However, while the diol conversion was increased to 84-98%, the decene yield fell to between 0.3 and 1.1%, indicating a large reduction in selectivity. These results indicate that while tungsten may be active for DODH, selectivity remains very low.

Tungsten catalysts were also tested using ammonium chloride as the reductant; specifically ammonium metatungstate tetrahydrate and 4 wt% loading WO_x/ZrO_2 were tested using 0.23 M ammonium chloride reductant, 0.2 M 1,2-decanediol reactant and toluene solvent. After a 5 hour, 180 °C reaction, no decene product was observed for either tungsten catalyst by GC-FID, indicating that ammonium is not an effective reductant for tungsten-catalyzed deoxydehydration.

4.4. Manganese Catalysts

Manganese is an interesting candidate as an alternative metal because it is a group VII element like rhenium which is also stable in many oxidation states but is far more abundant[69] and cheaper. Furthermore, Aboukis et al.[86] have studied H_2 TPR of TiO_2-supported manganese showing a first reduction of MnO_2 to Mn_3O_4 at 350 °C, and a second reduction of Mn_3O_4 to MnO at 410 °C. This would theoretically give us a redox couple that may be capable of performing DODH, especially in the presence of activated hydrogen. There are also numerous papers published producing supported manganese catalysts on oxide supports using incipient wetness impregnation, which should make catalyst preparation using a procedure similar to the one used for the molybdenum catalysts relatively easy.[86,87]

4.4.1. Manganese Catalyst Preparation

Manganese catalysts were prepared using incipient wetness impregnation using P25-TiO_2 (Sigma Aldrich) and manganese acetate (Sigma Aldrich) as the manganese precursor. Manganese acetate was used based on the work by Kapteijn et al.[87] which showed that manganese acetate was an effective precursor for incipient wetness impregnation that achieved good dispersion in comparison to a manganese nitrate precursor. Two different manganese loadings were prepared as seen in Table 4.8.

Table 4.8: Titania-supported manganese catalysts.

Catalyst	Weight % Mn Loading
MnO_x/TiO_2, 1 wt%	0.9
MnO_x/TiO_2, 4 wt%	3.6

4.4.2. Manganese Catalyst Reactivity

The manganese acetate and titania supported catalysts were tested for DODH activity with 2-propanol as a secondary alcohol, triphenylphosphine, and ammonium chloride reductants. After 5 hours, no decene formation was measured for using the secondary alcohol or triphenylphosphine reductants for any of the tested manganese catalysts, however, as seen in Table 4.9, after the 5 h reaction, some decene production was observed with ammonium chloride reductant. The catalysts were tested in a 24 h reaction, however alkene yield did not improve, remaining below stoichiometric yield of decene compared to total manganese content of the catalyst.

Table 4.9: Manganese catalyst deoxydehydration activity. Reaction conditions: 180 °C, 0.23 M 1,2-decanediol, 0.23 M NH_4Cl, diol:Mn=20.

Catalyst	Time (h)	Reductant	Diol Conv (%)	Alkene Yield (%)	Selectivity (%)	Activity (mol alkene)(mol Metal)$^{-1}h^{-1}$
None	5	None	3	0	0	
None	5	NH_4Cl	14	0	0	
$Mn(CH_3CO_2)_2$	5	NH_4Cl	13	1	7	0.05
MnO_x/TiO_2 1 wt%	5	NH_4Cl	22	2	7	0.14
MnO_x/TiO_2 4 wt%	5	NH_4Cl	17	1	5	0.05
None	24	NH_4Cl	4	1	37	
$Mn(CH_3CO_2)_2$	24	NH_4Cl	9	2	19	0.01
MnO_x/TiO_2 1 wt%	24	NH_4Cl	16	1	9	0.02
MnO_x/TiO_2 4 wt%	24	NH_4Cl	10	1	10	0.01

While manganese is in the same group as rhenium and can access many different oxidation states, it is a very powerful oxidant at higher oxidation states and tends to be stable at lower oxidation and coordination states than rhenium. The larger rhenium atom can more easily access the high coordination states necessary to form the glycolate intermediate necessary for deoxydehydration.

4.5. Vanadium Catalysts

Vanadium oxides have been shown to be active homogeneous DODH catalysts when functionalized with a bulky chelated complex that allows for dioxovanadate species.[9] The economic argument for vanadium is clear as it is cheap and abundant, however, on oxides it tends to prefer tetrahedral coordination with a single oxo group.[64] This may be mitigated by using a reducible support, as earlier work in the Jentoft group with supported vanadium catalysts on the reducible ceria support showed VO_x/CeO_2 with non-activated H_2 as a reductant was able to yield 2% of the alkene DODH product.[39]

4.5.1. Vanadium Catalyst Preparation

Supported vanadium catalysts were synthesized using incipient wetness impregnation. Ammonium metavanadate (Sigma Aldrich) was used as the vanadium precursor and pre-calcined G2 hydrous zirconia (MEL Chemicals) was used as the support to create a 2 wt% vanadium loading catalyst. The lower loading was necessary to maintain below monolayer surface coverage because of the relatively low molecular weight of vanadium. After drying in a muffle furnace for 12 h at 115 °C, the catalyst was calcined at 550 °C for 4 h.

4.5.2. Vanadium Catalyst Reactivity

The prepared zirconia-supported vanadium and homogeneous ammonium vanadate precursor were tested with ammonium chloride and triphenylphosphine reductants. Catalytic test results of the vanadium catalysts are shown in Table 4.10.

Table 4.10: Vanadium catalyst reactivity. Reaction conditions: 180 °C, solvent toluene, 0.2 M 1,2-decanediol reactant, 0.23 M reductant, Diol:V=20.

Catalyst	Temp (°C)	Time (h)	Reductant	Diol Conv (%)	Alkene Yield (%)	Selectivity (%)	Activity (mol alkene)(mol V)$^{-1}$h^{-1}
None	180	5	None	3	0	0	
None	180	5	NH_4Cl	14	0	0	
VO_x/ZrO_2	180	5	PPh_3	27	1	5	0.05
NH_4VO_4	180	5	NH_4Cl	33	4	11	0.14
VO_x/ZrO_2	180	5	NH_4Cl	33	1	2	0.03
None	180	24	NH_4Cl	4	1	37	
NH_4VO_4	180	24	NH_4Cl	68	14	20	0.10
VO_x/ZrO_2	180	24	NH_4Cl	65	6	9	0.05

From our reaction, we see that vanadium catalysts produce a small amount of deoxydehydration products using triphenylphosphine and ammonium chloride reductants. The homogeneous ammonium metavanadate catalyst was especially active and demonstrated a 14% alkene yield using ammonium chloride as a reductant after 24 h, which demonstrates that the reaction is catalytic rather than stoichiometric. However, the activity, selectivity and yield remain too low overall under these conditions as compared to rhenium and molybdenum catalysts. Kwok et al.[37] have reported silica-supported vanadium as a deoxydehydration catalysts, however they used a reaction temperature of 400 °C in a gas phase reaction of 2,3-butanediol. Increasing the reaction temperature may make the vanadium catalysts viable, however it would make liquid phase reactions difficult because it would be a very high pressure, 180 °C is near the maximum rating of the 150 psig rated ace glass pressure tubes that were utilized for our reactions, and solvent free reactions impose some additional limitations on substrates.

4.6. Rhenium Catalysts with Ammonium Chloride Reductant

As demonstrated in Chapter 2, rhenium-based catalysts have been found to be the most active deoxydehydration catalysts for a variety of reductants. When using triphenylphosphine and ReO_x/TiO_2 catalyst and temperature of 150 °C, we were able to achieve 83.6% selectivity to the alkene product with a turn over frequency (TOF) of 27.2 (mol decene)(mol Re)$^{-1}$h^{-1}. To test whether

ammonium-based reductants can be effective for rhenium catalysts, we tested both the homogeneous precursor ammonium perrhenate (NH_4ReO_4) and the zirconia-supported rhenium catalysts (ReO_x/ZrO_2) with ammonium chloride, ammonium sulfate, and urea as reductants.

Table 4.11: Rhenium catalysts with ammonium-based reductants. Reaction conditions: 1 h, toluene solvent.

Catalyst	Temp (°C)	Reductant	Diol Conversion (%)	Alkene Yield (%)	Selectivity (%)	TOF (mol alkene)(mol Metal)$^{-1}h^{-1}$
NH_4ReO_4	150	NH_4Cl	12.5	0.7	5.6	0.16
NH_4ReO_4	180	NH_4Cl	13.2	0.9	7.1	0.21
NH_4ReO_4	150	$(NH_4)_2SO_4$	4.4	0.0	0.0	0.00
NH_4ReO_4	150	Urea	8.1	1.9	23.1	0.39
NH_4ReO_4	180	Urea	34.5	1.7	4.9	0.39
ReO_x/ZrO_2	150	NH_4Cl	22.9	1.7	7.2	0.60
ReO_x/ZrO_2	180	NH_4Cl	31.4	8.6	27.6	2.81
ReO_x/ZrO_2	150	$(NH_4)_2SO_4$	18.0	1.9	10.4	0.60
ReO_x/ZrO_2	150	Urea	36.4	0.0	0.0	0.00
ReO_x/ZrO_2	180	Urea	52.0	1.4	2.7	0.45

As seen in Table 4.11, only modest amounts of the decene product were produced, all below stoichiometric yield aside from the higher temperature 180 °C reaction of ReO_x/ZrO_2 catalyst in which an 8.6% alkene yield was achieved. Overall, the low activity of the rhenium catalysts with ammonium-based reductants compares poorly to triphenylphosphine and secondary alcohol reductants.

CHAPTER 5

CONCLUSIONS AND FUTURE DIRECTIONS FOR SOLID DEOXYDEHYDRATION CATALYSTS

5.1. Concluding Remarks

The overarching goal of this theses was to develop active, selective, stable and inexpensive solid catalyst for deoxydehydration, that is, the conversion of vicinal diols into olefins. This transformation requires a sacrificial reductant. Towards the objective, several families of catalysts were synthesized. The general approach was to impregnate a support with suitable transition metal compounds by the incipient wetness method, followed by calcination. One synthesis strategy sought to improve a known but leach-prone carbon-supported perrhenate catalyst by replacing the carbon support with more polar oxide supports in order to more firmly anchor the active rhenium species.

A variety of oxides, including silica, titania, alumina, iron oxide, and zirconia were used as supports for oxo-rhenium catalysts in deoxydehydration. The supports were also tested for catalytic activity using 1,2-decanediol as a model diol reactant, and triphenylphosphine as the model reductant, both of which are highly soluble in non-polar benzene solvent used. The supports were first tested for activity under deoxydehydration reaction conditions. The supports were found to be inactive, however, the 1,2-decanediol was found to adsorb on the support surface. This makes it more difficult to close the mass balance for incomplete conversion, but ultimately no side reaction is catalyzed by the support. This yielded the result that the support has no adverse effect, and the supported rhenium catalysts retain high selectivity and reductant efficiency for deoxydehydration with the most active SiO_2 and TiO_2-supported catalysts demonstrating activity on par with the methyltrioxorhenium homogeneous benchmark catalyst.

High initial activity of the supported rhenium catalysts was correlated with rapid deactivation. It was found that rhenium leaching is the primary cause of deactivation and is induced via association of the catalyst with the diol to give a soluble glycolate complex. Homogeneous catalysis contributions were significant. In addition to choosing a suitable (i.e., reducible or Lewis-acidic) support, leaching can be minimized through an appropriately low rhenium loading that depends on the support. We have demonstrated that rhenium leaching is enabled by the presence of the diol which induces solubility through the formation of the intermediate glycolate species. We demonstrated that the severity of leaching depends on the nature of the solvent and diol due to differing the solubility of the glycolate complex. Since the leaching is promoted by the presence of the diol, we demonstrated that driving the reaction to 100% substrate conversion results in re-deposition of rhenium, which could be used to mitigate the effects of catalyst leaching using a release and catch strategy.

In an effort to implement new strategies for reducing rhenium leaching, a preliminary investigation of microporous supports was undertaken based on the idea of trapping the glycolate intermediate within a zeolite pore. Beta zeolite with two different concentrations of silicon-aluminum acid sites were tested as rhenium supports. The initial results did not show an improvement in activity and stability as compared to the titania and zirconia supports, and it could not be proven that the catalytic activity arose from rhenium species inside the micropores. However, it was shown that the presence of acid sites in the zeolite served to reduce rhenium leaching, while also reducing selectivity due to side reactions catalyzed by the acid site.

In order to produce more economical deoxydehydration catalysts, alternative transition metals were tested for deoxydehydration activity. Tungstate, vanadate, molybdate, and manganese salts were used to synthesize oxide-supported catalysts. Tungsten and manganese catalysts were found to have very low activity at the tested temperatures which were reasonable for liquid phase reactions. Vanadium exhibited slightly higher activity, and up to 14% alkene yield was achieved

for ammonium vanadate using ammonium chloride as the reductant. Molybdenum catalysts were the most promising, achieving over 50% alkene yield using ammonium molybdate as the catalyst and triphenylphosphine as the reductant, and up to 20% yield for the supported molybdenum catalysts.

Upon the observation that the molybdenum catalysts with an ammonium counterion were the most selective, ammonium was investigated as a possible reductant for deoxydehydration. Ammonium chloride, ammonium sulfate, and urea were all found to be active reductants, and 32% decene yield was achieved for a sodium molybdate catalyst using ammonium chloride as the reductant, the first time ammonium has been reported as a reductant for deoxydehydration. Preliminary investigation of side products showed that triphenylphosphine and secondary alcohol reductants tended to result in more aldehyde, ketone, and alcohol side products, where the ammonium reductants had much more exclusively large side products that indicate the formation of oligomers from the 1,2-decanediol reactant.

5.2. Future Directions

5.2.1. Support Effect and Surface Chlorine Impurities

For oxide-supported rhenium catalysts, the choice of support plays a strong role on the activity of the solid catalyst. As reported in Chapter 3, we observed a strong correlation between high activity in the first run with high rhenium leaching and subsequent deactivation as seen with the silica and titania supports. This implies that the leached rhenium species are highly active, while the catalysts that leach less are initially less active, which implies that the rhenium species is more strongly bound to the catalyst surface and less active overall, as seen with the zirconia, alumina, and iron oxide supports. This possible difference in rhenium binding strength may be corroborated in part by the UV-Vis spectroscopy on the supported catalysts. While for the silica-supported catalyst, we only see the perrhenate-associated band at 233 nm, for alumina and zirconia we see the formation of an additional band at 320 nm, possibly arising from interaction between

the surface rhenium species and the support. Additional characterization of the surface rhenium species for coordination and oxidation state by X-ray photoelectron spectroscopy (XPS) or X-ray absorption fine structure (XAFS) analysis may be valuable in elucidating the support interaction.

Samples have previously been sent to Brookhaven National Laboratory to test for the oxidation and coordination of the titania and zirconia-supported rhenium catalysts as prepared and post reaction. The results were not conclusive, however, from the XANES white line peak intensity seemed to suggest that the as prepared titania-supported catalyst was under-coordinated in comparison to the zirconia-supported catalysts and the used titania-supported catalyst. This may indicate that the persistent rhenium species on the titania catalyst were more strongly coordinated to the support, potentially explaining why persistent titania-supported rhenium species are seen in Figure 3.2. It may also help to explain why Sandbrink et al. observed that pre-reduction of ReO_x/TiO_2 improves the catalyst stability.

Additionally, in comparing our recyclability study to Sandbrink et al.,[24] they observed less deactivation of their titania supported catalysts. Upon investigation, it was found that they used a different titania support, which could have also contributed to the discrepancy in the results. Our experiments used a P25-TiO_2 (Sigma Aldrich) which is a mixture of anatase and rutile phase and contains chlorine impurities from the titanium tetrachloride precursor used in the flame hydrolysis (aeroxide) preparation method. Sandbrink et al. used a titania from Saint Gobain (ST61120) which is purely of anatase phase and contains sulfur as an impurity (<0.3wt%).

We have tested the Saint Gobain titania versus the P25-TiO_2 supported catalyst used in previous experiments, and it was found to be more stable. There was an attempt to test whether the performance of the P25 titania could be improved by removing chlorine impurities either by pre-washing or pre-calcining the titania before depositing rhenium by incipient wetness impregnation. The results were somewhat inconclusive, the catalysts made from pre-calcined supports were less

active, possibly due to either sintering, or the formation of more stable, less active rhenium. The initial vacuum filtration wash did not seem to have a significant effect.

The chlorine impurity in the P25-TiO2 may be more concentrated on the surface. It may form a passivating layer which inhibits a strong rhenium, support interaction as compared to the Saint Gobain catalyst. Alternatively, the difference could be an effect of titania phase, with the anatase phase having a stronger interaction with the rhenium, lowering leaching. To test this hypothesis, leaching and recyclability of both P25-TiO_2- and Saint Gobain TiO_2-supported rhenium catalysts should be measured with and without pre-washing to remove surface impurities. This should allow us the test whether previous results could be ascribed to titania phase or presence of surface impurities. Wash could be done sequentially by vacuum filtration until presence of chlorine is not detected in the wash fluid by precipitation with silver nitrate. Alternatively, heat treatment could be used to remove the surface chlorine. The characterization of activity, leaching, and recyclability could be pursued in a similar way as the leaching study reported in Chapter 3.

5.2.2. Microporous Supports

In Chapter 3, a preliminary investigation of using microporous supports as a means of reducing active species was explored for beta zeolite with two different concentrations of silicon-aluminum acid sites. We see that the presence of the acid sites reduces rhenium leaching, however also lowers selectivity due to the acid site catalyzing side reactions. The acidity of the zeolite acid sites can be adjusted by substituting the aluminum for alternative atoms such as boron and gallium.[88–91] The wide variety of microporous materials such as zeolites available also provides a large parameter space for optimizing pore size and structure to inhibit leaching based on the size of the target feedstock.

Additional characterization would be necessary. ICP-MS could be used to determine the rhenium loading on the microporous support. It would also be important to determine whether the deposited rhenium is primarily a surface species, or whether the rhenium is largely entrained in the

micropore network. This could be verified in part using tranmission electron microscopy, or using the technique by Wu et al.[58] who applied FTIR-spectroscopy to track the replacement of the acidic hydrogens with rhenium.

5.2.3. Heat Treatment for Catalyst Regeneration

As demonstrated in Chapter 3, rhenium can leach considerably during the reaction due to the formation of the glycolate intermediate with the diol, which leads to significant catalyst deactivation. By driving the reaction to complete diol conversion, we find that the leached rhenium largely precipitates out of of the solubilized phase as measured by ICP-MS. This in turn leads to higher activity of the recycled catalyst as compared to a recycled catalyst after incomplete diol conversion, but less activity than that of the fresh catalyst.

The active catalytic rhenium species is redeposited on the support, but in a less active form. This could be due to the presence of a more reduced rhenium species, the formation of rhenium oligiomers, or the formation of less active, but more stable supported rhenium species. By performing a calcination heat treatment between runs after 100% diol conversion, we may be able to re-oxidize the rhenium to a state more similar to the fresh catalyst, thereby regaining more of the original catalyst activity.

Sandbrink et al. found that pre-reducing the supported rhenium catalysts improved recyclability. They hypothesized that the reduced rhenium was less soluble leading to greater recyclability. Further, XAFS was performed to determine rhenium oxidation state. When catalysts were pre-reduced at 300 °C, it was found that the rhenium was reduced from Re(VII) to both Re(VI) and Re(0). The resulting catalyst had similar initial activity and better recyclability than the fresh catalyst. When the pre-reduction was done at 400 °C and above in hydrogen, more rhenium was reduced to Re(0), resulting in a less active catalyst. Sandbrink et al. hypothesized that the Re(0) form was largely inactive, however the Re(VI) may be more active even than Re(VII) due to pre-

reduction resulting in similar initial activity to the fresh catalyst despite formation of some inactive Re(0).

It may be valuable to explore the pre-reduction of supported catalysts in hydrogen to verify the results of Sandbrink et al., and use ICP-MS to test rhenium leaching vs pre-reduction. Further, since titania is a reducible support it would be interesting to see whether it is purely the rhenium being reduced, or if there is also reduction of the support occurring and compare the results to a less reducible support such as alumina.

5.2.4. Identification of Intermediates

From the work demonstrated in Chapter 3 showing the leaching behavior of supported rhenium catalysts by ICP-MS, work was also done in an attempt to characterize the solubilized intermediates present in the supernatant by a variety of means, including UV-Vis absorption spectroscopy, EPR, and XAFS. We see a strong indication of a solubilized rhenium intermediate with different and distinct bands that are dependent on the choice of reductant. When triphenylphosphine was used as a reductant, we observed a UV-Vis transmission band in the supernatant at 500 nm, whereas with secondary alcohol reductants, a band would form at 400 nm. From EPR, we did not observe any paramagnetic species when using triphenylphosphine reductant but did note a small concentration of paramagnetic species for secondary alcohol reductants.

These results indicate differing predominant rhenium intermediates depending on the choice of the reductant, but positive identification of these intermediates has not yet been made. This identification is made challenging due to the many possible oxidation and coordination states available to rhenium, and the possibility of the formation of dimers and oligomers of oxo-rhenium species.[74,75] Further, it was noted that the reaction mixture changed color upon cooling, and that the reaction mixture may be prone to oxidation over time for ex-situ measurements.

The use of in situ-NMR and FTIR may give additional insight into the intermediate glycolate species which would help to elucidate the mechanism. This has been attempted for homogeneous catalysts using secondary alcohol reductants using NMR by Abu-Omar and co-workers,[17] and by in-situ FTIR spectroscopy by Toste and co-workers.[19] They suggest a variety of intermediate species, including oxo-rhenium dimers. It would be especially interesting to extend this work to alternative reductants to see how the choice of reductant effects the mechanistic pathway.

5.2.5. Further Investigation of Ammonium Reductants

As demonstrated in Chapter 4, we have discovered that ammonium-based reductants are especially effective for molybdenum catalysts. There is some precedent for this sort of reductant seen for molybdenum catalysts in selective catalytic reduction, but it is curious that it is so much more effective for molybdenum than the other screened transition metal catalysts. It would be valuable to characterize the side products of this reaction in greater detail and identify the oxidation products of the reductant. This would help to give greater mechanistic insight into deoxydehydration using molybdenum catalysts with ammonium reductants and may result in further insights to help improve the selectivity of molybdenum catalysts for DODH.

5.2.6. Alternative Metals with Gold Promoted Hydrogen Reductants

From the work of Tomishige and coworkers, we see that ceria-supported rhenium using gold-promoted hydrogen reductants makes for a very active and robust catalyst.[27] The key optimization challenge they faced was in activating the hydrogen such that it reduced the rhenium, but did not hydrogenate the alkene product of deoxydehydration into the alkane. Previous work in our group performed by Alana Denning using hydrogen as a reductant for supported rhenium catalysts without a noble metal promoter was not found to be especially active, showing that the noble metal is necessary to dissociate the hydrogen to make it an effective reductant for the rhenium catalyst.[39]

Further, DFT work studying DODH with secondary alcohol and triphenylphosphine reductants indicated that the reduction step is the highest energy barrier step in the reaction.[21,92] A DFT study was also performed by Wang et al. on the ceria supported rhenium catalysts and hydrogen reductants with and without the noble metal promoter.[93] This study indicated that in the absence of the noble metal promoter, the energy barrier for the hydrogen dissociation and reduction was prohibitively high, however, the presence of the noble metal promoter makes the reduction step facile. This makes the noble metal activated hydrogen a promising reductant for the cheaper alternative metals.

BIBLIOGRAPHY

(1) IEA. Oil information overview https://webstore.iea.org/oil-information-2019-overview (accessed Jan 22, 2020). https://doi.org/10.1017/CBO9781107415324.004.

(2) Pauly, M.; Keegstra, K. Cell-Wall Carbohydrates and Their Modification as a Resource for Biofuels. *Plant Journal*. 2008, pp 559–568. https://doi.org/10.1111/j.1365-313X.2008.03463.x.

(3) Alonso, D. M.; Bond, J. Q.; Dumesic, J. A. Catalytic Conversion of Biomass to Biofuels. *Green Chem.* **2010**, *12* (9), 1493. https://doi.org/10.1039/c004654j.

(4) Cook, G. K.; Andrews, M. A. Toward Nonoxidative Routes to Oxygenated Organics: Stereospecific Deoxydehydration of Diols and Polyols to Alkenes and Allylic Alcohols Catalyzed by the Metal Oxo Complex (C5Me5)ReO3. *J. Am. Chem. Soc.* **1996**, *118* (39), 9448–9449. https://doi.org/10.1021/ja9620604.

(5) Raju, S.; Jastrzebski, J. T. B. H.; Lutz, M.; Klein Gebbink, R. J. M. Catalytic Deoxydehydration of Diols to Olefins by Using a Bulky Cyclopentadiene-Based Trioxorhenium Catalyst. *ChemSusChem* **2013**, *6* (9), 1673–1680. https://doi.org/10.1002/cssc.201300364.

(6) Dethlefsen, J. R.; Lupp, D.; Oh, B.-C.; Fristrup, P. Molybdenum-Catalyzed Deoxydehydration of Vicinal Diols. *ChemSusChem* **2014**, *7* (2), 425–428. https://doi.org/10.1002/cssc.201300945.

(7) Dethlefsen, J. R.; Lupp, D.; Teshome, A.; Nielsen, L. B.; Fristrup, P. Molybdenum-Catalyzed Conversion of Diols and Biomass-Derived Polyols to Alkenes Using Isopropyl Alcohol as Reductant and Solvent. *ACS Catal.* **2015**, *5* (6), 3638–3647. https://doi.org/10.1021/acscatal.5b00427.

(8) Galindo, A. DFT Studies on the Mechanism of the Vanadium-Catalyzed Deoxydehydration of Diols. *Inorg. Chem.* **2016**, *55* (5), 2284–2289. https://doi.org/10.1021/acs.inorgchem.5b02649.

(9) Gopaladasu, T. V.; Nicholas, K. M. Carbon Monoxide (CO)- and Hydrogen-Driven, Vanadium-Catalyzed Deoxydehydration of Glycols. *ACS Catal.* **2016**, *6* (3), 1901–1904. https://doi.org/10.1021/acscatal.5b02667.

(10) Vkuturi, S.; Chapman, G.; Ahmad, I.; Nicholas, K. M. Rhenium-Catalyzed Deoxydehydration of Glycols by Sulfite. *Inorg. Chem.* **2010**, *49* (11), 4744–4746. https://doi.org/10.1021/ic100467p.

(11) Ahmad, I.; Chapman, G.; Nicholas, K. M. Sulfite-Driven, Oxorhenium-Catalyzed Deoxydehydration of Glycols. *Organometallics* **2011**, *30* (10), 2810–2818. https://doi.org/10.1021/om2001662.

(12) Liu, P.; Nicholas, K. M. Mechanism of Sulfite-Driven, $MeReO_3$ -Catalyzed Deoxydehydration of Glycols. *Organometallics* **2013**, *32* (6), 1821–1831. https://doi.org/10.1021/om301251z.

(13) Larson, R. T.; Samant, A.; Chen, J.; Lee, W.; Bohn, M. A.; Ohlmann, D. M.; Zuend, S. J.; Toste, F. D. Hydrogen Gas-Mediated Deoxydehydration/Hydrogenation of Sugar Acids: Catalytic Conversion of Glucarates to Adipates. *J. Am. Chem. Soc.* **2017**, *139* (40), 14001–14004. https://doi.org/10.1021/jacs.7b07801.

(14) Michael McClain, J.; Nicholas, K. M. Elemental Reductants for the Deoxydehydration of Glycols. *ACS Catal.* **2014**, *4* (7), 2109–2112. https://doi.org/10.1021/cs500461v.

(15) Boucher-Jacobs, C.; Nicholas, K. M. Oxo-Rhenium-Catalyzed Deoxydehydration of Polyols with Hydroaromatic Reductants. *Organometallics* **2015**, *34* (10), 1985–1990. https://doi.org/10.1021/acs.organomet.5b00226.

(16) Boucher-Jacobs, C.; Nicholas, K. M. Catalytic Deoxydehydration of Glycols with Alcohol Reductants. *ChemSusChem* **2013**, *6* (4), 597–599. https://doi.org/10.1002/cssc.201200781.

(17) Liu, S.; Senocak, A.; Smeltz, J. L.; Yang, L.; Wegenhart, B.; Yi, J.; Kenttämaa, H. I.; Ison, E. A.; Abu-Omar, M. M. Mechanism of MTO-Catalyzed Deoxydehydration of Diols to Alkenes Using Sacrificial Alcohols. *Organometallics* **2013**, *32* (11), 3210–3219. https://doi.org/10.1021/om400127z.

(18) Shiramizu, M.; Toste, F. D. Expanding the Scope of Biomass-Derived Chemicals through Tandem Reactions Based on Oxorhenium-Catalyzed Deoxydehydration. *Angew. Chemie Int. Ed.* **2013**, *52* (49), 12905–12909. https://doi.org/10.1002/anie.201307564.

(19) Dethlefsen, J. R.; Fristrup, P. In Situ Spectroscopic Investigation of the Rhenium-Catalyzed Deoxydehydration of Vicinal Diols. *ChemCatChem* **2015**, *7* (7), 1184–1196. https://doi.org/10.1002/cctc.201403012.

(20) Qu, S.; Dang, Y.; Wen, M.; Wang, Z. X. Mechanism of the Methyltrioxorhenium-Catalyzed Deoxydehydration of Polyols: A New Pathway Revealed. *Chem. - A Eur. J.* **2013**, *19* (12), 3827–3832. https://doi.org/10.1002/chem.201204001.

(21) Shakeri, J.; Hadadzadeh, H.; Farrokhpour, H.; Joshaghani, M.; Weil, M. Perrhenate-Catalyzed Deoxydehydration of a Vicinal Diol: A Comparative Density Functional Theory Study. *J. Phys. Chem. A* **2017**, *121* (45), 8688–8696. https://doi.org/10.1021/acs.jpca.7b08884.

(22) Shakeri, J.; Hadadzadeh, H.; Farrokhpour, H.; Weil, M. A Comparative Study of the Counterion Effect on the Perrhenate-Catalyzed Deoxydehydration Reaction. *Mol. Catal.* **2019**, *471* (December 2018), 27–37. https://doi.org/10.1016/j.mcat.2019.04.014.

(23) Denning, A. L.; Dang, H.; Liu, Z.; Nicholas, K. M.; Jentoft, F. C. Deoxydehydration of Glycols Catalyzed by Carbon-Supported Perrhenate. *ChemCatChem* **2013**, *5* (12), 3567–3570. https://doi.org/10.1002/cctc.201300545.

(24) Sandbrink, L.; Klindtworth, E.; Islam, H. U.; Beale, A. M.; Palkovits, R. ReOx/TiO2: A Recyclable Solid Catalyst for Deoxydehydration. *ACS Catal.* **2016**, *6* (2), 677–680. https://doi.org/10.1021/acscatal.5b01936.

(25) Ota, N.; Tamura, M.; Nakagawa, Y.; Okumura, K.; Tomishige, K. Hydrodeoxygenation of Vicinal OH Groups over Heterogeneous Rhenium Catalyst Promoted by Palladium and Ceria Support. *Angew. Chemie Int. Ed.* **2015**, *54* (6), 1897–1900. https://doi.org/10.1002/anie.201410352.

(26) Liu, S.; Okuyama, Y.; Tamura, M.; Nakagawa, Y.; Imai, A.; Tomishige, K. Catalytic Conversion of Sorbitol to Gasoline-Ranged Products without External Hydrogen over Pt-Modified Ir-ReOx/SiO2. *Catal. Today* **2016**, *269*, 122–131. https://doi.org/10.1016/J.CATTOD.2015.10.023.

(27) Tazawa, S.; Ota, N.; Tamura, M.; Nakagawa, Y.; Okumura, K.; Tomishige, K. Deoxydehydration with Molecular Hydrogen over Ceria-Supported Rhenium Catalyst with Gold Promoter. *ACS Catal.* **2016**, *6* (10), 6393–6397. https://doi.org/10.1021/acscatal.6b01864.

(28) Li, X.; Zhang, Y. Highly Selective Deoxydehydration of Tartaric Acid over Supported and Unsupported Rhenium Catalysts with Modified Acidities. *ChemSusChem* **2016**, *9* (19), 2774–2778. https://doi.org/10.1002/cssc.201600865.

(29) Sharkey, B. E.; Denning, A. L.; Jentoft, F. C.; Gangadhara, R.; Gopaladasu, T. V.; Nicholas, K. M. New Solid Oxo-Rhenium and Oxo-Molybdenum Catalysts for the Deoxydehydration of Glycols to Olefins. *Catal. Today* **2018**, *310*, 86–93. https://doi.org/10.1016/J.CATTOD.2017.05.090.

(30) BASF. Engelhard Industrial Bullion (EIB) Prices https://apps.catalysts.basf.com/apps/eibprices/mp/ (accessed Jan 22, 2020).

(31) Sádaba, I.; López Granados, M.; Riisager, A.; Taarning, E. Deactivation of Solid Catalysts in Liquid Media: The Case of Leaching of Active Sites in Biomass Conversion Reactions. *Green Chem.* **2015**, *17* (8), 4133–4145. https://doi.org/10.1039/C5GC00804B.

(32) Hübner, S.; de Vries, J. G.; Farina, V. Cover Picture: Why Does Industry Not Use Immobilized Transition Metal Complexes as Catalysts? (Adv. Synth. Catal. 1/2016). *Adv. Synth. Catal.* **2016**, *358* (1), 1–1. https://doi.org/10.1002/adsc.201501096.

(33) Eremin, D. B.; Ananikov, V. P. Understanding Active Species in Catalytic Transformations: From Molecular Catalysis to Nanoparticles, Leaching, "Cocktails" of Catalysts and Dynamic Systems. *Coord. Chem. Rev.* **2017**, *346*, 2–19. https://doi.org/10.1016/J.CCR.2016.12.021.

(34) Sheldon, R. A.; Wallau, M.; Arends, I. W. C. E.; Schuchardt, U. Heterogeneous Catalysts for Liquid-Phase Oxidations: Philosophers' Stones or Trojan Horses? *Acc. Chem. Res.* **1998**, *31* (8), 485–493. https://doi.org/10.1021/ar9700163.

(35) Richardson, J. M.; Jones, C. W. Strong Evidence of Solution-Phase Catalysis Associated with Palladium Leaching from Immobilized Thiols during Heck and Suzuki Coupling of Aryl Iodides, Bromides, and Chlorides. *J. Catal.* **2007**, *251* (1), 80–93. https://doi.org/10.1016/J.JCAT.2007.07.005.

(36) Köhler, K.; Heidenreich, R. G.; Soomro, S. S.; Pröckl, S. S. Supported Palladium Catalysts for Suzuki Reactions: Structure-Property Relationships, Optimized Reaction Protocol and Control of Palladium Leaching. *Adv. Synth. Catal.* **2008**, *350* (18), 2930–2936. https://doi.org/10.1002/adsc.200800575.

(37) Kwok, K. M.; Choong, C. K. S.; Ong, D. S. W.; Ng, J. C. Q.; Gwie, C. G.; Chen, L.; Borgna, A. Back Cover: Hydrogen-Free Gas-Phase Deoxydehydration of 2,3-Butanediol to Butene on Silica-Supported Vanadium Catalysts (ChemCatChem 13/2017). *ChemCatChem* **2017**, *9* (13), 2609–2609. https://doi.org/10.1002/cctc.201701012.

(38) Sandbrink, L.; Beckerle, K.; Meiners, I.; Liffmann, R.; Rahimi, K.; Okuda, J.; Palkovits, R. Supported Molybdenum Catalysts for the Deoxydehydration of 1,4-Anhydroerythritol into 2,5-Dihydrofuran. *ChemSusChem* **2017**, *10* (7), 1375–1379. https://doi.org/10.1002/cssc.201700010.

(39) Denning, A. L. Supported Transition Metal-Oxo Compounds for the Deoxydehydration of Polyols to Olefins, University of Oklahoma, 2014.

(40) Morris, D. S.; van Rees, K.; Curcio, M.; Cokoja, M.; Kühn, F. E.; Duarte, F.; Love, J. B. Deoxydehydration of Vicinal Diols and Polyols Catalyzed by Pyridinium Perrhenate Salts. *Catal. Sci. Technol.* **2017**, *7* (23), 5644–5649. https://doi.org/10.1039/C7CY01728F.

(41) Lee, E. L.; Wachs, I. E. In Situ Spectroscopic Investigation of the Molecular and Electronic Structures of SiO 2 Supported Surface Metal Oxides. *J. Phys. Chem. C* **2007**, *111* (39), 14410–14425. https://doi.org/10.1021/jp0735482.

(42) Lee, E. L.; Wachs, I. E. Molecular Design and In Situ Spectroscopic Investigation of Multilayered Supported M 1 Ox/M 2 Ox/SiO 2 Catalysts. *J. Phys. Chem. C* **2008**, *112* (51), 20418–20428. https://doi.org/10.1021/jp805265m.

(43) Shiramizu, M.; Toste, F. D. Deoxygenation of Biomass-Derived Feedstocks: Oxorhenium-Catalyzed Deoxydehydration of Sugars and Sugar Alcohols. *Angew. Chemie - Int. Ed.* **2012**, *51*, 1–6. https://doi.org/10.1002/anie.201203877.

(44) Reichardt, C. *Solvents and Solvent Effects in Organic Chemistry*; Wiley, 2002. https://doi.org/10.1002/3527601791.

(45) Zhang, F.; Szeto, K. C.; Taoufik, M.; Delevoye, L.; Gauvin, R. M.; Scott, S. L. Enhanced Metathesis Activity and Stability of Methyltrioxorhenium on a Mostly Amorphous Alumina: Role of the Local Grafting Environment. *J. Am. Chem. Soc.* **2018**, *140* (42), 13854–13868. https://doi.org/10.1021/jacs.8b08630.

(46) Wachs, I. E. Raman and IR Studies of Surface Metal Oxide Species on Oxide Supports: Supported Metal Oxide Catalysts. *Catal. Today* **1996**, *27* (3–4), 437–455. https://doi.org/10.1016/0920-5861(95)00203-0.

(47) Lupacchini, M.; Mascitti, A.; Canale, V.; Tonucci, L.; Colacino, E.; Passacantando, M.; Marrone, A.; D'Alessandro, N. Deoxydehydration of Glycerol in Presence of Rhenium Compounds: Reactivity and Mechanistic Aspects. *Catal. Sci. Technol.* **2019**, *9* (12), 3036–3046. https://doi.org/10.1039/C8CY02478B.

(48) Zhao, F.; Shirai, M.; Arai, M. Palladium-Catalyzed Homogeneous and Heterogeneous Heck Reactions in NMP and Water-Mixed Solvents Using Organic, Inorganic and Mixed Bases. *J. Mol. Catal. A Chem.* **2000**, *154* (1–2), 39–44. https://doi.org/10.1016/S1381-1169(99)00369-6.

(49) Heidenreich, R. G.; Krauter, J. G. .; Pietsch, J.; Köhler, K. Control of Pd Leaching in Heck Reactions of Bromoarenes Catalyzed by Pd Supported on Activated Carbon. *J. Mol. Catal. A Chem.* **2002**, *182–183*, 499–509. https://doi.org/10.1016/S1381-1169(01)00499-X.

(50) Köhler, K.; Heidenreich, R. G.; Krauter, J. G. E.; Pietsch, J. Highly Active Palladium/Activated Carbon Catalysts for Heck Reactions: Correlation of Activity, Catalyst Properties, and Pd Leaching. *Chem. - A Eur. J.* **2002**, *8* (3), 622–631. https://doi.org/10.1002/1521-3765(20020201)8:3<622::AID-CHEM622>3.0.CO;2-0.

(51) Pröckl, S. S.; Kleist, W.; Gruber, M. A.; Köhler, K. In Situ Generation of Highly Active Dissolved Palladium Species from Solid Catalysts—A Concept for the Activation of Aryl Chlorides in the Heck Reaction. *Angew. Chemie Int. Ed.* **2004**, *43* (14), 1881–1882. https://doi.org/10.1002/anie.200353473.

(52) Thathagar, M. B.; ten Elshof, J. E.; Rothenberg, G. Pd Nanoclusters in C□C Coupling Reactions: Proof of Leaching. *Angew. Chemie Int. Ed.* **2006**, *45* (18), 2886–2890. https://doi.org/10.1002/anie.200504321.

(53) Richardson, J. M.; Jones, C. W. Poly(4-Vinylpyridine) and Quadrapure TU as Selective Poisons for Soluble Catalytic Species in Palladium-Catalyzed Coupling Reactions – Application to Leaching from Polymer-Entrapped Palladium. *Adv. Synth. Catal.* **2006**, *348* (10–11), 1207–1216. https://doi.org/10.1002/adsc.200606021.

(54) Soomro, S. S.; Ansari, F. L.; Chatziapostolou, K.; Köhler, K. Palladium Leaching Dependent on Reaction Parameters in Suzuki–Miyaura Coupling Reactions Catalyzed by Palladium Supported on Alumina under Mild Reaction Conditions. *J. Catal.* **2010**, *273* (2), 138–146. https://doi.org/10.1016/J.JCAT.2010.05.007.

(55) Phan, N. T. S.; Van Der Sluys, M.; Jones, C. W. On the Nature of the Active Species in Palladium Catalyzed Mizoroki–Heck and Suzuki–Miyaura Couplings – Homogeneous or Heterogeneous Catalysis, A Critical Review. *Adv. Synth. Catal.* **2006**, *348* (6), 609–679. https://doi.org/10.1002/adsc.200505473.

(56) Jones, C. W. On the Stability and Recyclability of Supported Metal–Ligand Complex Catalysts: Myths, Misconceptions and Critical Research Needs. *Top. Catal.* **2010**, *53* (13–14), 942–952. https://doi.org/10.1007/s11244-010-9513-9.

(57) Kirchnerová, J.; Cave, G. C. B. The Solubility of Water in Low-Dielectric Solvents. *Can. J. Chem.* **1976**, *54*, 3909–3916. https://doi.org/10.1139/v76-562.

(58) Wu, Y.; Holdren, S.; Zhang, Y.; Oh, S. C.; Tran, D. T.; Emdadi, L.; Lu, Z.; Wang, M.; Woehl, T. J.; Zachariah, M.; et al. Quantification of Rhenium Oxide Dispersion on Zeolite: Effect of Zeolite Acidity and Mesoporosity. *J. Catal.* **2019**, *372*, 128–141. https://doi.org/10.1016/j.jcat.2019.02.024.

(59) Lacheen, H. S.; Cordeiro, P. J.; Iglesia, E. Structure and Catalytic Function of Re-Oxo Species Grafted onto H-MFI Zeolite by Sublimation of Re2O7. *J. Am. Chem. Soc.* **2006**, *128* (47), 15082–15083. https://doi.org/10.1021/ja065832x.

(60) Association, I. Z. Database of Zeolite Structures http://www.iza-structure.org/databases/ (accessed Feb 6, 2019).

(61) Wu, Y.; Holdren, S.; Zhang, Y.; Oh, S. C.; Tran, D. T.; Emdadi, L.; Lu, Z.; Wang, M.; Woehl, T. J.; Zachariah, M.; et al. Quantification of Rhenium Oxide Dispersion on Zeolite: Effect of Zeolite Acidity and Mesoporosity. *J. Catal.* **2019**, *372*, 128–141. https://doi.org/10.1016/j.jcat.2019.02.024.

(62) Yang, H.; Ma, Z.; Zhou, T.; Zhang, W.; Chao, J.; Qin, Y. Encapsulation of an Olefin Metathesis Catalyst in the Nanocages of SBA-1: Facile Preparation, High Encapsulation Efficiency, and High Activity. *ChemCatChem* **2013**, *5* (8), 2278–2287. https://doi.org/10.1002/cctc.201300021.

(63) Védrine, J. Heterogeneous Catalysis on Metal Oxides. *Catalysts* **2017**, *7* (11), 341. https://doi.org/10.3390/catal7110341.

(64) Wachs, I. E. Catalysis Science of Supported Vanadium Oxide Catalysts. *Dalt. Trans.* **2013**, *42* (33), 11762. https://doi.org/10.1039/c3dt50692d.

(65) Shetty, M.; Murugappan, K.; Green, W. H.; Román-Leshkov, Y. Structural Properties and Reactivity Trends of Molybdenum Oxide Catalysts Supported on Zirconia for the Hydrodeoxygenation of Anisole. *ACS Sustain. Chem. Eng.* **2017**, *5* (6), 5293–5301. https://doi.org/10.1021/acssuschemeng.7b00642.

(66) Hu, H.; Wachs, I. E. Catalytic Properties of Supported Molybdenum Oxide Catalysts: In Situ Raman and Methanol Oxidation Studies. *J. Phys. Chem.* **1995**, *99* (27), 10911–10922. https://doi.org/10.1021/j100027a035.

(67) Kamata, K.; Yonehara, K.; Sumida, Y.; Hirata, K.; Nojima, S.; Mizuno, N. Efficient Heterogeneous Epoxidation of Alkenes by a Supported Tungsten Oxide Catalyst. *Angew. Chemie - Int. Ed.* **2011**, *50* (50), 12062–12066. https://doi.org/10.1002/anie.201106064.

(68) Wachs, I. E.; Deo, G.; Weckhuysen, B. M.; Andreini, A.; Vuurman, M. A.; De Boer, M.; Amiridis, M. D. Selective Catalytic Reduction of NO with NH3 over Supported Vanadia Catalysts. *J. Catal.* **1996**, *161*, 211–221. https://doi.org/10.1006/jcat.1996.0179.

(69) United States Geological Survey. Mineral Commodity Summaries https://www.usgs.gov/centers/nmic/mineral-commodity-summaries (accessed Apr 6, 2019).

(70) Weber, R. S. Effect of Local Structure on the UV-Visible Absorption Edges of Molybdenum Oxide Clusters and Supported Molybdenum Oxides. *J. Catal.* **1995**, *151* (2), 470–474. https://doi.org/10.1006/jcat.1995.1052.

(71) Rousseau, R.; Dixon, D. A.; Kay, B. D.; Dohnálek, Z. Dehydration, Dehydrogenation, and Condensation of Alcohols on Supported Oxide Catalysts Based on Cyclic (WO3)3 and (MoO3)3 Clusters. *Chemical Society Reviews*. The Royal Society of Chemistry October 20, 2014, pp 7664–7680. https://doi.org/10.1039/c3cs60445d.

(72) Mitchell, P. C. H. Speciation of Molybdenum Compounds in Water Ultraviolet Spectra and REACH Read Across. *Rep. Int. Molybdenum Assoc. Reach Molybdenum Consort.* **2009**.

(73) Navarro, C. A.; John, A. Deoxydehydration Using a Commercial Catalyst and Readily Available Reductant. *Inorg. Chem. Commun.* **2019**, *99*, 145–148. https://doi.org/10.1016/j.inoche.2018.11.015.

(74) Abu-Omar, M. M.; Appelman, E. H.; Espenson, J. H. Oxygen-Transfer Reactions of Methylrhenium Oxides. *Inorg. Chem.* **1996**, *35*, 7751–7757. https://doi.org/10.1021/ic960701q.

(75) Harms, R. G.; Herrmann, W. A.; Kühn, F. E. Organorhenium Dioxides as Oxygen Transfer Systems: Synthesis, Reactivity, and Applications. *Coord. Chem. Rev.* **2015**, *296*, 1–23. https://doi.org/10.1016/j.ccr.2015.03.015.

(76) Cheng, X.; Bi, X. T. A Review of Recent Advances in Selective Catalytic NOx Reduction Reactor Technologies. *Particuology* **2014**, *16*, 1–18. https://doi.org/10.1016/j.partic.2014.01.006.

(77) Sorrel, J. Selective Catalytic Reduction. In *Economic and Cost Analysis Air Pollution Regulation*; Randall, David D., Schaffner, Karen S., Fry, C. R., Ed.; Environmental Protection Agency: Research Triangle Park, NC, 2016.

(78) IHS Markit. Urea https://ihsmarkit.com/products/urea-chemical-economics-handbook.html (accessed Jan 22, 2020).

(79) Tran, R.; Kilyanek, S. M. Deoxydehydration of Polyols Catalyzed by a Molybdenum Dioxo-Complex Supported by a Dianionic ONO Pincer Ligand. *Dalt. Trans.* **2019**, *48*, 16304–16311. https://doi.org/10.1039/c9dt03759d.

(80) Demidova, Y. S.; Suslov, E. V.; Simakova, I. L.; Mozhajcev, E. S.; Korchagina, D. V.; Volcho, K. P.; Salakhutdinov, N. F.; Simakov, A.; Murzin, D. Y. Selectivity Control in One-Pot Myrtenol Amination over Au/ZrO2 by Molecular Hydrogen Addition. *J. Mol. Catal. A Chem.* **2017**, *426*, 60–67. https://doi.org/10.1016/j.molcata.2016.10.034.

(81) Wang, T.; Ibañez, J.; Wang, K.; Fang, L.; Sabbe, M.; Michel, C.; Paul, S.; Pera-Titus, M.; Sautet, P. Rational Design of Selective Metal Catalysts for Alcohol Amination with Ammonia. *Nat. Catal.* **2019**, *2* (9), 773–779. https://doi.org/10.1038/s41929-019-0327-2.

(82) Patil, R. D.; Adimurthy, S. Catalytic Methods for Imine Synthesis. *Asian J. Org. Chem.* **2013**, *2* (9), 726–744. https://doi.org/10.1002/ajoc.201300012.

(83) Nakajima, M.; Fava, E.; Loescher, S.; Jiang, Z.; Rueping, M. Photoredox-Catalyzed Reductive Coupling of Aldehydes, Ketones, and Imines with Visible Light. *Angew. Chemie Int. Ed.* **2015**, *54* (30), 8828–8832. https://doi.org/10.1002/anie.201501556.

(84) Horsley, J. A.; Wachs, I. E.; Brown, J. M.; Via, G. H.; Hardcastle, F. D. Structure of Surface Tungsten Oxide Species in the Tungsten Trioxide/Alumina Supported Oxide System from x-Ray Absorption near-Edge Spectroscopy and Raman Spectroscopy. *J. Phys. Chem.* **1987**, *91* (15), 4014–4020. https://doi.org/10.1021/j100299a018.

(85) Lwin, S.; Wachs, I. E. Olefin Metathesis by Supported Metal Oxide Catalysts. *ACS Catal.* **2014**, *4* (8), 2505–2520. https://doi.org/10.1021/cs500528h.

(86) Aboukaïs, A.; Abi-Aad, E.; Taouk, B. Supported Manganese Oxide on TiO2 for Total Oxidation of Toluene and Polycyclic Aromatic Hydrocarbons (PAHs): Characterization and Catalytic Activity. *Mater. Chem. Phys.* **2013**, *142* (2–3), 564–571. https://doi.org/10.1016/j.matchemphys.2013.07.053.

(87) Kapteijn, F.; Vanlangeveld, A. D.; Moulijn, J. A.; Andreini, A.; Vuurman, M. A.; Turek, A. M.; Jehng, J. M.; Wachs, I. E. Alumina-Supported Manganese Oxide Catalysts. *J. Catal.* **1994**, *150* (1), 94–104. https://doi.org/10.1006/jcat.1994.1325.

(88) Shamzhy, M.; Opanasenko, M.; Concepción, P.; Martínez, A. New Trends in Tailoring Active Sites in Zeolite-Based Catalysts. *Chem. Soc. Rev.* **2019**, *48*, 1095–1149. https://doi.org/10.1039/c8cs00887f.

(89) Coudurier, G.; Védrine, J. C. Catalytic and Acidic Properties of Boron Pentasil Zeolites. *Stud. Surf. Sci. Catal.* **1986**, *58* (10), 1389–1396. https://doi.org/10.1016/S0167-2991(09)60930-7.

(90) Fricke, R.; Kosslick, H.; Lischke, G.; Richter, M. Incorporation of Gallium into Zeolites: Syntheses, Properties and Catalytic Application. *Chem. Rev.* **2000**, *100* (6), 2303–2406. https://doi.org/10.1021/cr9411637.

(91) Yuan, S. P.; Wang, J. G.; Li, Y. W.; Jiao, H. Brønsted Acidity of Isomorphously Substituted ZSM-5 by B, Al, Ga, and Fe. Density Functional Investigations. *J. Phys. Chem. A* **2002**, *106* (35), 8167–8172. https://doi.org/10.1021/jp025792t.

(92) Wu, D.; Zhang, Y.; Su, H. Mechanistic Study on Oxorhenium-Catalyzed Deoxydehydration and Allylic Alcohol Isomerization. *Chem. - An Asian J.* **2016**, *11* (10), 1565–1571. https://doi.org/10.1002/asia.201600118.

(93) Xi, Y.; Yang, W.; Ammal, S. C.; Lauterbach, J.; Pagan-Torres, Y.; Heyden, A. Mechanistic Study of the Ceria Supported, Re-Catalyzed Deoxydehydration of Vicinal OH Groups. *Catal. Sci. Technol.* **2018**, *8* (22), 5740–5752. https://doi.org/10.1039/c8cy01782d.